Performance Evaluation of Sucrose-Based Rocket Fuel with Additives and Multi-Oxidizer

Raga Chali Geleta

A Thesis Submitted to the

Department of Mechanical Engineering

School of Mechanical, Chemical and Materials Engineering

Presented in Partial Fulfillment of the Requirement for the Degree of

Master of Science in Thermal Engineering

Office of Graduate Studies

Adama Science and Technology University

September, 2023

Adama, Ethiopia

Performance Evaluation of Sucrose-Based Rocket Fuel with Additives and Multi-Oxidizer

Raga Chali Geleta

Advisor: Dr. Gezahegn Habtamu (Assistant Professor)

A Thesis Proposal Submitted to

The Department of Mechanical Engineering

School of Mechanical, Chemical and Materials Engineering

Presented in Partial Fulfillment of the Requirement for the Degree of

Master of Science in Thermal Engineering

Office of Graduate Studies

Adama Science and Technology University

September, 2023

Adama, Ethiopia

DECLARATION

I hereby declare that this Master Thesis entitled "***Performance Evaluation of Sucrose-Based Rocket Fuel with Additives and Multi-oxidizer***" is my original work. That is, it has not been submitted for the award of any academic degree, diploma or certificate in any other university. All sources of materials that are used for this thesis have been duly acknowledged through citation.

__ Raga Chali Geleta ___	______________	____________________
Name of the student	Signature	Date of Submission

RECOMMENDATION

I, the advisor of this thesis, hereby certify that I have read the revised version of the thesis entitled "***Performance Evaluation of Sucrose-Based Rocket Fuel with Additives and Multi-oxidizer***" prepared under my guidance by Raga Chali Geleta submitted in partial fulfillment of the requirements for the degree of Mater's of Science in Thermal Engineering. Therefore, I recommend the submission of revised version of the thesis to the department following the applicable procedures.

____ Dr. Gezahegn Habtamu ______	____________	__________________
Name major of Advisor	Signature	Date

APPROVAL FROM BOARD OF EXAMINERS

I, the advisor of the thesis entitled "***Performance Evaluation of Sucrose-Based Rocket Fuel with Additives and Multi-oxidizer***" developed by Raga Chali Geleta, hereby certify that the recommendation and suggestions made by the board of examiners are appropriately incorporated into the final version of the thesis.

____ Dr. Gezahegn Habtamu _____	____________	__________________
Name major of Advisor	Signature	Date

We, the undersigned, members of the Board of Examiners of the thesis by Raga Chali Geleta have read and evaluated the thesis entitled "***Performance Evaluation of Sucrose-Based Rocket Fuel with Additives and Multi-oxidizer***" and examined the candidate during open defense. This is, therefore, to certify that the thesis is accepted for partial fulfillment of the requirement of the degree of Master of Science in Thermal Engineering.

_______________________	____________	__________________
Chairperson	Signature	Date
_______________________	____________	__________________
Internal Examiner 1	Signature	Date
_______________________	____________	__________________
External Examiner 2	Signature	Date

Final approval and acceptance of this thesis proposal is contingent upon submission of its final copy to the Office of Postgraduate Studies (OPGS) through the Department Graduate Council (DGC) and School Graduate Committee (SGC).

_______________________	____________	__________________
Department Head	Signature	Date
_______________________	____________	__________________
School Dean	Signature	Date
_______________________	____________	__________________
Office of Postgraduate Studies, Dean	Signature	Date

ACKNOWLEDGEMENT

I would like to express my heartfelt gratitude to God, the source of all wisdom, strength, and blessings. Without His guidance and grace, none of my accomplishments would have been possible. Also, I would like to extend my deepest appreciation to my advisor, Dr. Gezahegn Habtamu for his unwavering dedication, expertise, and mentorship. His guidance and encouragement have been invaluable in shaping my research and academic pursuits. I am grateful for his patience, constructive feedback, and belief in my abilities.

I would also like to express my sincere thanks to my family for their constant love, encouragement, and unwavering support. Their sacrifices and understanding have played an instrumental role in my academic achievements. Also, I am grateful to Dr. Esaias from Orlando Florida, USA for his invaluable support, and contributions to my research.

I would also like to acknowledge and thank my colleagues for their collaboration, camaraderie, and support. Finally, I would like to express my gratitude to all the individuals, whether mentioned here or not, who have contributed to my growth, learning, and success in various ways.

Thank you all for being an integral part of my journey and for making it truly meaningful and rewarding.

TABLE OF CONTENTS

ACKNOWLEDGEMENT v
LIST OF TABLES ix
LIST OF FIGURES x
LIST OF SYMBOLS AND NOMENCLATURE xii
ACRONYMS xii
ABSTRACT xvi
CHAPTER ONE 1
INTRODUCTION 1
1.1. Background of the Study 1
1.2. Introduction to Sounding Rocket 2
1.3. Statement of the Problem 4
1.4. Objectives of the study 5
1.4.1. General Objective 5
1.4.2. Specific Objective 5
1.5. Significance of the Study 5
1.6. Scope and Limitations of the Study 5
CHAPTER TWO 7
2. LITERATURE REVIEW 7
2.1. Significance of Space Science to Developing Countries and Space Science History of Ethiopia 7
2.2. Classification of Rocket Propulsion Systems 9
2.3. Chemical Rocket Propulsion 10
2.3.1. Liquid Propellant Rocket 10
2.3.2. Hybrid Propellant Rockets Motors 11
2.4. Solid propellant rocket motors 12
2.4.1. Casing 13
2.4.2. Case Material Development 13
2.4.3. Nozzle 15
2.4.4. Nozzle Material Development 15
2.4.5. Thermal protection system 18
2.5. Sugar-based Solid Fuels 21
2.6. Small Scale Model Rockets 24
2.7. Summary and Gap of Reviewed Literature 28
CHAPTER THREE 30

3. MATERIALS AND METHODS 30
3.1. Introduction 30
3.2. Procedures and Methods Followed 30
3.2.1. Review of Literature 30
3.2.2. Analytical Formulas 30
3.2.3. Design 31
3.2.4. Result Validation 31
3.2.5. Results and discussion 31
3.3. Sub scale Motor Design 33
3.3.1. Structural Design 33
3.3.2. Materials used in the Experiment 35
3.3.3. Electrical Circuit Design 35
3.4. Propellant preparation 37
3.5. Utilized Software 39
3.5.1. NASA's CEA Software 39
CHAPTER FOUR 41
4. THEORETICAL PERFORMANCE ANALYSIS OF THE FUEL AND MOTOR 41
4.1. Chemical Composition of the Propellant 41
4.2. Combustion Analysis 42
4.2.1. Ideal Gas Mixtures 42
4.2.2. Thermodynamic Analysis of the Reacting Systems 43
4.3. Solid Propellant Rocket Motor Fundamentals 45
4.4. Performance Parameters of Solid Propellants 47
4.5. Basic Relations of Propellant Burning Rate with Chamber Pressure 48
4.5.1. Mass Flow Relations and Burning Rate Relation with Pressure 49
4.5.2. More Accurate Burning Rate Relation with Pressure 50
4.6. Nozzle Theory and Thermodynamic Relations 51
4.7. Thrust and Thrust Coefficient 53
4.8. Motor Casing Structural Integrity Design 54
CHAPTER FIVE 55
5. RESULTS AND DISCUSSION 55
5.1. Thermo-physical and Performance Results from CEA NASA Software 55
5.2. Design for the Rocket for an Apogee of 20km and payload of 1kg 58
5.2.1. Initial Design Consideration 58
5.2.2. Fuel Grain Design 59

5.2.3. Nozzle Design 59
5.3. Flight Trajectory Simulation 61
CHAPTER SIX 65
6. CONCLUSION AND RECOMMENDATION 65
6.1. Conclusion 65
6.2. Recommendation 66
REFERENCES 68
APPENDIXES 74
A. Small Scale Rocket Motor Test Results 74
B. CEA NASA chemical equilibrium analysis and performance parameter result for 5% of Mg powder by mass. 77
C. CEA NASA chemical equilibrium analysis and performance parameter result for 10% of Al powder by mass. 79
D. Measuring Instrument Description and Specifications 80
E. Arduino Code for the Test Stand 81
F. Python Code for the Flight Trajectory Simulation 85
G. Drawings of Test Stand and Solid Rocket 89

LIST OF TABLES

Table 1: Typical Motor Nozzle Materials and Their Functions (George & Oscar, 2017) .. 17
Table 2: Slow burning transonic UAV (Matthew, 2017) 24
Table 3: Materials used for the test setup 35
Table 4: Chemical composition of fuel samples prepared 38
Table 5: Physical states of reactants and products 41
Table 6: Chemical Composition of samples using Mg as additive 55
Table 7: Chemical Composition of Samples using Al as additive 56
Table 8: Chemical Composition of Samples using ammonium nitrate and potassium nitrate as a multi-oxidizer 57
Table 9: Chemical equilibrium and performance data obtained from CEA NASA 59
Table 10: Burn rate and burn time data (obtained by approximation) 59

LIST OF FIGURES

Figure 1: James Webb Telescope and its orbit (Michael et al., 2021) 1
Figure 2: Sounding Rockets (Elaine, 2004).. 3
Figure 3: Solid Rocket Motor (SRM) (George et al., 2018).. 3
Figure 4: 2 and 3D view of the liquid rocket engine (George & Oscar, 2017) 11
Figure 5: Hybrid Rocket Engine (Zolla et al., 2021).. 12
Figure 6: Filament wound composites for rocket motor cases (Mateduc Composites, n.d.) 14
Figure 7: End and internal burn grain (Jonathan, 2018).. 20
Figure 8: Full-scale mockup of the ILR-33 "Amber" sounding rocket.(Nowakowski et al., 2017)... 25
Figure 9: 2D axisymmetric section of SRM employed in analysis with its analysis result (Jan 2022) 26
Figure 10: Microthrusters configuration with igniter wafer and its electrical connection (Rossi et al., 2002)... 27
Figure 11 CATIA drawing of the sounding rocket.. 30
Figure 12: Procedures followed to undertake the thesis.. 32
Figure 13: Isometric view of the test stand drawing 33
Figure 14: Dimensions of Small Scale Motor 34
Figure 15: Experimental Setup.. 34
Figure 16: Diagram for electrical connections 36
Figure 17: Sensors and Microprocessor (a) Industrial pressure transducer, (b) HX711 Load cell, (c) Arduino Uno, (d) MAX6637 thermocouple.. 37
Figure 18: Chemical ingredients of the tested fuel.. 37
Figure 19: Weighting scale and fuel grinding machine... 38
Figure 20: Fuel samples.. 38
Figure 21: Small scale motor... 39
Figure 22: Classification of Grains according to their pressure-time characteristics.......... 46
Figure 23: Mass balance in combustion chamber 50
Figure 24: Thermochemical and Performance Result from CEA 56
Figure 25: Thermochemical and Performance Result from CEA 57
Figure 26: Thermo-physical and performance data results from NASA CEA.................... 58
Figure 27: Fuel grain 59

Figure 28: Area ratio, temperature ration, pressure ratio and exhaust velocity vs Mach number 61
Figure 29: Force balance on the rocket while the fuel is burning 62
Figure 30: Flight trajectory (a) velocity vs time and (b) height vs time.............................. 64
Figure 31: The captions of first round tests.. 74
Figure 32: Caption of second round test... 75
Figure 33: Pressure and thrust vs time 76

LIST OF SYMBOLS AND NOMENCLATURE

ACRONYMS

TPS Thermal Protection System

SRM Solid Rocket Motor

KNSB Potassium Nitrate-Sorbitol

KNDX Potassium Nitrate-Dextrose

KNSU Potassium Nitrate-Sucrose

SP Sugar Propellant

APCP Ammonium Perchlorate Composite Propellants

TVC Throttle Vector Control

NASA National Aeronautics and Space Administration

GPS Global Positioning System

ESSGI Ethiopian Space Science and Geospatial Institute

CNC Computerized Numerical Control

DB Double Base propellant

O/F Oxidizer to Fuel

CFRP Carbon Fiber Reinforced Plastic

HATM Hypervelocity Anti-Tank Missile

UAV Unmanned Aerial Vehicle

CEA Chemical Equilibrium Analysis

NOMENCLATURES

mf Mass fraction

m Mass (Kg)

y Molar ratio

N Number of mole (Mole)

M Molar mass of the mixture (g/mol)

h Enthalpy (KJ/kg or KJ/mol)

u Internal energy (KJ/kg or KJ/kg)

s Entropy (KJ/kg^{o}c)

C_v Specific heat at constant volume (J/kg^{o}c)

C_p Specific heat at constant pressure (J/kg^{o}c)

k Specific heat ration

h_f Enthalpy of formation (KJ/kg)

Q Heat (J)

W Work (J)

n Mole fraction

P_o Atmospheric Pressure (atm)

R_u Universal gas constant (KJ/kmol.K)

P Pressure (Pa)

T	Temperature (K/ ^oC)
X	Exergy (J)
g	Gibbs energy (KJ/mol)
ζ	Mass fraction
I_t	Total Impulse (Ns)
F	Force (N)
t	Time (s)
I_{sp}	Specific Impulse (s)
c	Effective Exhaust Velocity (m/s)
g_0	Gravity at sea level (9.8m/s^2)
c^*	Characteristic Velocity (m/s)
R	Specific Gas Constant (KJ/Kmol.K)
C_F	Thrust Coefficient
A	Area (m^2)
A_t	Throat Area (m^2)
r	Burn rate (mm/s)
ρ	Density (Kg/m^3)
V	Volume (m^3)
a	Temperature Coefficient
n	Pressure Exponent
a	Speed of sound (m/s)
M	Mach number
T_0	Stagnation Temperature (K)
P_0	Stagnation Pressure (Pa)
v	Velocity (m/s)
L	Length (m)
D	Diameter (m)
d	Thickness (m)
ν	Poisson's Ratio
σ_θ	Hoop Sress, (N/m^2)
σ_l	Longitudinal Stress (N/m^2)
E	Young's Modulus of Elasticity

SUBSCRIPT AND SUPERSCRIPT

i	ith Component
m, mix	Mixture
$-$	A given quantity per unit mole
.	A given quantity per unit time
o	Standard state
0	Stagnation
in	Inlet
out	Outlet
p	Product
r	Reactant
gen	Generated
rev	Reversible
P	Propellant
b	Burning

t	Throat
$*$	Critical
2	Nozzle Exit
1	Nozzle Inlet (Combustion Chamber)
3	Ambient

ABSTRACT

Sounding rockets are space technologies that take probes into space to provide information about the earth's atmosphere and radiation. Sounding rocket has two main parts: rocket motor and payload. The primary technical challenges in sounding rocket technology include cost reduction and the search for new propellant. Sucrose-based propellants may be a cost-effective alternative to expensive ammonia-based propellants. This thesis analyzes sucrose-based fuels with additives and multi-oxidizers to improve propulsion efficiency and design a rocket capable of reaching 20 km with a 1 kg payload. The thesis employs the CEA NASA software to evaluate the performance of the formulated fuel. To improve the performance of the KNSU propellant fuel, three different additives are introduced and evaluated. The addition of varying amounts of magnesium powder (1% to 5% of the fuel's mass) leads to a enhancement of 5.4% in specific impulse. By incorporating aluminum powder in concentrations up to 10%, an increase in specific impulse up to 10 % was observed. Furthermore, gradually substituting potassium nitrate with ammonium nitrate results in a steady improvement in specific impulse from 110 to 174 seconds; however, relying solely on ammonium nitrate as the oxidizer has some drawback as they are hygroscopic and of low burn rate. Finally, the rocket motor needed to send the specified payload to the set apogee was designed. The rocket's design includes a de Laval nozzle, with an optimized ratio of exit area to throat area set at 5.0. The total mass of the rocket is 12.345 kg, with fuel accounting for 75.7% and payload accounting 8.1%. Python simulations show a rocket achieves a 20 km peak altitude in 55 seconds, with a 165-second flight duration. Additionally, a small-scale rocket motor test setup is prepared, equipped with sensors and a microprocessor with a potential use, in the future, to experimentally test the fuel. Initial tests on the prepared test setup confirmed the setup's functionality, while challenges arose in accurately measuring temperature during short burn times. Subsequent tests provided valuable performance data, despite limitations with thermocouples. The thesis contributes to rocket design and propulsion. The thesis contributes to rocket design and propulsion by providing insights into improved conventional fuel. The simulations validates the design.

Keywords: Sounding rocket, Specific impulse, Sucrose based solid rocket fuel, potassium nitrate oxidizer,

CHAPTER ONE

INTRODUCTION

1.1. Background of the Study

Right at this moment, NASA is receiving data from James Webb Telescope which is found 1.5 million km away from the earth. This telescope doesn't orbit the earth but the sun, just like planets, at what is called second Lagrange point (NASA, Goddard Space Flight Center, 2021). Not only for sophistications, but also for basic necessities like agriculture, natural disaster prevention and security, space is being utilized. However, the backwardness of Ethiopia in the field of space science exposed the country to many disadvantages. Limited access to internet, Global Positioning System (GPS), and high rental costs for television broadcasting satellites and weather forecasting satellite are some of the problems. Millions of dollars are expended each year to rent other Arab countries' satellite for above mentioned uses. As a result, the Ethiopian Space Science and Geospatial Institute (ESSGI) was established in 2016. The main goals of ESSTI were to train professionals in the field of aerospace science, develop and strengthen national infrastructures for space science and technology, and give the country the means to fully take advantage of the many applications of space science and technology. (Wondwosen, 2022).

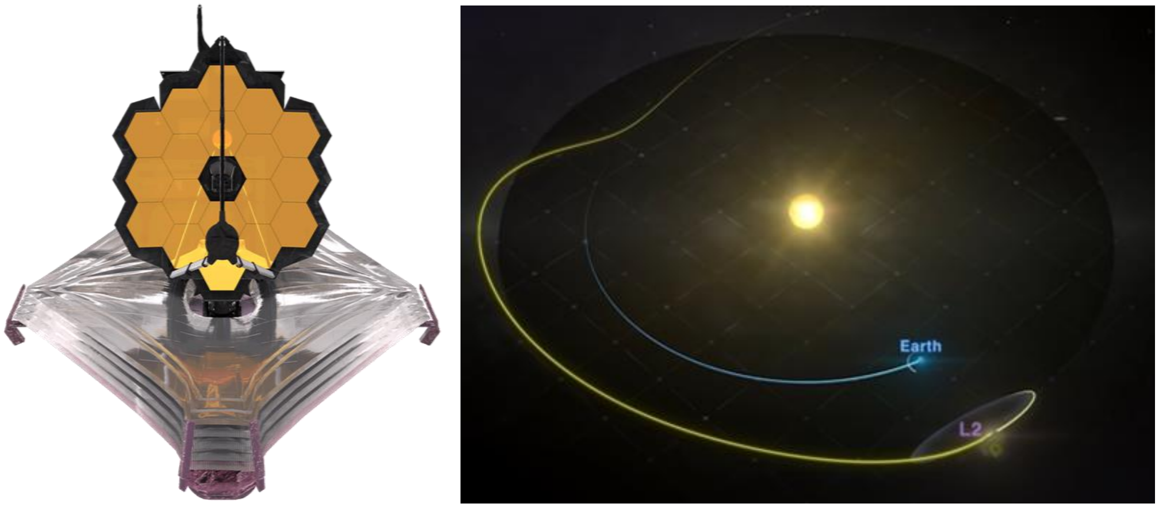

Figure 1: James Webb Telescope and its orbit (Michael et al., 2021)

Satellites are sent into orbit by rockets and rockets only. However, it is quite expensive to launch satellites or any other cargo into space. As an example, Ethiopia spent millions of dollars to launch its first satellite by Chinese government. The country could have saved significant amount of money if it was possible to produce in the country. This indicates that there is still considerable disparity between existing aerospace technology and the nation's stand, indicating that there is still more work to be done.

1.2. Introduction to Sounding Rocket

Rockets are vehicles that travel to a great distance using jet propulsion without the aid for the surrounding air as an oxidizer. It works by Newton's third law saying there is reaction for any action, and the reaction of the engine to the high-speed exhaust gases is what generates thrust. Rockets have both fuel and oxidizer on the vehicle and hence, can fly in the vacuum of space and even operate more effectively in a vacuum rather than in the earth's air (Sandra, 2017).

Rockets are the only means to get humans and cargos into space (Weinzierl, 2018). Weather it is deep space exploration to investigate the outer universe or sending satellites to lower orbit for enhancing human life on the earth, it involves using rockets and rockets alone. Rocket technology is now employed extensively in research and thus any advancement done on the science of rocket contributes to space science. Therefore, to achieve independence and wealth, it will take constant work in this fields.

Sounding rockets, as shown in figure 2, are one- or two-staged solid-propellant rockets that are used for studying the upper atmosphere and undertaking space exploration. They also function as low-cost means for testing or proving prototypes of novel components or subsystems for use in launch vehicles and satellites (Indian Space Research Organization, 2022)

Solid Rocket Motor

Solid rocket motor (SRM), as in figure 3, is the main component of the solid rocket to provide a thrust. It is composed of motor casing, nozzle, igniter, thermal protection systems, and throttle vector controller (TVC). Thrust is created when the combustion gases' high thermal energy is transformed into kinetic energy in the exhaust.

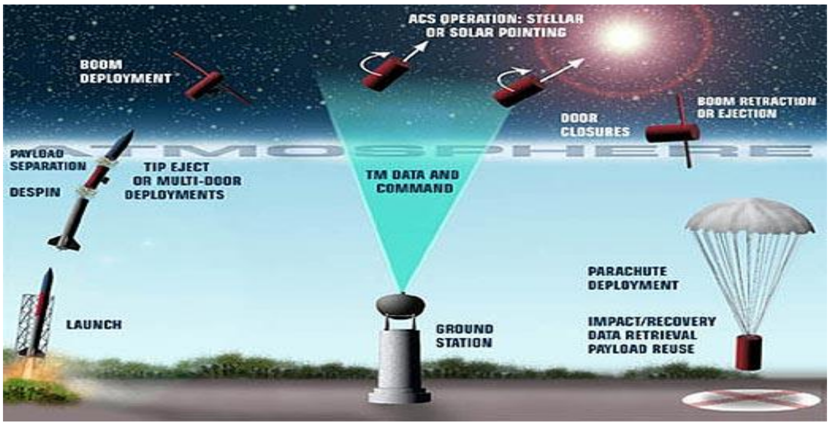

Figure 2: Sounding Rockets (Elaine, 2004)

For many rocket propulsion applications, SRMs are a desirable option because of their simplicity. Because there aren't many structural parts, the SRM is effective in its weight. (George & Oscar, 2017).

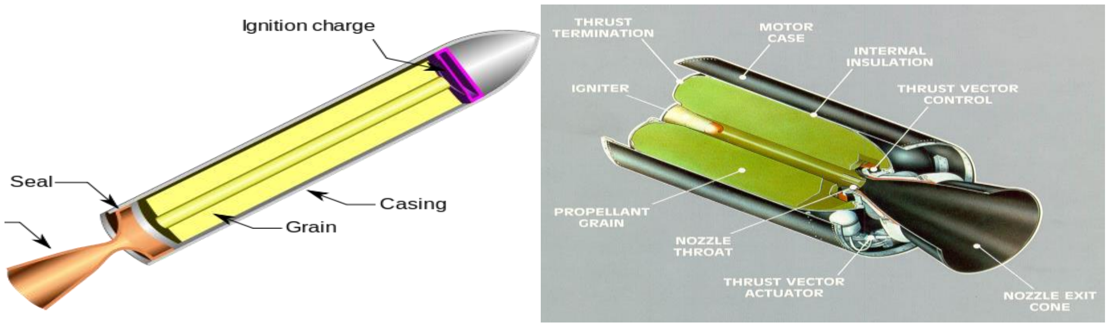

Figure 3: Solid Rocket Motor (SRM) (George et al., 2018)

Sucrose Based Solid Rocket Motor

Propellants, are the chemical fuels and can be in different physical states. Solid propellant is one from them in which both the fuel and oxidizer are in solid phase and there are different types of it, such as gun powder, Zink Sulfur (ZS), Candy, double base (DB), Composite, High Energy propellants, and others (George & Oscar, 2017). Sugar propellants (SP), sometimes known as candy rockets, are also one of them which have oxidizer and sugar-based rocket fuel for model rockets. SP are intermediate performance propellants in which the binder-fuel is one of the common sugars (sucrose, dextrose, maltose, etc.) or one of the so-called "sugar alcohols," such as sorbitol. The fuel, oxidizer, and additive are the three ingredients that make up the propellant. Sucrose is the most often utilized sugar as a fuel while Potassium nitrate is the most prevalent oxidant (KNO3). There are several different types of additives that either function as catalysts or improve the aesthetics of the takeoff or flight. Typically, the classic sugar propellant is made with an oxidizer to fuel ratio of 65:35.

The binder-fuel, however, is not a polymer and has already undergone some oxidation. These features provide the propellants two desirable characteristics. First, because the binder breaks down more quickly than a polymer does, a lower-energy oxidizer like potassium nitrate may (and is) used successfully. Second, using less oxidizer can still produce satisfactory results. Although there are isolated accounts of their utilization, sulfur, charcoal, and other auxiliary fuels are not frequently incorporated in sugar propellants. The typical specific impulse (Isp) supplied is in the range of 130 seconds and is not greatly influenced by the fuel. Black powder typically has an Isp of 80–90 seconds, but the majority of ammonium perchlorate composite propellants (APCP) have an Isp of 190–210 seconds. The rates at which sugar propellants burn are similar to those of APCP. The somewhat high melting point of this combination increased processing complexity and perhaps decreased repeatability. However, the production of propellants is more easy and, hopefully, much safer because of the more recent researches on lower-melting sugars and sugar alcohols (Singh, 2015).

Finally, this thesis is undertaken to investigate the performance of aluminized-sucrose based solid fuel rand design a sounding rocket motor that has a payload of 1kg and an apogee of 20 km. Static test setup has been made to measure the performance parameters and the rocket is designed using the optimum fuel.

1.3. Statement of the Problem

The easily available and cheap fuel for rockets is sugar based rockets. While they are cheap and easy to get, the performance of sugar based fuels are low when compared to the APCP one and needed to be improved. Also, simple and explicit rocket motor designing approach is not available.

The thesis works to improve the performance of the fuel by incorporating additives such as Mg and Al powder and replacing portion of the oxidizer by other strong oxidizer NH4NO3. CEA NASA software is utilized to evaluate the performances of the formulated fuel. Also A static test stand is prepared which, in the future, can be used to characterize the fuel. The simplified design approach is utilized to design a rocket motor for a specified requirement.

1.4. Objectives of the study

1.4.1. General Objective

The general objective of this thesis is to enhance sugar based fuel by testing different composition of a solid propellant numerically using software and design a rocket motor using the optimum fuel.

1.4.2. Specific Objective

To attain the aforementioned general objective, the following specific objectives are drawn. Specifically this thesis aimed to:

- Formulate different fuels with varying composition of additives and oxidizers and Study the combustion characteristics and performance parameters.
- Design and model a rocket motor that can move a sounding rocket and its payload to an apogee of 20 km.
- Simulate the flight dynamics
- Model and build a small static test stand facility for future experiments
- Prepare different composition of propellants (using sucrose, potassium nitrate and aluminum powder)
- Test the experimental setup's functionality.

1.5. Significance of the Study

The absence of endeavors in the country on space science, specifically rockets, have impacted the country's growth rate in today's competitive world. This research will explore solid propellant rocket that may, in the future, be used for a sounding rockets that takes scientific probes in to space for short term experiments. Hence, this thesis while also expanding the research domain it paves a way for future domestic researchers to start an effort to cope up with the ongoing technology. The work was hoped to have a significant potential to influence young engineers who were scared to pursue their passion around this area. Interested individuals will have better opportunity to further advance the work.

1.6. Scope and Limitations of the Study

The thesis focuses on enhancing the performance of sugar-based fuel for rockets by incorporating additives such as Mg and Al powder and replacing a portion of the oxidizer with NH4NO3. Moreover, the evaluation of the formulated fuel will be done using CEA

NASA software, which will allow for numerical analysis and performance assessment. Also, A static test stand will be designed and prepared and test for its functionality. Finally, the thesis will utilize a simplified design approach to design a rocket motor that meets specified requirements.

The evaluation of the formulated fuel will rely on the CEA NASA software, which may have limitations in accurately representing real-world performance. The results should be interpreted with caution. Also, the static test stand will be designed and prepared, and functionality of the setup will be assessed, but actual rocket motor performance testing is beyond the scope of this thesis. In addition, the simplified design approach used in this thesis may not account for all complexities and nuances involved in rocket motor design. It should be considered as an initial design approach rather than a comprehensive methodology.

CHAPTER TWO

2. LITERATURE REVIEW

This section discusses relevant published works on rocket sciences specifically, solid rocket motors. It presents an unpretentious summary of the information while it also has structural pattern and combines both summary and synthesis.

2.1. Significance of Space Science to Developing Countries and Space Science History of Ethiopia

There are countless earth-impacting space uses such as: weather monitoring and climate, access to education and healthcare, water management, transportation and agricultural efficiency, peacekeeping, security, humanitarian aid and other further useful developments are currently under consideration. Space technology aids in enhancing "Life on Land" by maintaining natural habitats and slowing the loss of biodiversity through monitoring ecosystems, protecting animals, and teaching people about deforestation and desertification.

For instance, (Simonetta, 2022) said that at the beginning of 2018, the European Global Navigation Satellite System Agency (EGNSSA) and the United Nations Office for Outer Space Affairs (UNOOSA) worked together to assess the impact of space technology on the Sustainable Development Goals (SDG). The analysis revealed that 65 out of 169 SDG objectives directly benefit from the use of Earth observation and satellite navigation technology. When communications satellites are taken into account, the number of targets that are directly impacted rises. In relation to this, Space-based Information for Disaster Management and Emergency Response (UN-SPIDER) is a fantastic example of how disaster reduction and emergency operations may be carried out with the use of space technology; it typically strives to save lives and reduce property damage.

(Wondwosen, 2022) stated that Space science and technology have too long been seen as the sole purview of rich nations and a luxury for underdeveloped nations. However, many developing nations are coming to understand the criticality of space technology in their hopes for the future. Its values are now widely acknowledged in a variety of fields, including smart agriculture and food security, telecommunications, catastrophe risk reduction and humanitarian crisis prevention, as well as natural resource and environmental management.

This idea was expressed in the remarks made by Ethiopia's Deputy Prime Minister and Minister of Foreign Affairs, Demeke Mekonnen, at the country's satellite launch event in 2019: "This will be the cornerstone for our historic road to wealth. Space is a technology, sovereignty, job creation, hunger relief, and everything else Ethiopia needs to achieve inclusive and sustainable development (Wondwosen, 2022). A similar realization prompted the African Union (AU) to draft a policy on the development of African space in 2017. According to the AU, developing natural resource management and economic success depends on space research and technology.

Moreover, (Ouzemou et al., 2018)) stated that in order to boost food production and consume less water, tracing crops and their locations as well as their spatial extent helps agricultural planning, better irrigation water resource management, and crop health monitoring. High spatial resolution multispectral remote sensing images are frequently used for mapping crops in broad agricultural systems at the global and regional scales.

In particular, (Goel et al., 2021) talked about how smart agriculture might benefit underdeveloped countries. Research, invention, and space technology are the three major foundations of smart agriculture. Protecting soil quality, reducing irrigation water waste, and arming farmers with agricultural information all depend on space technology. Several of these concepts are already in use in industrialized nations. With the help of terrestrial, aquatic, and aerial sensors, satellites, and surveillance technologies, a sizable quantity of geospatial data from several sources is acquired, evaluated, and used for smart farming and crop protection. By 2030, it's expected that 85% of the world's population will live in developing countries, and because agriculture is so important to growing economies, the adoption of digital farming in rural regions will be good for the agricultural business. Emerging nations urgently need data-driven technical progress in this respect to increase GDP and ensure that the populace has access to food.

However, Ethiopia seldom makes use of all the advantages of space. The Addis Abeba Geophysical Observatory was established in 1957, the same year that the nation launched its first 4-inch optical telescope. The science department of Addis Ababa University (AAU), originally the University College of Addis Ababa, was in charge of supervising this institution. A.A. Geophysical Observatory was established in response to the call for a geomagnetic observatory made during the Rome meeting on the Global Geophysical Year in 1957 (Wondwosen, 2022). In addition to providing data to enable worldwide research, the AAU telescope has been used to examine a range of astronomical objects and events, including as the solar eclipses in 1959 and 1961 and Halley's Comet in 1986. This telescope is situated in what is now known as Eritrea, and at the same time, Bishoftu, Ethiopia, set up its first satellite laser range tracking station.

Recently, the Ethiopian Space Science Society (ESSS) was founded in 2004 with 47 founding members and until that, it appears that not much has been accomplished in the subject since that time. Tefera Walwa, a former deputy prime minister and fervent supporter of space science, was one among the individuals who worked tirelessly to establish the organization. Many first mocked the effort and referred to the group as "a mad man's club" but now, over 10,000 people belong to the ESSS, which includes 19 branches and 100 space clubs. In its varied activities, it collaborates with universities, research facilities, governmental organizations, and trade associations for realization of its objectives (Wondwosen, 2022).

2.2. Classification of Rocket Propulsion Systems

A rocket's propulsion systems can be divided into different categories according to their function (booster stage, sustainer or upper stages, attitude control, orbit station keeping, etc.), the vehicle they are used to launch (aircraft, missile, assisted takeoff, space vehicle, etc.), size, propellant type, construction, and the quantity of rocket propulsion units used (George & Oscar, 2017). But the most common base for classification is its energy source. On this basis, the three major groups are:

1. Chemical Propulsion,
2. Electric Propulsion, and
3. Nuclear Propulsion

In the case of chemical propulsion, combustion of chemicals release fluid, commonly gas, and thermal energy and the hot working fluid creates high pressure in the combustion chamber. Then, the pressurized gases pass through a nozzle to change their high pressure in to kinetic energy and hence to produce thrust.

Electric propulsion is another kind of spacecraft thruster that speeds a mass fast using electrostatic or electromagnetic fields to generate thrust. It works by positively charging xenon or krypton-based gas propellants and forcing the ions out through a thruster to accelerate the spaceship forward and because they operate at a higher specific impulse than chemical rockets and have a faster exhaust speed, electric thrusters often require a lot less fuel. Power electronics are used to regulate the thrusters and hence electric propulsion delivers thrust for a longer period of time than its counterpart, chemical rockets. However, the thrust is much weaker due to the limited electric power available in the space.

Thirdly, nuclear propulsion technologies come in two forms: nuclear electric and nuclear thermal. Nuclear electric propulsion technology produce a small amount of thrust but utilize propellants far more effectively than chemical rockets because they create electricity in a reactor and then utilize electric propulsion. Nuclear electric propulsion systems has a potential propel the future Mars missions using small amount of fuel used because of their ability to deliver thrust for a long periods of time to accelerate the spacecraft to so high speed. On the other hand, nuclear thermal propulsion system delivers high thrust and twice the propellant efficiency of chemical rockets. A liquid propellant receives heat from the reactor to work. This heat changes the liquid into high pressure gas and the gas expands through a nozzle to create thrust and propel the spaceship (Clare, 2021).

2.3. Chemical Rocket Propulsion

Chemical Rockets are further classified in to three classes depending on their fuel-oxidizer state. Those are Liquid propellant rockets, solid- liquid hybrid propellant rockets and solid propellant rockets. Each of these engines has application that it is best suited for. Therefore, Engineers take into account factors other than engine efficiency when selecting an engine type; these factors include dry weight, reusability, and complexity, throttability, and etc.

2.3.1. Liquid Propellant Rocket

The rocket engine employing liquid propellant is one common kind of propulsion. American scientist Robert H. Goddard produced the first practical construct of the device in 1921, despite the fact that the idea was first conceived more than a century before (George & Oscar, 2017). In a liquid propellant rocket propulsion system, the fuel and the oxidizer are both liquids, hence tanks are employed to store and deliver the propellants. The liquid propellants are then fed under pressure from the tanks into the thrust chamber. A liquid fuel (such as kerosene) and a liquid oxidizer (such as liquid oxygen) make up the propellant's usual composition. On the other hand, a mono propellant is a single liquid that, when properly catalyzed, changes into hot gases.

The majority of low-thrust, low-energy propulsion systems, including those used to control the height of flying objects utilize gas pressure feed systems (George & Oscar, 2017).

However, one or more liquids fed by a turbo pump are used in the larger bipropellant rocket engines. This rocket engine is made up of one or more thrust chambers, a feed mechanism for moving liquid propellants under pressure from tanks, a power source to provide the feed mechanism with energy, appropriate plumbing or piping to transmit the thrust force, and control devices (including valves) to start and stop the propellant flow as well as occasionally to vary the flow.

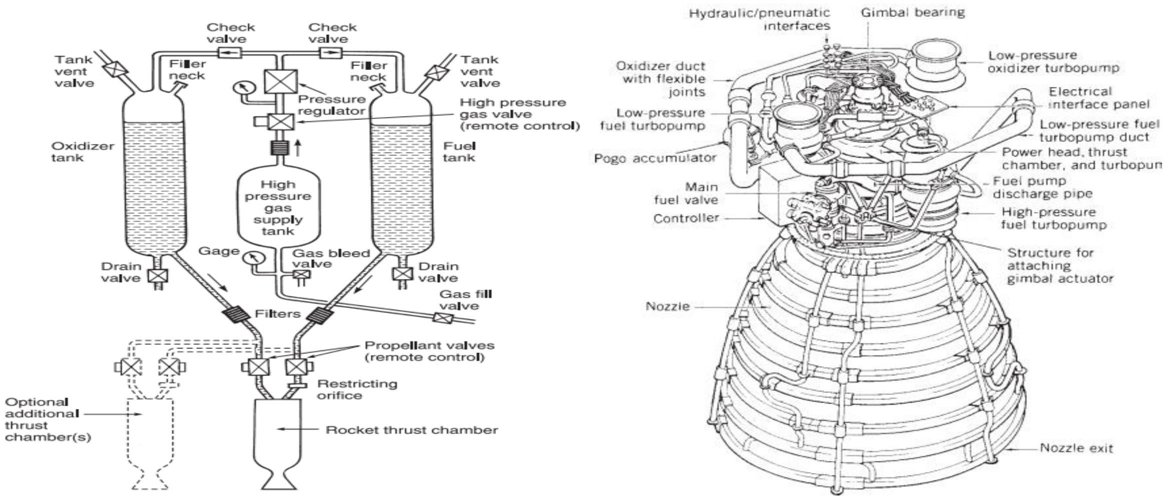

Figure 4: 2 and 3D view of the liquid rocket engine (George & Oscar, 2017)

In certain applications, a thrust vector control system, a random variable thrust feature, an engine condition monitoring or engine health monitoring subsystem, and other instrumentation/measuring devices may also be incorporated into a rocket engine.

2.3.2. Hybrid Propellant Rockets Motors

Hybrid propulsion systems or hybrid rocket engines are bipropellant engine designs in which one component propellant is stored in the liquid phase and the other as a solid (George & Oscar, 2017). Currently, there are three different hybrid propulsion system designs. For the first, the oxidizer is held as a liquid while the fuel is in the solid phase, and this arrangement is by far the most popular and has undergone extensive experimental investigation. In the opposite or reverse design\, the fuel is in liquid state and the oxidizer is solid; practically little research has been done on this configuration. A third variant, known as the mixed hybrid configuration, burns extra liquid oxidizer that is either fed in an afterburner chamber or simultaneously at the head and end of the grain cavity after the solid fuel-rich combination has been burned (Frederick et al., 2007). The final layout is the result of efforts to improve fuel regression rates, which would boost thrust and chamber pressure. With metallized fuel added to the grain in the traditional setup, increased regression rates could be attained.

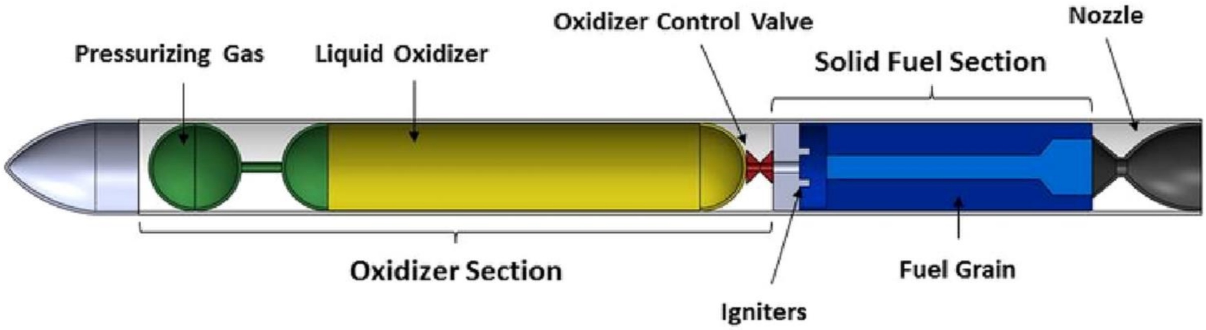

Figure 5: Hybrid Rocket Engine (Zolla et al., 2021)

According to Armold et al., (2013), hybrid rocket motors include some of the best aspects of both liquid and solid rockets. Because the oxidizer does not come into contact with the fuel until the oxidizer is injected and ignition is begun, they are fundamentally safer than solid propellant motors. Since the solid-fuel grain may be made of a variety of inert polymers or paraffin wax, it can be disseminated using conventional methods without the need for additional expensive and prohibitive safety measures. In contrast to solid propellant rocket motors, hybrid rocket systems may be throttled, and the optimal oxidizer/fuel ratios produce greater Specific Impulse. Hybrid motors have half the piping of liquid systems but could have a greater specific impulse.

Hybrid rocket motors have a number of disadvantages in addition to all of these benefits, the most important of which is the relatively low regression rate of polymeric solid fuels (Armold et al., 2013). This is due to the insufficient heat transfer rates between the diffusion flame, which is about 1 mm above the fuel surface, and the exposed solid-fuel grain surfaces. Several tactics have recently been developed to address this problem and enhance the hybrid rocket's potential for usage in space propulsion. Examples include altering the composition of the fuel and the flow field of the oxidizer (whether by the layout of oxidizer injectors, mechanical modifiers like discs and turbulators or the shape of the solid fuel grains, etc.).

2.4. Solid propellant rocket motors

In solid rocket engines, the materials that are to be burned are already kept in a combustion chamber or casing in solid state. The term "grain" refers to the solid propellant that contains all of the necessary chemical components for combustion. Once lit, it is intended to burn uniformly and steadily at a set rate over all of the visible internal solid substrate. With each burn and use of propellant, the internal pressure rises. In order to provide thrust, the heated gases flow into the supersonic nozzle (George & Oscar, 2017).

2.4.1. Casing

The solid rocket motor case is a thin-walled pressure vessel that holds solid propellant and its insulation. The fundamental purposes of the solid rocket motor case have not changed since the start of solid rocket motor development. The quantity of payload carried, internal propellant pressures, inertia, and aerodynamic loads on the casing skin all influence the material choice. The weight to area ratio initially appeared to be a suitable criterion to compare various designs for diverse purposes when all other design variables were identical. By making the material thinner, an object's area can be increased; but at a certain point, the greatest area that can be achieved depends on the material's strength. As a result, the strength-to-weight ratio of the material utilized is used to compare other potential materials. Finding lighter materials is necessary if the weight is to become the solid rocket motor's minimal components.

2.4.2. Case Material Development

The first generation of solid rocket motor cases were made of steel, aluminum, titanium and recently from fiber glass composites. A significant amount of investigation was done on steel alloy, aluminum alloy, and titanium alloy in order to find ways to lighten the casings. In the early 1960s, the second stage of the Minuteman ICBM missile case was made of titanium alloys, which had a wider variety of uses for both low and high temperatures (Bachrach, 1987).

In order to make the motor casing lighter, three separate materials were investigated in 1960: sandwich panels, maraging steels (alloys of nickel, cobalt, molybdenum, and titanium), and composites. Over time, fiberglass composite materials became more significant in the solid rocket business. The fiberglass composite is constructed from matted fiberglass filaments, as seen in figure 6, and any open spaces are filled with plastic resin. Designers must choose the orientation layup for the motor casing depending on the internal and exterior stresses applied since a composite's strength in any direction is the sum of the components of strength of all the affected fibers.

There have been several substantial improvements made in glass, and these improvements will greatly improve filament-wound motor casings. S-994 glass, which includes 10% MgO and is 30% stronger than E-glass and titanium alloys, has a strength-to-weight ratio that is twice that of steel and titanium alloys. While gigantic rocket boosters were being investigated and constructed, a new material known as whiskers, or discontinuous fibers, was also being produced. Aligned whiskers can stiffen the matrix to a degree equivalent to continuous filaments, but they can't match continuous filament composites' strength. Regardless of aspect ratios, the longitudinal strength of whisker composites was never going to be higher than 55% of the strength of equivalent filamentary composites. Therefore, continuous filament- wound composites represented the cutting edge in the 1970s and 1980s. Using filament-wound S-994 glass or E-glass composites, the Polaris' first and second stage rocket engines were created (Bachrach, 1987).

Since the early 1990s, attention has been focused on the integration of metallic attachment rings with insensitive munitions (IM) (Fossumstuen et al., 2005). Pre-preg towing has proven to be a crucial feature for high capacity composite boxes with integrated attachment rings that are wrapped in filament. TCR-pre-preg technology with M30S fiber was chosen for the Hyper Velocity Anti-Tank Missile (HATM).

Figure 6: Filament wound composites for rocket motor cases (Mateduc Composites, n.d.)

The HATM's rocket engine case had to be made of carbon fiber reinforced plastic (CFRP) with titanium connecting rings because of the high propellant to inert mass ratio. A thin layer of aramide fiber reinforced epoxy is used to protect the CFRP structure from the hot combustion gases and to withstand external aero-thermal loads. During the case's construction, titanium bosses are incorporated forward and backward (filament winding process). The vehicle assembly can be mounted on the titanium polar boss in the front, and the submerged nozzle can be mounted on the titanium attachment ring in the back. The motor case was successfully employed in static motor flings and flight tests after being verified in a number of tests that included hydro burst testing, bending tests, and environmental tests.

2.4.3. Nozzle

A nozzle is an attachment to the casing that transforms the chaotic motion of the gas produced inside the motor case into ordered velocity. The design of the rocket nozzle must be able to resist the high temperature created by the expelled propellant since it is exposed to greater heat than other parts of the rocket. Today's combustion gases temperatures are higher than 6000°F, compared to a range of 1000° to 2000°F some decades ago. Therefore, unlike the solid rocket motor case design, the nozzle material's fundamental capacity to tolerate significant temperature swings is more crucial than its basic strength. (Bachrach, 1987). The primary factor affecting a rocket engine's thrust is the momentum that the combustion gases give when they are released through an exhaust nozzle. The speed of the exhaust gases continuously rises as they pass through the nozzle, going from low subsonic speeds to high supersonic speeds at the nozzle exit. For the purpose of comprehending the flow mechanism, the nozzle may be divided into three sections: the converging subsonic portion, the throat section, and the divergent supersonic area.

The size of the throat section and the conditions in which the combustion chamber is functioning affect the mass flow rate through a rocket nozzle. Design modifications to the convergent portion of the nozzle's convergent section would have an impact on the mass flow of exhaust gases and, to a lesser degree, the combustion efficiency. Expansion in the divergent supersonic region of the nozzle can further boost the sonic velocity of the exhaust gases (Rao, 1961)**.**

2.4.4. Nozzle Material Development

An effective nozzle design can result in significant weight savings because, at first, the weight of the rocket nozzle can account for a sizeable portion of the entire mass of the solid rocket engine, including the propellant. This is why, for certain early test vehicles, the nozzle's weight was especially problematic; for example, the X-17 rocket test vehicle from Lockheed, which was developed in 1959, had a nozzle mass to overall mass ratio of about 0.04 (Bachrach, 1987).

Graphite and copper were the first materials employed as inserts in the rocket nozzle; these materials served as heat sinks for the blazing fuel. Lighter weight nozzles were created by changing the insulating material and nozzle wall thicknesses (Bachrach, 1987). Refractory metals, graphite, cermets, and ceramics were also the primary materials used for the nozzle design because they are lighter and can tolerate higher temperatures. The refractory metals mentioned were tungsten, molybdenum, or tantalum; their densities were 19.4, 10.2, and 16.6 g/cm^3 respectively. These metals' melting points range from 2024.4°C to 3410°C; they are so high that the sounding rocket's blazing propellant temperature range would be low for them (Bachrach, 1987).

Unfortunately, due to their weight, tungsten and tantalum could not be considered for many applications; molybdenum appeared to have the best chance of success. Unluckily, none of these three metals are heat-resistant against oxidation. Their oxides are fairly flammable and burn rapidly at temperatures above 704.44°C. Ceramics are a different class of refractory materials that can withstand extremely high temperatures without dimensional change or property alteration. They would not work for rocket nozzle inserts because they are too fragile and sensitive to heat shock. Now two groups of materials arose as the result: ceramic refractory materials, which are strong at high temperatures but brittle and sensitive to heat shock, and refractory metals, which are ductile and impact-resistant but lose strength at the needed high temperatures. It was reasonable to think of combining these two materials to create a new substance known as "cermet"; two such cermets were produced: titanium carbide and molybdenum boride. The cermet materials made an effort to resist the flaws of each class while capturing their strengths (Bachrach, 1987).

Unfortunately, most of the materials listed above were not used as rocket nozzle inserts; instead, current rocket nozzles are composed of 3D carbon-carbon composite. A material belonging to the graphite family is called 3D Carbon-Carbon Composite. In spite of oxidizing very slowly and having a relatively low strength at room temperature, graphite is noteworthy in that it maintains its strength at temperatures as high as 2426.7°C. However, graphite had a downside that outweighed its advantages of stability and strength at high temperatures: it was constantly brittle (Kattus, 1957).

Nowadays, composite materials make up practically all of the solid rocket motor's components. For instance, carbon fiber composites are 25% lighter than steel counterparts while maintaining the same stiffness and strength. Epoxies and phenolics with graphite and fiber reinforcement are now the most often used materials to create nozzles for SRM applications. These materials are desired due to their low rates of erosion, cheap production costs, and/or lighter weights (McClain et al., 2019). The bulk of the standard nozzle materials are summarized in Table 1.

For instance, Above cited (Fossumstuen et al., 2005) discussed the design of a nozzle that includes a molded silica phenolic immersed converging-diverging nozzle. The titanium structural shell housing, which is threadedly attached to the rear attachment ring of the rocket engine CFRP casing, has the exit cone and nozzle pre-molded onto it.

Table 1: Typical Motor Nozzle Materials and Their Functions (George & Oscar, 2017)

Function	Material	Remarks
Structure and container	-Aluminum -Low-carbon steel: high-strength steels special alloys	-Limited to 515 ^{o}C, -Good between 625 and 1200 ^{o}C
Heat sinks and heat-resistant materials at the intake and throat sections; a hot environment with fast-moving gas that is eroding	-Carbon-carbon -Carbon or Kevlar fiber with phenolic or plastic resin -Molded graphite -Tungsten, molybdenum	- Interwoven filaments with three or four directions, strong, pricey, and a maximum temperature of 3300oC -Used with large throats - Low cost; only for low chamber pressure and temperature - Rarely used, heavy, costly, susceptible to cracking, and erosion-resistant
Insulator; shielded from flowing gas by a heat sink or flame barrier.	Ablative polymers, silica or Kevlar fillers, and phenolic resins	Want low conductivity, good adhesion, ruggedness, erosion resistance; can be filament wound or impregnated cloth layup with subsequent machining

A pyro-mesh igniter and weather seal were also included in the complete nozzle assembly. The nozzle is made of high-pressure molded phenolic with silica fiber reinforcement and a titanium shell construction. The submerged solution has a throat diameter of 53.3 mm, an exit diameter of 139.2 mm, and a length of 128 mm, which includes the intake and throat area. It was created to be a lightweight solution. The nozzle is fastened to the motor case's rear attachment ring using threaded hardware. Titanium serves as the foundation for the nozzle's metallic construction. The total weight of the nozzle assembly is around 980 grams.

2.4.5. Thermal protection system

Most of the time, a layer of heat-barrier material is positioned between the propellant and the inside surface of the casing of a solid rocket motor to act as internal insulation (Mohan et al., 2017). Internal insulation's main purpose is to keep the rocket engine casing from getting hot enough to risk its structural integrity. Typically, solid propellant grains are housed inside an exterior casing or shell that is part of solid rocket motors. The casing is often made of a robust, long-lasting material like steel or filament wrapped composite but it will burn away when exposed to the hostile combustion for long time.

In the course of ablation, a number of unique processes happen. The temperature of the ablation material rises as a result of the hot gas passing over the surface and transferring some of its heat to it. In addition to charring and absorbing part of the heat as the temperature rises, organic materials also break down and release gasses that are blown along the surface to create a thin insulating layer. Erosion and decomposition removes the char layer, with erosion being a function of the rate of mass flow over the surface and breakdown being a function of heat and oxidation. Thus, when the char is removed, the heat sinks deeper, producing additional char, and so on until the ablation material has been entirely removed. Additionally, when propellants are burned, gases are often include particles. These entrained particles have the potential to damage the rocket motor insulation in a turbulent environment. Therefore, motor case and other vehicle systems must be protected from the heat of propellant combustion through this mechanism which otherwise will damage the casing and other systems.

According to (Mohan et al., 2017), the rocket engine's case is prone to melting or degrading if the insulating layer and liner are punctured while it is operating, which might cause the rocket motor to total destruction. Therefore, it is essential that insulating compositions endure the severe circumstances encountered during the combustion and safeguard the casing from the blazing propellant. Hence, strong thermal protection system is applied to the exposed surfaces of the motor to stop heat transfer that causes the casing and other vehicle components to overheat. Since regenerative liquid cooling is not an option for solid rockets motors, ablative liners are the preferred thermal protection strategy for solid rockets. Non-ablative insulators or refractory structures are also possible remedy but they typically weight and cost more than ablative solutions. Given that it adds to the vehicle's inert mass and takes up space that could be used to store fuel, the thermal shielding should be as thin as is practical.

The insulation is often made of a material that can survive the high-temperature gases created when the propellant grains burn, and it is usually bonded to the inside surface of the casing. Extreme conditions are created within the rocket motor's housing during the combustion of solid rocket fuel. For instance, the rocket motor case's interior temperatures routinely reach 2760 ^{0}C and its internal pressures can approach 10.35 MPa (Mohan et al., 2017).

TPS is employed in almost all rockets. For instance, (Matthew, 2017) modeled, developed and tested slow burning rocket propulsion system. The thermal protection for his UAV consisted of two layers between the combustion gases and the motor case: an ablative liner and fibrous insulation. Silicone polymer ablative composites was the material of choice for ablative liner because of their low thermal conductivity and low ablation rates in oxidizing environments. The second layer, between the ablative and the case, is a thermal insulating layer made of a low-density fiberglass cloth. Because of its fibrous composition, the insulating layer has poor paths for heat conduction. If ablative material alone were used in a thin layer, an unacceptable amount of heat would leak through the ablative via conduction into the case. The fibrous insulating layer behind the ablative reduces this thermal leakage, allowing for a thinner, more performant thermal protection system.

To optimize the TPS of the for the slow burning rocket propulsion system, (Jonathan, 2018)) studied its thermal protection in depth. The thermal protection challenge is more challenging for small, slow-burning solid rockets than for ordinary small solid rockets due to the end-burning grain arrangement and extended burn period. Small, slow-burning rockets require the design of specialized thermal protection systems. The case's interior is more exposed to combustion gases as a result of the end-burning grain. The leftover propellant is located between the flame front and the motor casing in an internal burning grain. Only a tiny portion of the case, at the throat (and sometimes the front), is exposed to combustion gases since the propellant insulates the remainder of the case. In contrast, the propellant in an end-burning grain burns away, exposing a sizable internal surface. A silicone-based thermally ablative liner ringed by an additional layer of fiber insulation was recommended as the best thermal protection material for a slow-burning SRM in order to maintain the temperature-sensitive parts of the car within a safe operating range. Following the selection of the proper materials, the problem of increasing their thickness was resolved using a combination of computational and experimental methods.

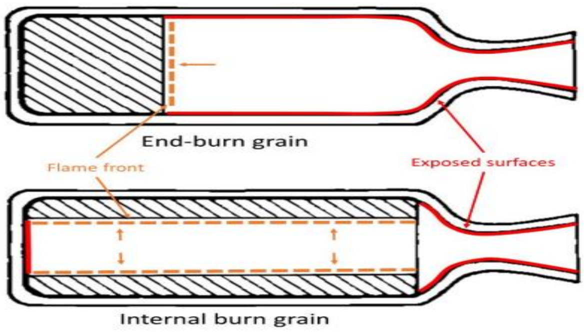

Figure 7: End and internal burn grain (Jonathan, 2018)

Also in (Mosa et al., 2022) conducted a detailed analysis of the four types of elastomeric heat shielding materials (EHSMs), comprising silicon rubber, polyurethane (PU), ethylene propylene diene monomer (EPDM), and nitrile rubber (NBR). The author also considered several filler types to enhance the thermal, mechanical, and ablative capabilities of the EHSMs. The virgin polymer layer is shielded from direct flame by the charring phenomenon. We also considered the possibility of a synergistic interaction between fillers and polymer matrices. Every technique, tool, and approach used to characterize the manufacture of EHSMs is described in great depth. Different approaches to describing the EHSMs are discussed in regard to this. Additionally, the empirical models that link filler concentration and thermal insulation performance are provided.

The effects of the orientation of the reinforced fibers and the presence of aluminum on the ablation and erosion performance of the Ethylene Propylene Diene Monomer type insulation were also examined by (Sapozhnikov et al., 2022). A subscale solid rocket motor used hydroxyl-terminated polybutadiene and ammonium perchlorate as propellant. Seven static firing tests, six with low Al content and one with high Al level. In the EPDM articles, Kevlar fibers were arranged in four different patterns: random, circumferential, longitudinal, and diagonal (45°). Numerical simulations were used to decipher the experiment's results. The numerical results indicate a tendency to exaggerate the issue, but they also show that the insulation's post-fire charring is not particularly significant. According to the test results, the longitudinal fiber arrangement has the lowest ablative resistance.

(Ji et al., 2022) also examined the impact of differences in carbon fiber length on ablation. Commonly, silicone rubber-based ablative composites that have been fortified with carbon fibers (CFs) are used to protect the casing of solid rocket motors (SRMs). However, the influence of the length of the CFs on the microstructure and ablation properties of silicone rubber-based ablative composites has been ignored. In this work, different CF lengths were added to silicone rubber-based ablative composites, and as a result, ceramic layers with various morphologies were produced after ablation. This allowed us to examine the effect of fiber length. The formation of a complete and continuous skeleton in ceramic layers by CFs longer than 3 mm was shown to be possible. The oxyacetylene ablation results also showed that the maximum back-face temperature reduced from 117.7 to 107.9 C and the linear ablation rate decreased from 0.233 to 0.089 mm/s as the length of the CFs increased from 0.5 to 3 mm. This is due to the fact that later skeletons concatenated and cemented the fillers and ceramic leftovers to produce a cohesive, long-lasting ceramic layer.

2.5. Sugar-based Solid Fuels

Solid-fuel rockets are widely utilized in military applications like missiles because they may be stored for extended periods of time and launched successfully when necessary. Solid propellants perform worse (relative to liquids) in today's medium- to large-sized launch vehicles, which are regularly used to orbit commercial satellites and launch enormous space projects, and are not recommended for use as the primary propulsion. However, when higher-than-average velocities are necessary, solids are typically utilized as strap-on boosters or add-on upper stages with spin stabilization to maximize cargo capacity. Solid rockets are used as lightweight launch vehicles for payloads entering low Earth orbit (LEO) under 2 tons or for escape payloads weighing up to 1100 pounds. Only solid rocket engines based on sucrose are the focus of this section (Singh, 2015).

For instance, (Singh, 2015) Performed research on sugar based fuel. The project's main goal was to use model rocketry to comprehend the mechanics of rockets. The project included building model rockets, testing them for thrust, and then launching them. This made it possible to clearly grasp how a rocket is designed, built, and launched. The project's secondary goal was to alter the propellant and engine architecture in order to improve the performance of the rocket. After conducting the necessary study, the team decided on three potential propellants for development. Every propellant had a straightforward formula of an oxidizer, fuel, and catalyst. Potassium nitrate was selected as the oxidizer and Iron III oxide as the catalyst for all three propellants. Due of its reasonable performance and accessibility, potassium nitrate was chosen.

The three propellants used were potassium nitrate and sucrose (KNSU), potassium nitrate and dextrose (KNDX), and potassium nitrate and sorbitol (KNSB). The oxidizer to fuel ratio for all three fuels was 65 to 35. The propellant was "oxidizer rich" to ensure that all of the fuel was burnt during combustion. The fuel used by the example motors in this proposal was sorbitol. This fuel has an excellent working time and a little longer burn time when melted than sugar motors. At a relatively modest temperature of 250oF, it also melts. Theoretical combustion equation for the 65/35 oxidizer fuel ratio KNSU propellant is as follows:

$$\mathbf{48\ KNO_3 + 5\ C_{12}H_{22}O11 \longrightarrow 24\ K_2CO_3 + 24\ N_2 + 55\ H_2O + 36\ CO_2} \qquad (2.1)$$

Additionally, Felix et al., (2021) worked on the design, analysis, and testing of a solid-propellant rocket motor that could lift a model rocket to an apogee of 50 meters. Since the engine and propulsion system had to be fitted into an airframe with a minimal payload, they had to provide enough thrust to lift the aircraft to the target height while still being tiny and light. All of this had to be accomplished while adhering to the restriction of utilizing only locally produced materials. Software called OpenMotor was used to simulate the motor's performance. The flow inside the motor chamber and nozzle was examined using ANSYS Fluent. This article presents data from static testing for the various engine designs and tested fuels. Sucrose and Dextrose, two different sugar kinds, were employed as fuel in the rocket motor. Potassium nitrate was utilized as the oxidizer. The various fuels employed are contrasted in the study, along with the preparation techniques. The chosen engine was able to launch the rocket to an apogee of 34 meters with a maximum thrust of 48 Newton and an average thrust of 35 Newton.

Additionally, Moody et al., (2020) built and made solid potassium-nitrate/sorbitol (KNSB) rocket motors, then measured their performance for use in an undergraduate lab. Since commercially available solid rocket motors have excellent performance and dependability, but they are pricey, pose doubts about safety, and are challenging to use in the classroom. Therefore, it was imperative to develop a production technique for a low-cost, high-reliability propellant that is secure enough to be used in a laboratory exercise for undergraduate aerospace propulsion. A tubular core was used to cast the KNSB rocket grains, which would then be launched on a specially made static thrust platform. To measure chamber pressure and thrust for use in the undergraduate laboratory, the thrust stand is equipped with instrumentation. They designed and tested procedures for tabulating data for use in the lab, including total impulse, specific impulse, characteristic velocity, and others. This laboratory practice compared theoretical and analytical data from theoretical and modeled values derived from chemical analysis and simulation tools. The use of KNSB solid rocket motors enabled the production of low-cost propellants using straightforward manufacturing processes, increasing access to educational possibilities. The students and graduate teaching assistants applied a technique that has been improved for mixing, casting, testing, and analysis. The students got the ability to analyze rocket motor burn profiles and evaluate them against theoretical predictions on a quantitative and qualitative level.

(Adeniyi et al., 2021) also investigated how the use of dual fuel may improve the ballistic performance of a low energy sugar-based solid rocket propellant. The threshold ratio of sucrose to sorbitol that provided the highest ballistic efficiency could be found using a beam load cell (type single-point 2,000 kg linearly described by 0-20 kN force, with.005 percent precision). Seven different propellant formulations were developed, loaded, and shot into the rocket engine, and their performance was evaluated thereafter. The primary performance factors that mattered were thrust, total impulse, burn time, delivered specific impulse, delivered characteristic velocity, and chamber pressure. The tested formulations included (65% KNO3 and 35% sucrose); (65% KNO3 and 35% sorbitol); (65% KNO3, 32% sucrose, and 3% carbon); (65% KNO3, 25% sucrose, and 10% sorbitol); (65% KNO3, 24% sucrose, 10% sorbitol, and 1% carbon); and finally a propellant made from KNO3, sucrose, sorbitol, carbon and iron II oxide combinations in 65, 30, 3, 1, 1% proportion respectively. The developed dual-fuel propellant formulation (MODKNERK) has effectively achieved an appropriate ratio as a trade-off for the advantages and disadvantages of both sucrose and sorbitol as fuels in solid rocket propellant. Additionally, it has been proven that propellant additives improve ballistic indices. The MODKNERK was founded in order to create a motor that is both the most effective and delivers all of its ballistic energy. A lower energy rocket motor's ballistic and rocket motor efficiency were also found to be improved by commencing the ignition of such a motor using fast-burning rocket dual-fuel propellant.

2.6. Small Scale Model Rockets

Matthew, (2017) Worked on development of slow-burning rocket propulsion for UAVs. The capabilities of aviation systems are being increased by small unmanned aerial vehicles (UAVs). However, there is a gap in the size and performance of aircraft: no aircraft lighter than 10 kilos can fly at a speed greater than 100 meters per second. Current UAV propulsion technologies fall short of the criteria for a high-power, compact propulsion system needed for a small, swift aircraft. A slow-burning solid rocket motor has been created to fill this purpose. Such motors need solid propellants that burn slowly and have adjustable burn rates. This thesis presents experimental findings and combustion theory for a solid propellant that burns slowly. It also covers a rocket motor made to utilize this propellant as well as the production method for it.

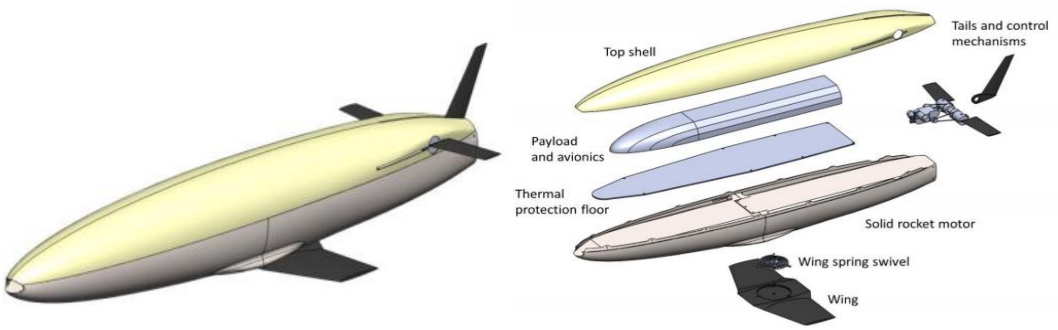

Table 2: Slow burning transonic UAV (Matthew, 2017)

For the low-thrust, long-endurance requirements of UAV propulsion, this propellant burns slowly enough. Oxamide, a burn rate suppressor, can be used to predictably modify its burn rate. Additionally, this thesis offers an idea for a compact, quick airplane built on a cutting-edge propulsion system. A small thermal protection device isolates other vehicle systems *from* the heat of combustion while the motor integrates smoothly into the aircraft's structure. These findings show that slow-burning rocket propulsion systems are practical and can be used to tiny aircraft. Small UAVs launched by rockets ought to be able to maintain powered, transonic flight for several minutes. With this innovation, kilogram-scale UAVs could be able to rapidly deploy over distances of tens of kilometers and conduct combined operations with human fighter planes.

The technological challenges associated with small, low-thrust solid rocket motors were also examined by (Vernacchia et al., 2022), including slow-burning solid propellants, motors with low chamber pressure due to their low thrust for size, thermal shielding for the motor casing, and tiny nozzles with lengthy burn periods. Ammonium perchlorate and a burn rate suppressor with a range of 0 to 20 percent were used to create slow-burning propellants with burn rates of 1-4 mm s1 at 1 MPa. These propellants allowed a low-thrust engine to run effectively with a thrust to burn area ratio ten times lower than that of conventional solid rocket motors. This engine can provide 5–10 N of thrust for 1–3 minutes on a kilogram scale. These firings evaluated a novel ceramic-insulated nozzle and tested an ablative thermal protection liner. In this study, the viability of such motors is shown, and a fundamental design for compact, low-thrust solid motors integration into small unmanned aerial vehicles (UAVs) is given.

Additionally, (Nowakowski et al., 2017) developed a solid rocket engine with a 6000 Newton thrust rating for suborbital application. The major goal of the experiment was to show that it was feasible to launch a small payload (5 kg) to a height of 100 kilometers. In addition, the project's goal was to create a test-bed platform for microgravity research that would be inexpensive, simple to use, and wholly made in Poland. The configuration for the internal ballistics design is described, along with the computations' outcomes. The Polish Small Sounding Rocket Program's H1 experimental in-flight test platform is displayed with the first use of the motor as its primary propulsion system. Both on-ground and in-flight tests were discussed, and comparisons of performance between theory and experiment are demonstrated. It was discovered that a unique composite-case manufacturing technique could produce substantial propellant mass fractions while generating considerable financial savings. The method for modifying the design for use as the booster stage of the ILR-33 sounding rocket was the main topic of the study.

Figure 8: Full-scale mockup of the ILR-33 "Amber" sounding rocket.(Nowakowski et al., 2017)

Additionally, Jan (2022) developed a solid-propellant rocket engine that can lift the Phobos model rocket up to a height of 3 km for the European EuRoC (European Rocketry Challenge) competition. The thesis also tried to develop an engine that student organizations like the UPCSP (UPC Space Program) would find easier to use and more affordable than the commercial engines now in use. A 2D axisymmetric piece of the structure has been subjected to a thermomechanical study to determine how temperature affects the structural integrity of elements. On the one hand, the performance of the motor, the thrust, and the chamber pressure curves have been evaluated using a Matlab internal ballistics technique. The combustion process was described using the ProPEP 3 program (Propellant Performance Evaluation Program), and the rocket's top height was calculated using the OpenRocket software. Additionally, a price range for the motor's estimated production costs has been provided.

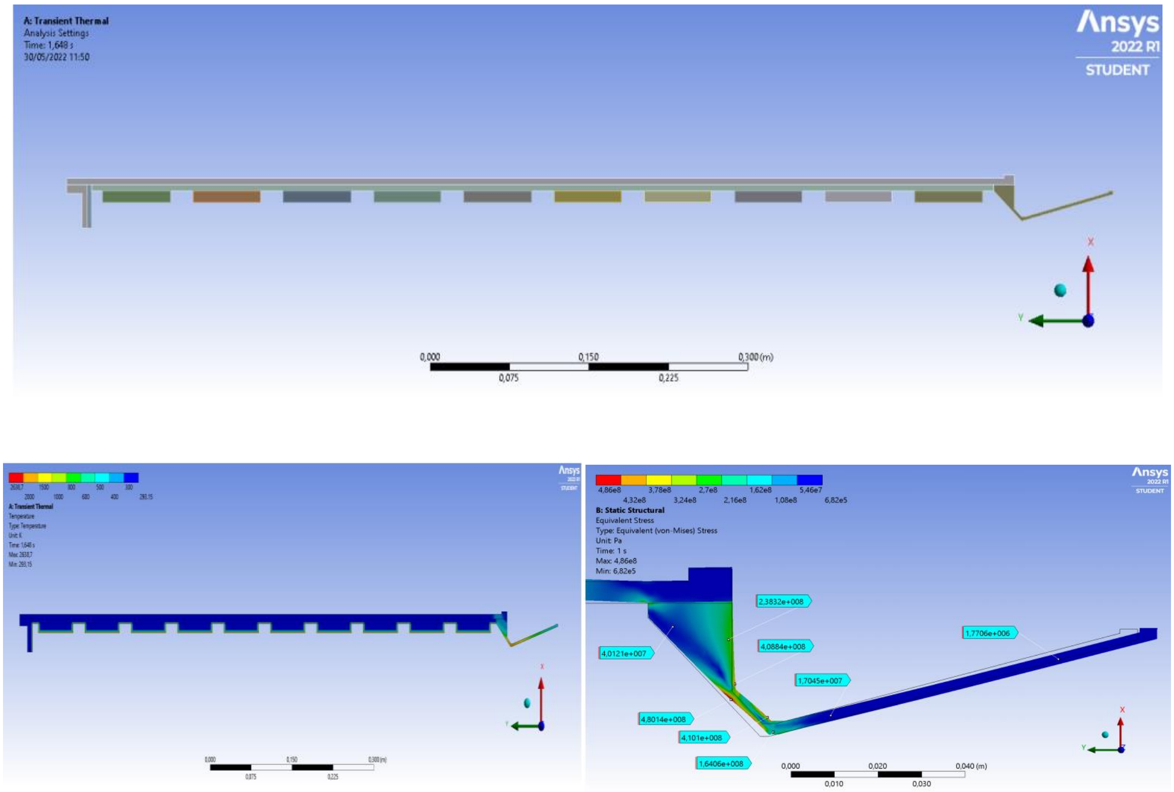

Figure 9: 2D axisymmetric section of SRM employed in analysis with its analysis result (Jan 2022)

The results show that high-performance fuels like APCP (Ammonium Perchlorate Composite Propellant) should be employed given the geometric constraints of the scenario in order to attain the target height. The findings also indicate that the materials used to make this component must have a greater melting point and better heat conductivity than steel, while yet having limit strengths comparable to steel, due to the high temperatures that are achieved in the nozzle's throat.

Besides, Rossi et al., (2002), modeled, designed and fabricated a novel class of MEMS devices termed microscale rockets by the incorporation of propellant into silicon micromachined systems. These new instruments appear to fill a need in the market for high-energy microscale actuation. Their primary novelty is the use of just one solid propellant, which is put into a tiny tank that has been micro manufactured in either ceramic or silicon. The structure is made out of a sandwich of three micromachined silicon substrates: nozzles, igniters, and propellant chambers. The solid propellant burns with a thrust force that varies from 1 mN to a few mN. The thrust impulse may be modified based on application needs simply by taking into account geometrical and dimensional factors.

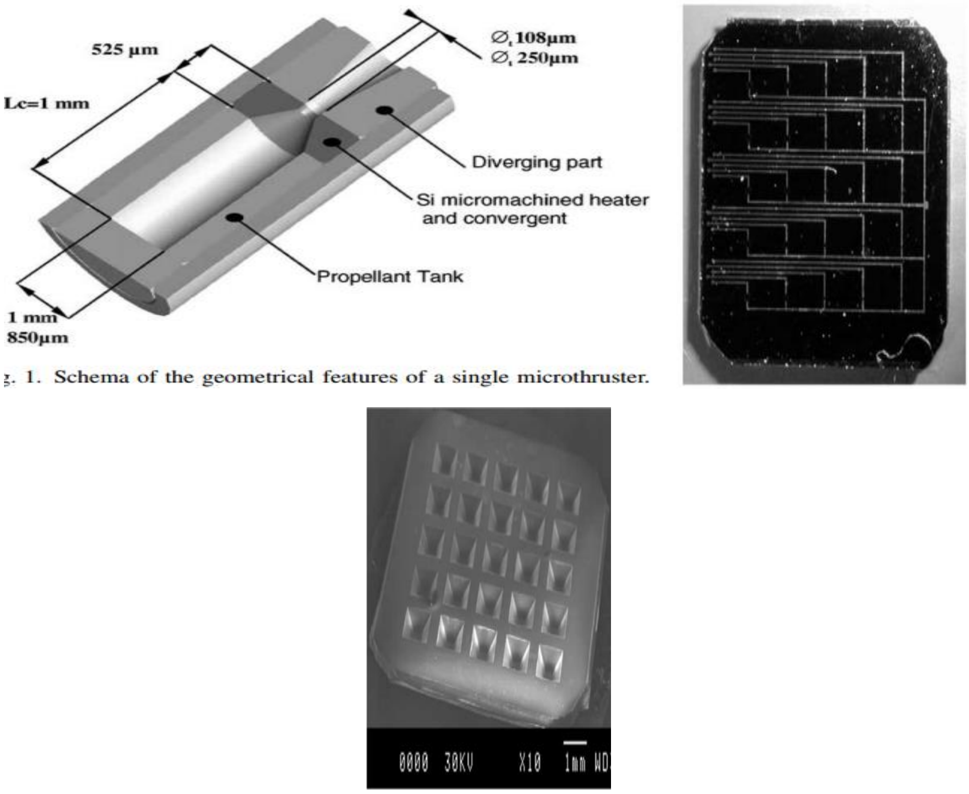

Figure 10: Microthrusters configuration with igniter wafer and its electrical connection (Rossi et al., 2002)

The development of microscale thrusters for the attitude control or/and station maintaining of extremely small satellites is one known use of microrockets in space. The manufacturing and assembly and modeling procedure for microthrusters as well as the unique machinery designed to load solid propellant into microcavities are discussed.

2.7. Summary and Gap of Reviewed Literature

Numerous space applications have a significant impact on Earth, including monitoring climate and weather conditions, facilitating access to healthcare and education, managing water resources, improving transportation and agricultural efficiency, promoting peacekeeping and security, providing humanitarian aid, and exploring other beneficial advancements that are currently being contemplated. The primary criterion for categorizing rockets is their energy source, and based on this, they can be grouped into three main categories: Chemical Propulsion, Electric Propulsion, and Nuclear Propulsion.

Based on the condition of their fuel and oxidizer, chemical rockets may be divided into three classes. These include rockets that use liquid propellant, solid-liquid hybrid propellant, and solid propellant. A solid rocket's major component is its motor, which is made up of two main components: the casing and the nozzle. The solid propellant and insulation are contained in a thin-walled pressure vessel that is the motor case. The nozzle, which is fastened to the casing, is intended to create ordered momentum out of the chaotic motion of the gases created in the motor case. A layer of heat-barrier material is often positioned between the propellant and the inside surface of the rocket engine casing to keep it from heating up to a point where it might endanger its structural integrity.

SP, or sugar-based propellant, are a category of propellants that exhibit medium-level performance. These propellants employ a binder-fuel composed of commonly used sugars like sucrose, dextrose, maltose, and sugar alcohols like sorbitol. Efforts have been made to enhance the performance of sugar-based propellants by incorporating additives such as aluminum, magnesium, and iron III oxide.

Although numerous attempts have been made to enhance the performance of sucrose-based fuels and develop a compact rocket using such fuel, there is still a lack of literature to substantiate these research endeavors and facilitate further improvement. The following gaps were identified during the review of existing literature:

- There is a dearth of clear evidence regarding the specific percentage improvement in specific impulse resulting from the incorporation of additives.

- The exploration of mixing a low-level oxidizer with a higher-level oxidizer (such as KNO_3 with NH_4NO_3) to mitigate their drawbacks and enhance performance has not been undertaken.
- The investigation of utilizing epoxy in conjunction with a multi-oxidizer fuel to enhance the mechanical properties of the fuel were unexplored.
- There has been no pursuit of developing small-scale motors test set up with minimal production costs.

CHAPTER THREE

3. MATERIALS AND METHODS

3.1. Introduction

The paper intended to come up with sucrose based fuel with improved performance and, design a motor for solid rocket with a maximum height of 20 km. To attain the aforementioned objectives, the methodologies expected to be followed are discussed under this heading. Well planned measures have to be taken in order to achieve the target because of the unavailability of adequate materials and laboratories dedicated for the projects.

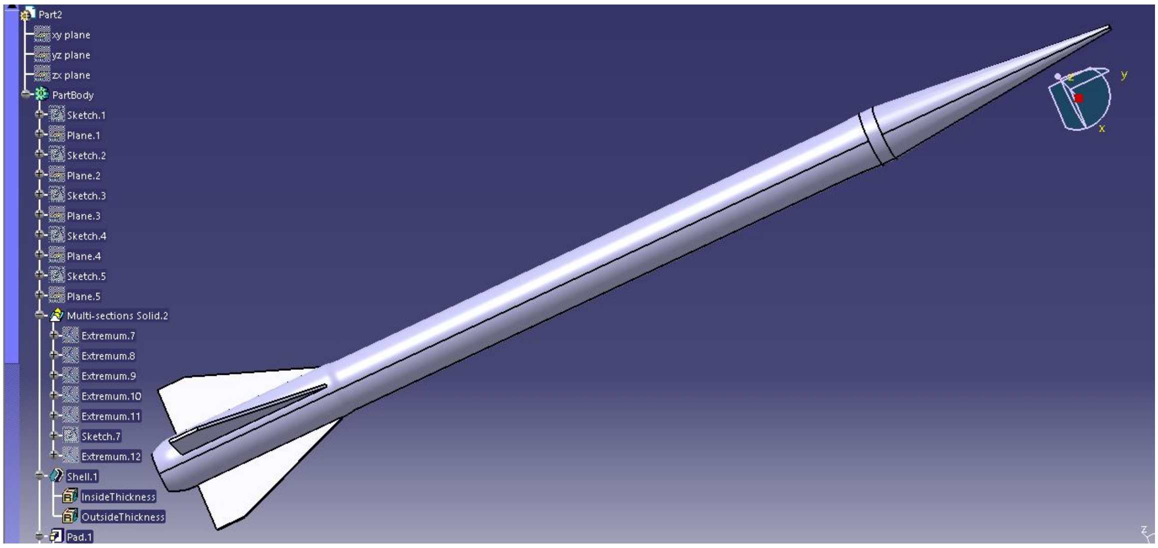

Figure 11 CATIA drawing of the sounding rocket

3.2. Procedures and Methods Followed

3.2.1. Review of Literature

This is the most common and important part of this thesis. Previous works on Rockets focusing on propulsion technology is performed. Particularly, as the analysis of internal ballistic involves turbulent flow and because of hostile nature of the conditions created in the chamber, it is of paramount importance to refer to already undertaken works.

3.2.2. Analytical Formulas

In order to forecast or get insight of the reality, mathematical modeling is employed to act as a representation of a real-world phenomenon. This thesis only applies previous mathematical formulas correlating chamber pressure, nozzle throat area, and mass flow rate and burn area.

3.2.3. Design

This involves the design configuration of motor case and nozzle. Additionally, different fuel composition will be examined in order to find best mixture Decision on the design of all parts majorly depended on availability of materials and manufacturing ease.

3.2.4. Result Validation

Output results from the software is compared with other paper's result to further confirm the reliability of the findings.

3.2.5. Results and discussion

After the constructed Rocket motor has been tested, the results with further discussion will be provided as the study moves forward. Under this topic, the outcomes of the analytical model and efficiency will be examined and addressed. The answer should be compared against the assumptions used to construct the mathematical model of the issue. Based on the findings, the results will be contrasted and discussed in order to address certain objectives-related concerns.

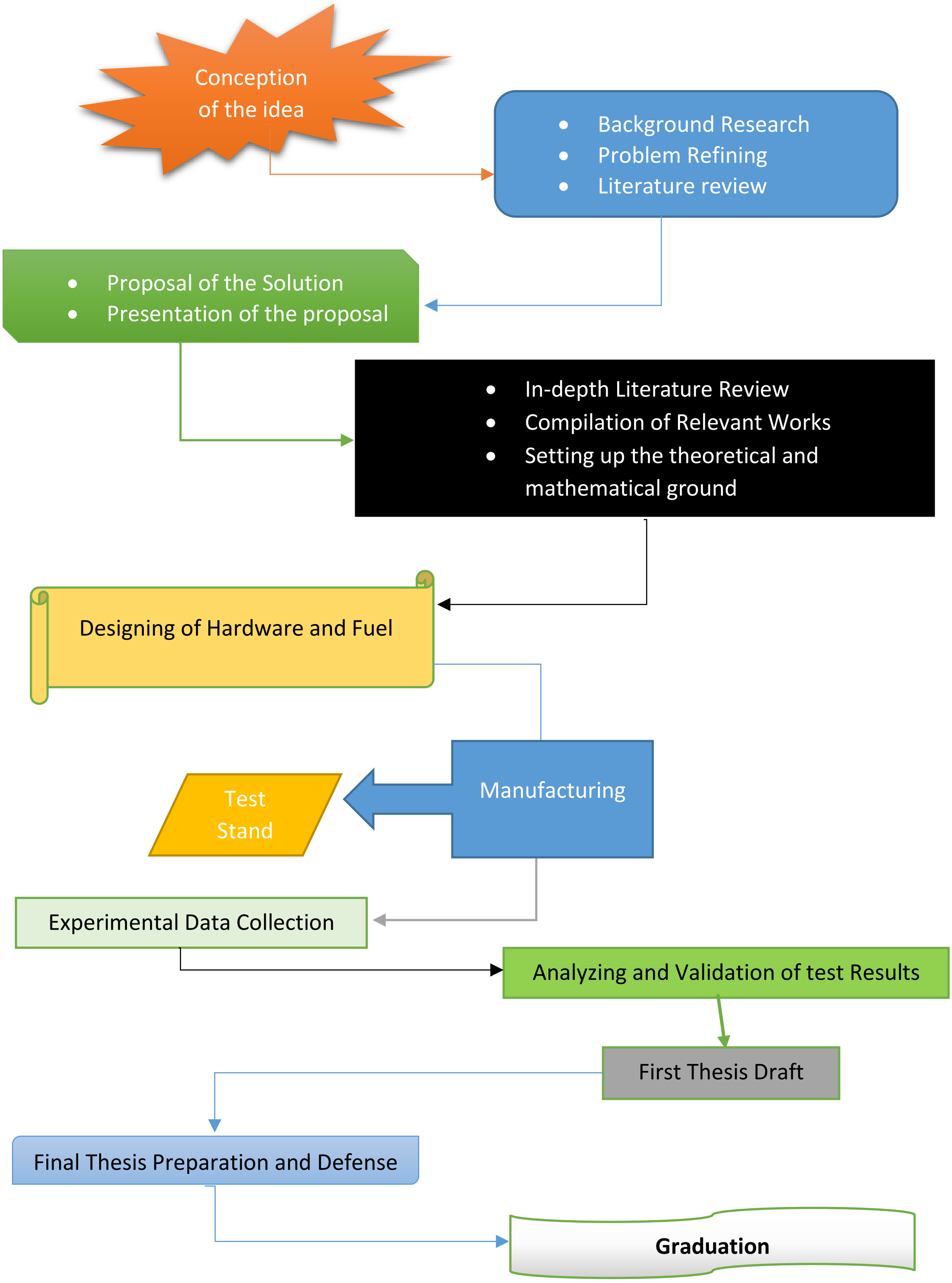

Figure 12: Procedures followed to undertake the thesis

3.3. Sub scale Motor Design

A subscale motor was then employed to examine the different propellant formulations. This process is required because propellants burn in strand burners differently than they do in motors.

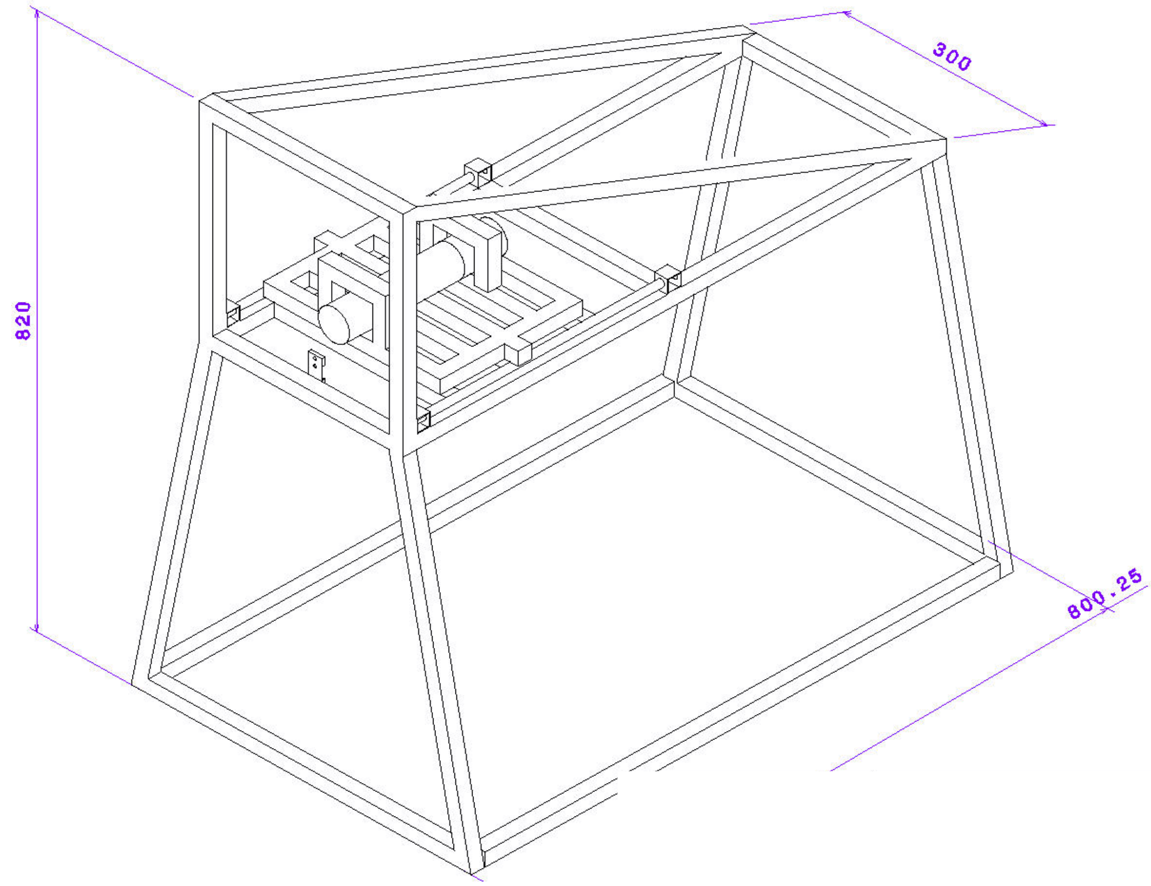

Figure 13: Isometric view of the test stand drawing

3.3.1. Structural Design

Test stand was designed to statically hold the vehicle. The modelling of test stand and motor were made using CATIA v5. The motor has a place where it is secured so that its performance parameters are measured. This test setup should withstand the stresses created due to the loads from the motor. To check whether it could withstand the estimated load, structural simulation had is done analytically. However, since the load is very small (on the order of few newton, the analysis of stress is omitted.

In addition to this, the pressure which develops in the chamber is on the order of mega Pascal which can destroy the motor. Hence, designing a motor with so many things put under consideration was tough. For this proper material was selected with high temperature, pressure and wear bearing capacity. Structural steel was the best option to be used as a motor casing because of its high melting pint, strength, wear resistance and ease of availability.

$$\sigma_\theta = 2\sigma_l = \frac{P*R*F.S}{t} = \frac{3447.4kpa*21.5mm*3}{2mm} = 185.3MPa$$

The obtained stress is well below the yield stress of a mild steel which is 250MPa. Based on the availability of mild steel tube on the market, the following tube with following dimension was utilized as a motor and for the nozzle the dimensions are given in appendix F:

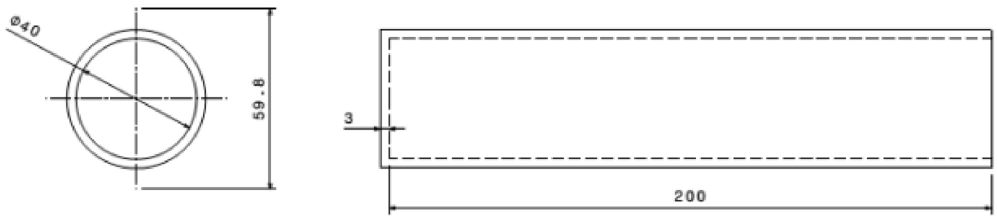

Figure 14: Dimensions of Small Scale Motor

The motor also has to be insulated to prevent the transfer of heat to the electrical equipment such as sensors, controllers and computers to log the data. Unless the motor is insulated, the high heat coming from it may damage the electrical equipment near it.

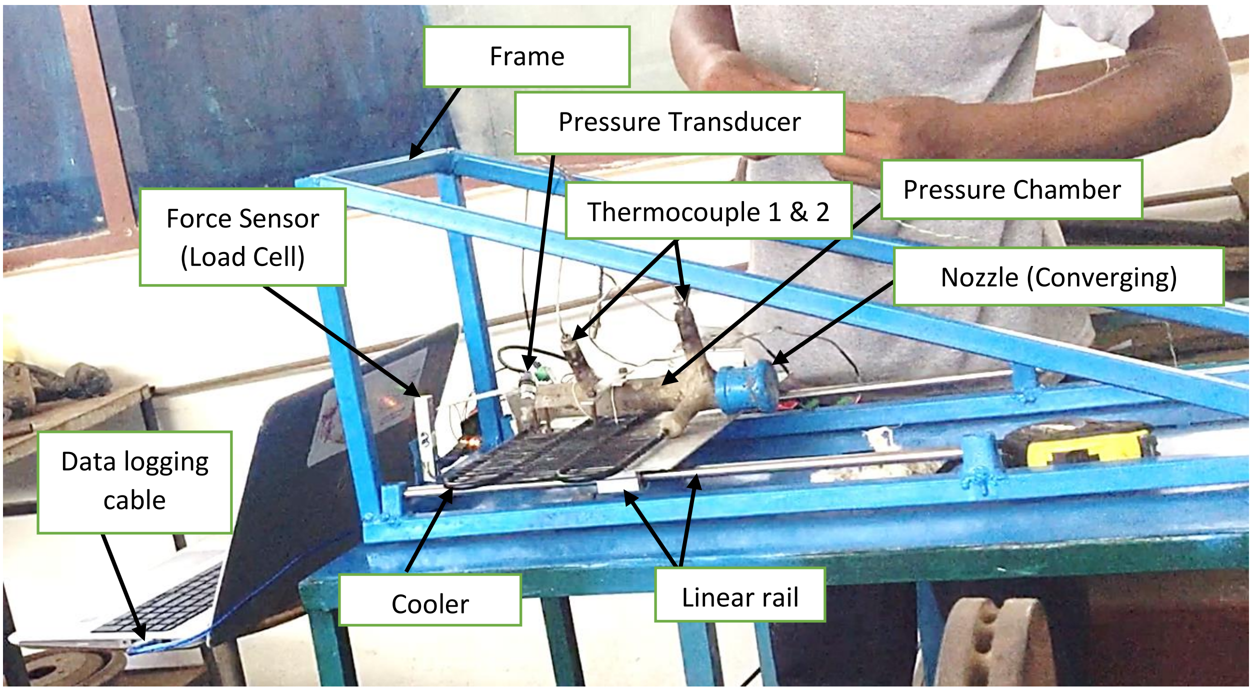

Figure 15: Experimental Setup

A resistor-based ignition system is selected for this test setup as it is a commonly employed method for small-scale solid rocket motor test stands. This ignition system utilizes a resistor as a heating element to initiate the combustion process in the rocket motor. When an electrical current is passed through the resistor, it generates heat, which is then transferred to the propellant material. This heat energy raises the propellant's temperature to the point where it ignites, initiating the thrust generation. The resistor-based ignition system is favored for its simplicity, reliability, and cost-effectiveness, making it an ideal choice for small-scale rocket motor testing, where precision and control are crucial in achieving successful ignition and subsequent performance evaluation.

3.3.2. Materials used in the Experiment

Critical materials used in the project are presented in this section. Almost all of the materials are found in the country. There were many things considered when selecting these materials from pool of other possible ones. These are their thermal and structural integrity, ease of availability, price, and manufacturing difficulty.

Table 3: Materials used for the test setup

Case and Nozzle	Structural steel
Temperature sensor	MAX6637 (K-type thermocouple)
Pressure Sensor	Industrial pressure transducer
Thrust sensor	Hx711 Load cell
Test stand frame and combustion chamber	Structural steel
Controller	Arduino UNO
Fuel	Sucrose ($C_{11}H_{22}O_{11}$)
Oxidizer	Potassium Nitrate (KNO_3)
Additive	Aluminum
Thermal protection system	Cement
Ignition System	Resister wire (Nickel Chromium)
Very low friction motor mounting mechanism	Linear rail (10mm rod and 10mm Bearing)

3.3.3. Electrical Circuit Design

The application of measuring techniques is essential for assessing the performance characteristics of propellants in the context of small-scale rocket motor testing. Tools utilized in this situation is an electrical circuit that incorporates an Arduino-based microprocessor, a thermocouple, a load cell, and a pressure transducer. Key performance metrics may be accurately and immediately monitored. The thermocouple detects temperature, the load cell calculates thrust, and the pressure transducer records the rocket motor's internal pressure. The Arduino microprocessor serves as the system's primary control unit. The data are then displayed and recorded on computer.

First, the equipment required for measuring the performance parameters were searched for on the market. This was because of the limit in the availability of needed apparatus such as high pressure sensor, high temperature sensors, load cells, microcontrollers, and sealants.

After all structural parts have been prepared, electrical devices used such as sensors (temperature sensor, pressure sensor, and load cell) and controller (Arduino) was installed. However, using a conventional industrial pressure sensors in this project was not is as it seemed. Most pressure sensors can tolerate a temperature of around 100 ^{0}c, which is very small compared to the temperature of gases in the combustion chamber. To mitigate this, a certain technique had to be followed, which needed the incorporation of copper tubes and piping.

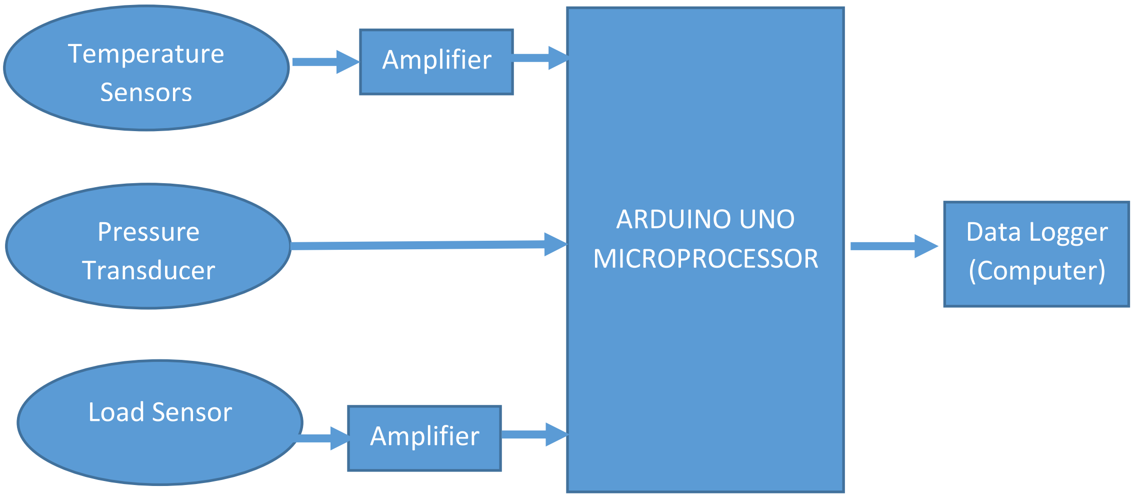

Figure 16: Diagram for electrical connections

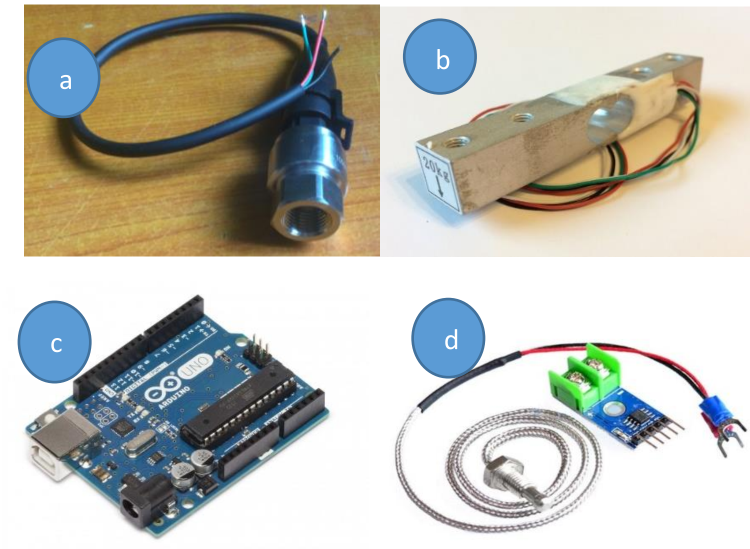

Figure 17: Sensors and Microprocessor (a) Industrial pressure transducer, (b) HX711 Load cell, (c) Arduino Uno, (d) MAX6637 thermocouple

3.4. Propellant preparation

The propellant components used for sample manufacture in this study were potassium nitrate and sucrose, both of which were industrial grade ingredients. To ensure proper blending and uniformity, each component underwent a milling process using a mill equipped with rotary blades. The milling procedure involved filling each mill up to 70% of its maximum volume and operating it for approximately three minutes. Once the grinding process was complete, the milled components were carefully stored in individual pots to maintain their integrity.

Figure 18: Chemical ingredients of the tested fuel

To achieve the desired chemical composition, precise adjustments were made by measuring the masses of the components using a scale with a resolution of 0.01 grams. This ensured accurate proportions of potassium nitrate and sucrose in the propellant mixture. After the adjustment phase, the components were returned to the rotary mill for another round of mixing and grinding, which lasted approximately three minutes. This additional milling step aimed to further enhance the homogeneity and consistency of the propellant mixture.

Figure 19: Weighting scale and fuel grinding machine

Table 4: Chemical composition of fuel samples prepared

Sample	Mole of **KNO3**	**Al** %	Mole of **Al**	Mole of **C**	Sucrose %	Mole of Sucrose
1	6.44	1.00	0.37	1.67	32	0.94
2	6.44	2.00	0.74	1.67	31	0.91
3	6.44	3.00	1.11	1.67	30	0.88
4	6.44	4.00	1.48	1.67	29	0.85
5	6.44	5.00	1.85	1.67	28	0.82

Figure 20: Fuel samples

Once all the samples of chemical powder with varying compositions of interest were meticulously prepared, the next step involved casting the propellant into the sub-scale motor. The casting process required a careful approach, ensuring that the powder was poured into the motor gradually. As each portion of the powder was added, it was compressed using a hand hammer weighing approximately 1kg and a solid metal rod with a diameter matching that of the chamber. To achieve the desired level of compaction, the hammering action was repeated around 20 times for each instance. This repetitive punching motion helped to enhance the density and stability of the propellant within the motor. Each sample used in the experiment weighed 28g when placed in the test chamber.

Figure 21: Small scale motor

3.5. Utilized Software

3.5.1. NASA's CEA Software

Chemical processes and their equilibrium characteristics, alternately, may be analyzed and predicted using the CEA (Chemical Equilibrium with Applications) program from NASA. The CEA is especially made for high-temperature chemical systems, such those found in combustion and rocket engines.

The equilibrium composition of a particular reactive mixture is calculated by CEA using the laws of chemical thermodynamics. it also takes into consideration variables like temperature, pressure, and the starting composition of the mixture to provide information on the chemical species present, their concentrations, thermodynamic characteristics (such as enthalpy, entropy), and other pertinent data.

The program makes use of both theoretical and empirical models to calculate the thermodynamic characteristics of diverse chemical species. It makes use of an extensive amount of thermodynamic data, including equilibrium constants, heat capacities, enthalpies, and entropies for a variety of chemical processes. This database is being updated and expanded constantly to include fresh theoretical calculations and experimental data.

To determine the equilibrium reactive system composition, CEA uses an iterative procedure. It begins with an initial compositional estimate and gradually modifies chemical species concentrations until the system achieves equilibrium. The program allows for the study of complicated chemical systems including solids, liquids, and gases while taking into consideration both gas and condensed phases.

CHAPTER FOUR

4. THEORETICAL PERFORMANCE ANALYSIS OF THE FUEL AND MOTOR

4.1. Chemical Composition of the Propellant

Common sugar (mostly sucrose,) or sugar alcohol (sorbitol) is used as the fuel in sugar propellant, while potassium nitrate (KNO3) is used as the oxidizer. The propellant is held together by a binder made from the fuel, which is sugar itself. But since the binder-fuel is not a polymer like APCP, it degrades quickly. These characteristics provide the propellants desirable properties. Since the binder degrades more quickly than a polymer while still generating acceptable results, a lower-energy oxidizer like potassium nitrate is efficiently used.

Following is the theoretical combustion equation for conventional KNSU at 68 atm:

$$\mathbf{48KNO_3 + 5C_{12}H_{22}0_{11} \rightarrow 24K_2CO_3 + 24N_2 + 55H_2O + 36CO_2}$$

Table 5: Physical states of reactants and products

Sucrose	$C_{12}H_{22}0_{11}$	Solid
Potassium nitrate	KNO_3	Solid
Potassium carbonate	K_2CO_3	Liquid, solid
Carbon dioxide	CO_2	Gas
Water	H_2O	Gas
Nitrogen	N_2	Gas

Specific impulse for propellants based on sucrose ranges from 115 to 130, and it is not significantly affected by the fuel. The I_{sp} of black powder is normally between 80 and 90 seconds, but the I_{sp} of most ammonium perchlorate composite propellants (APCP) is between 190 and 210 seconds. Similar to APCP, sugar propellants also have comparable burn rates. This blend of sucrose and potassium nitrate has a high melting point, which makes processing more difficult and may reduce reproducibility (Singh, 2015).

4.2. Combustion Analysis

4.2.1. Ideal Gas Mixtures

Non-reacting gas mixes consist of two or more gases that have the same chemical composition. The mole fraction or mass fraction of each component is used to describe the composition of a gas mixture, depending on the definition.

$$\mathrm{mf}_i = \frac{m_i}{m_m} \text{ and } y_i = \frac{N_i}{N_m} \tag{4.1}$$

Where

$$m_m = \sum_{i=1}^{k} m_i \text{ and } N_m = \sum_{i=1}^{k} N_i$$

The apparent molar mass and gas constant of a mixture are expressed as:

$$M_m = \frac{m_m}{N_m} = \sum_{i=1}^{k} y_i M_i \text{ and } R_m = \frac{R_u}{M_m} \tag{4.2}$$

Also

$$\mathrm{mf}_i = y_i \frac{M_i}{M_m} \text{ and } M_m = \frac{1}{\sum_{i=1}^{k} \frac{\mathrm{mf}_i}{M_i}} \tag{4.3}$$

The extensive characteristics of a gas mixture may often be calculated by adding the contributions of each component:

$$u_m = \sum_{i=1}^{k} \mathrm{mf}_i u_i \text{ and } \bar{u}_m = \sum_{i=1}^{k} y_i \bar{u}_i \tag{4.4}$$

$$h_m = \sum_{i=1}^{k} \mathrm{mf}_i h_i \text{ and } \bar{h}_m = \sum_{i=1}^{k} y_i \bar{h}_i \tag{4.5}$$

$$s_m = \sum_{i=1}^{k} \mathrm{mf}_i s_i \text{ and } \bar{s}_m = \sum_{i=1}^{k} y_i \bar{s}_i \tag{4.6}$$

$$c_{v,m} = \sum_{i=1}^{k} \mathrm{mf}_i c_{v,i} \text{ and } \bar{c}_{v,m} = \sum_{i=1}^{k} y_i \bar{c}_{v,i} \tag{4.7}$$

$$c_{p,m} = \sum_{i=1}^{k} \mathrm{mf}_i c_{p,i} \text{ and } \bar{c}_{p,m} = \sum_{i=1}^{k} y_i \bar{c}_{p,i} \tag{4.8}$$

$$\left(C_p\right)_{\mathrm{m}} \& = \frac{\sum_{j=1}^{m} n_j (C_p)_j}{\sum_{j=1}^{m} n_j} \tag{4.9}$$

$$k_{\mathrm{m}} \& = \frac{(C_p)_{\mathrm{m}}}{(C_p)_{\mathrm{m}} - R'} \tag{4.10}$$

The composition of the combustion products, such as chemical contents and concentrations, has a substantial impact on the average values of k and M for typical rocket exhaust gases containing many different elements. Cold monatomic gases like helium and argon have a k value of 1.67; cold diatomic gases like hydrogen, oxygen, and nitrogen have a k value of 1.4; while cold triatomic and higher gases like methane and carbon dioxide have a k value between 1.1 and 1.3. Generally speaking, the value of k decreases as molecular complexity increases.

4.2.2. Thermodynamic Analysis of the Reacting Systems

The study of the interactions between heat, work, chemical processes, and physical state changes is known as chemical thermodynamics, a branch of thermodynamics. Enthalpy is a thermodynamic parameter which is calculated by multiplying the internal energy of a system by the sum of its pressure and volume. As a result, on a unit mole basis, the enthalpy of a reactant and product is given by:

$$Enthalpy \;=\; \bar{h}_f^0 + \left[\bar{h} - \bar{h}^o\right] \tag{4.11}$$

Enthalpy of formation, or $\bar{h}_f^0$, is a basic characteristic that denotes an element's or a compound's chemical energy in a certain reference state. This property may be viewed as the enthalpy of a material in a certain state as a function of its chemical composition. The amount in parentheses represents the sensible enthalpy relative to the standard reference state because $\bar{h}$ is the sensible enthalpy in the provided state and $\bar{h}$° is the sensible enthalpy at the standard reference state of 25°C and 1 atm. With this definition, we may use the enthalpy values from tables regardless of the reference state that was used to generate them.

4.2.2.1. First Law Analysis of the Reaction

For a chemically reacting steady-flow system, the steady-flow energy balance relation, Ein = Eout, may be expressed as follows by disregarding kinetic and potential energy changes:

$$\dot{Q}in + \dot{W}in + \sum \dot{n}r(\overline{h_f^o} + \bar{h} - \overline{h^o})_r = \dot{Q}out + \dot{W}out + \sum \dot{n}p(\overline{h_f^o} + \bar{h} - \overline{h^o})_p \tag{4.12}$$

Where n_p and n_r represent the molal flow rates of the product p and the reactant r, respectively. It is easier to work with quantities stated per mole of fuel when doing a combustion analysis. Each component in the equation above is divided by the fuel's molal flow rate to produce the following relation:

$$\dot{Q}in + \dot{W}in + \sum Nr(\overline{h_f^o} + \bar{h} - \overline{h^o})_r = \dot{Q}out + \dot{W}out + \sum Np(\overline{h_f^o} + \bar{h} - \overline{h^o})_p \tag{4.13}$$

Where Nr and Np are the number of moles of the reactant r and the product p, respectively, per mole of fuel.

4.2.2.2. Adiabatic Flame Temperature

The adiabatic flame temperature for a steady-flow combustion process is determined from eqn. 4.3 by setting $\dot{Q} = 0$ and $\dot{W} = 0$. It yields:

$$\sum Nr(\overline{h_f^o} + \bar{h} - \overline{h^o})_r = \sum Np(\overline{h_f^o} + \bar{h} - \overline{h^o})_p \tag{4.14}$$

The enthalpy of the reactants H_{react} may be easily calculated if the reactants and their states are known. However, since the temperature of the products is unknown before to the computations, calculating the enthalpy of the products H_{prod} is not as simple. Therefore, unless equations for the sensible enthalpy changes of the combustion products are provided, iterative techniques must be used to determine the adiabatic flame temperature.

4.2.2.3. Second Law Analysis of the Reaction

So far, we've examined combustion processes from the perspectives of mass and energy conservation. However, a second-law analysis of a process is necessary to complete the thermodynamic analysis. The exergy and exergy destruction, both of which are connected to entropy, are of great importance. The entropy balance for any reacting system can be stated as:

$$S_{in} - S_{out} + S_{gen} = \Delta S_{system} \tag{4.15}$$

Where the term '$S_{in} - S_{out}$' is the entropy transfer by heat and mass, S_{gen} is the entropy generated and ΔS_{system} is the change in entropy. The entropy balance relation for a closed or steady-flow reactive system may be written more formally as follows using quantities per unit mole of fuel and assuming that the positive direction of heat transfer is toward the system:

$$\sum \frac{Q_k}{T_k} + S_{gen} = S_p - S_r \tag{4.16}$$

For any temperature T, absolute entropy values at pressures other than P_o=1 atm may be calculated by:

$$\bar{s}(T,P) = \overline{s^o}(T,P_O) - R_u ln\frac{P}{P_o} \tag{4.17}$$

For i component in an ideal-gas mixture, the relation can be written as:

$$\overline{s_i}(T,P_i) = \overline{s_i^o}(T,P_O) - R_u ln\frac{y_i P_m}{P_o} \tag{4.18}$$

Once the total entropy change or the entropy generation is evaluated, the exergy destroyed $X_{destroyed}$ associated with a chemical reaction can be determined by:

$$X_{destroyed} = T_0 S_{gen} \tag{4.19}$$

Reversible work, the maximum amount of work that can be accomplished in a process, is represented by W_{rev} and the reversible work relation for a steady-flow combustion process that involves heat transfer with only the surroundings at T_o in the absence of any changes in kinetic and potential energy may be calculated by:

$$\dot{W}_{rev} = \sum N_r(\overline{h_f^o} + \bar{h} - \overline{h^o} - T_0\bar{s})_r - \sum N_p(\overline{h_f^o} + \bar{h} - \overline{h^o} - T_0\bar{s})_p$$

Or

$$\dot{W}_{rev} = \sum N_r(\overline{g_f^o} + \bar{g}_{T_0} - \bar{g}^o)_r - \sum N_p(\overline{g_f^o} + \bar{g}_{T_0} - \bar{g}^o)_p \tag{4.20}$$

4.3. Solid Propellant Rocket Motor Fundamentals

The word motor is a common name for solid propellants as the word engine is for liquid propellants. There are several types and sizes of motors, with thrust ranging from around 2 N to over 12 million N. The body of the motor case is either composed of composite fiber-reinforced plastic or metal such as steel, aluminum, or titanium. The case must also have thermal protection or insulation layers on its interior surfaces that come into contact with hot gas. This serves to prevent the case from overheating to the point where it is unable to support the pressure and other loads. Additionally, every motor must have a thrust-carrying structure that secures it to its vehicle.

The grain which is the solid portion of the hardened propellant makes up 82 to 94% of the mass of the motor. The material and geometrical configuration of the grain govern motor performance characteristics.

Definitions and terminology relevant to grains are presented as follows:

***Configuration*:** The geometry or shape of the initial burning surfaces of a grain.

Burn Rate or rate of regression: The rate at which the fuel in the motor burns. It is usually in mm/s or in/s.

Cylindrical grain: A grain which has internal cross section of cylinder that is constant along the axis.

Neutral burning: a grain that burns with an approximate constant thrust, pressure, and burning surface area, usually within 15%.

Progressive burning: a grain where the as the burn duration increases the thrust, pressure, and burning surface area increase.

Regressive burning: a grain where the as the burn duration increases the thrust, pressure, and burning surface area decrease.

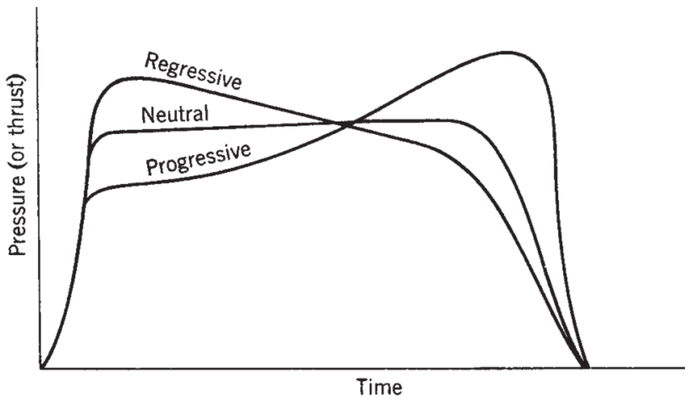

Figure 22: Classification of Grains according to their pressure-time characteristics

Perforation: a propellant grain's core cavity port or flow path; its cross-section may have the form of a cylinder, a star, or something similar.

Sliver: Propeller loss or unburned propellant residue i.e., ejected from the nozzle during web burnout.

Effective burning time* or just *burning time, t_b: Usually, the region between 10% maximum starting pressure and web burnout with web burnout being regarded as the pressure-time trace's aft tangent-bisector point.

Inhibitor* also called *restrictor: A coating of slow- or non-burning material, often a polymeric rubber type with filler materials placed (painted, sprayed, glued or dipped) on a portion of the grain's propellant surface to prevent burning on that surface.

Internal insulation* or *thermal protection: a thermally insulating, sticky interior layer made of a substance that won't burn easily that sits between the casing and the propellant grain. Its goal is to reduce the case's temperature rise and heat transmission during rocket operation.

Web thickness, b: In the case of an end-burning grain, b is equal to the grain's length. But for the radially burning one, it is the minimum thickness of the grain measured from the first internal burning surface to the insulated case wall.

Propellant Mass Fraction, ζ: The motor mass ratio and, consequently, the flight performance of the vehicle are directly connected to the propellant mass fraction, which is stated as:

$$\zeta = \frac{m_p}{m_o} \tag{4.21}$$

Where m_p is the useable solid propellant mass and m_o is the beginning rocket's total mass which is the addition of m_p and the rocket motor's non-burning, inert hardware mass. The payload mass and the non-propulsion inert mass (vehicle structure, guidance and control, communications equipment, and power supply) must be taken into account when calculating a vehicle's total propellant mass percentage. A high value of ζ suggests efficient hardware design and a low inert motor mass, but also frequently significant stresses.

4.4. Performance Parameters of Solid Propellants

One of the common performance parameters of rocket fuel is **total impulse, I_t**. To get the total impulse, the thrust force F, which may change over time, is integrated throughout the application period t:

$$I_t = \int_0^t F dt \tag{4.22}$$

This equation can be reduced the equation below if the thrust is considered constant with very short starting and stopping transient time:

$$I_t = Ft \tag{4.23}$$

The **specific impulse** is the second crucial performance parameter. The specific impulse I_s stands for the thrust per unit weight flow rate of propellant. It is an essential measure of the effectiveness of any rocket propulsion system and has an analogy to 'the miles per gallon' used with regard to cars. Better performance is frequently indicated by a higher number.

$$I_{sp} = \frac{\int_0^t F dt}{g_0 \int_0^t \dot{m} dt} \quad (4.24)$$

Values of I_s can be calculated using the integral above or by utilizing average values for F and m as m_p stands for the total effective propellant mass discharged, as seen below:

$$I_{sp} = I_t/(m_P g_0) \quad (4.25)$$

The third parameter is **effective exhaust velocity, c**. Since the exhaust velocity in actual rocket nozzles is not truly identical over the full exit cross section, it is challenging to evaluate such velocity profiles with accuracy. The average velocity at which fuel is being expelled from the rocket vehicle is represented by the effective exhaust velocity, or c. It's outlined as:

$$c = \frac{F}{\dot{m}} = I_s g_0 \quad (4.26)$$

$$c = v_2 + \frac{(P_2 - P_3)A_2}{\dot{m}} = I_s g_0 \quad (4.27)$$

It is specified in meters per second. Both c and I_{sp} may be used as indicators of rocket performance because their only difference is a constant, g_0.

Another parameter used in rocket propulsion literature is **characteristic velocity, c^***. Although it is not a physical velocity, the characteristic velocity, c^*, is used to compare the relative performance of various chemical rocket propulsion system designs and propellants. It may be easily calculated from measurements of $\dot{m}$, P_1, and A_t. It is given as:

$$c^* = \frac{P_1 A_t}{\dot{m}} = \frac{I_s g_0}{C_F} = \frac{c}{C_F} = \frac{\sqrt{kRT_1}}{k\sqrt{\left[\frac{2}{k+1}\right]^{\frac{k+1}{k-1}}}} \quad (4.28)$$

The fact that c^* is virtually unrelated to nozzle features means that it might possibly be connected to the effectiveness of the combustion. The effective exhaust velocity and the specific impulse, however, continue to be dependent on the nozzle geometry, specifically the nozzle area ratio A_2/A_t.

4.5. Basic Relations of Propellant Burning Rate with Chamber Pressure

The combustion parameters of the propellant, such as burning rate, burning surface, and grain shape, affect how a rocket motor operates and is built. Internal ballistics is the field of applied science that studies these traits. The ability to accurately predict the burning rate behavior of the chosen propellant under all conceivable motor operating conditions and limits of design is crucial for the design and development of successful rocket motors. The composition of the propellant affects burning rate.

The data of burning are rare and often are collected in through three testing ways: Standard strand burners, often called Crawford burners, small-scale motors and full-scale rocket motors, A strand burner is a little pressure vessel where a thin bar or strand of fuel is ignited at one end and burnt completely. The strand can be controlled such that it will only burn on the exposed cross-sectional surface by applying an exterior nonflammable coating; chamber pressure is achieved by pressurizing the container with an inert gas. Burning rates can be determined via optical, acoustic, or electric signals from wires that are buried in the ground. Due to the fact that strand burner testing does not accurately replicate the hot chamber environment, the observed burning rate is often lower than that achieved from full-scale motor firing. Because of scaling issues, small ballistic evaluation motors often also have a little lower burning rate than full-scale bigger motors.

4.5.1. Mass Flow Relations and Burning Rate Relation with Pressure

The mass flow rate m of the hot gases produced and exiting the engine at any given moment is provided by:

$$\dot{m}_{in} = A_b r \rho_b \tag{4.29}$$

Where Ab is the propellant grain burning area, r the burning rate, and ρ_b the density of solid propellant prior to ignition.

According to the conservation of mass principle, the mass of gaseous propellant emerging from a burning surface per unit time must equal the sum of the rate of change of gaseous mass storage in the combustion chamber (caused by increases in the volume of the grain cavity) and the rate of mass evaporating through the exhaust nozzle.

$$\dot{m}_{out} = \frac{A_t P}{c^*} \tag{4.30}$$

$$\dot{m}_{storage} = \frac{d}{dt}(\rho_1 V) \tag{4.31}$$

Figure 23: Mass balance in combustion chamber

$$A_b r \rho_b = \frac{d}{dt}(\rho_1 V) + \frac{A_t P}{c^*} \tag{4.32}$$

The term $\frac{d}{dt}(\rho_1 V)$ can usually be neglected except for very short operating durations. This results in the equation that is frequently used to describe the pressure in steady burning:

$$P = K r \rho_b c^* \quad where \ is \ K = \frac{A_b}{A_t} \tag{4.33}$$

Value of K, a crucial new dimensionless motor parameter, must remain constant for steady flow and steady burning. Be aware that in this derivative of V indicates the rate of growth of volume in the chamber hot-gas cavity whereas ρ_b represents the solid propellant density and ρ_1 the chamber hot-gas density; The nozzle throat area is represented by A_t, the chamber pressure is represented by P, the characteristic velocity is represented by c*, which is proportional to T, the absolute chamber temperature determined by the thermochemistry for a particular propellant.

4.5.2. More Accurate Burning Rate Relation with Pressure

The most popular empirical formula for the majority of propellants is:

$$r = aP^n \ 4.25 \tag{4.34}$$

Where r, the burning rate, is in mm/sec and the chamber operating pressure P is in MPa. The constant a, sometimes referred to as the temperature coefficient, is affected by the ambient grain temperature, T_b. The burning rate exponent n, also known as the pressure exponent or the combustion index, is independent of the propellant beginning temperature but affects both the burning rate and the chamber operating pressure. When n>1.0, any pressure disturbances will be magnified in the chamber and will not cause combustion stability.

Inserting Eq. 12–5 into eqn. 12–4 and 12–1, we may now write the generated mass flow rate and K as:

$$\dot{m}_{in} = A_b \rho_b a P_1^n \tag{4.35}$$

$$K = P_1^{(1-n)}/(\rho_b a c^*) \tag{4.36}$$

High values for n result in quick fluctuations in the burning rate as a function of pressure. This suggests that significant variations in the volume of hot gas generated can be caused by even a typically minor difference in chamber pressure. Most commercial propellants have a pressure exponent n ranging from 0.2 to 0.6. The chamber pressure and burning rate become extremely sensitive to one another as n gets closer to 1.0, and a devastating spike in chamber pressure might happen in just a few milliseconds.

4.6. Nozzle Theory and Thermodynamic Relations

The stagnation condition is the scenario that occur when flows are stopped isentropically and are denoted by the subscript 0. The term stagnation is sometimes replaced with the term "total". Stagnation enthalpy is the summation of static or local enthalpy and the fluid kinetic energy. The total or stagnation enthalpy per unit mass h_0 is assumed to be constant in nozzle flows under ideal conditions:

$$h_0 = h + \frac{v^2}{2} = Constant \tag{4.37}$$

This energy equation yields the absolute stagnation temperature T0 as:

$$T_0 = T + \frac{v^2}{2c_p} = Constant \tag{4.38}$$

In perfect gases, the velocity of sound (acoustic velocity) a, and Mach number is defined as:

$$a = \sqrt{RKT} \text{ And } M = \frac{v}{a} = \frac{v}{\sqrt{RKT}} \tag{4.39}$$

From basic thermodynamic equations,

$$cp = kR/(k-1), \tag{4.40}$$

Substituting these in the above equations yields:

$$\frac{T_0}{T} = 1 + \left(\frac{k-1}{2}\right) M^2 \tag{4.41}$$

In isentropic processes the following relations hold true between two cross-sections 1 and 2:

$$\frac{T_2}{T_1} = \left(\frac{P_2}{P_1}\right)^{\frac{k-1}{k}} = \left(\frac{V_1}{V_2}\right)^{k-1} \tag{4.42}$$

Using the above relation we can also derive the ratio of a stagnation pressure to pressure and the ratio of stagnation density to density:

$$\frac{P_0}{P} = \left[1 + \left(\frac{k-1}{2}\right) M^2\right]^{\frac{k-1}{k}} \tag{4.43}$$

$$\frac{\rho_0}{\rho} = \left[1 + \left(\frac{k-1}{2}\right) M^2\right]^{\frac{1}{k-1}} \tag{4.44}$$

The characteristics of a fluid at the throat are given by:

$$\frac{T^*}{T_0} = \frac{2}{k+1} \tag{4.45}$$

$$\frac{P^*}{P_0} = \left(\frac{2}{k+1}\right)^{\frac{k}{k-1}} \tag{4.46}$$

$$\frac{\rho^*}{\rho_0} = \left(\frac{2}{k+1}\right)^{\frac{1}{k-1}} \tag{4.47}$$

The rate at which mass flows through the nozzle is constant in steady-flow circumstances and may be written as:

$$\dot{m} = \frac{AMP_0\sqrt{k/RT_0}}{[1+(k-1)M^2/2]^{(k+1)/2(k-1)}} \tag{4.48}$$

Inserting Ma = 1 at the nozzle for choked flow yields the maximum mass flow rate:

$$\dot{m} = AP_0\sqrt{\frac{k}{RT_0}}\left(\frac{2}{k+1}\right)^{\frac{k+1}{2(k-1)}} \tag{4.49}$$

From conservation of energy, the enthalpy of the fuel plus its kinetic energy will be the conserved in combustion chamber and at nozzle exit and neglecting all other energy losses such as potential energy. From conservation of energy:

$$h_1 + v_1^2 = h_2 + v_2^2 \tag{4.50}$$

For a solid-fuel rocket, the **ideal nozzle exhaust velocity**, V2, is given by:

$$v_2 = \sqrt{(h_1 - h_2) + v_1^2} \tag{4.51}$$

$$v_2 = \sqrt{\frac{2k}{k-1} RT_1 \left[1 - \left(\frac{P_1}{P_2}\right)^{\frac{(k-1)}{k}}\right] + v_1^2} \tag{4.52}$$

By neglecting the kinetic energy of the combustion gases prior to entering the nozzle,

$$v_2 = \sqrt{\frac{2k}{k-1} RT_1 \left[1 - \left(\frac{P_1}{P_2}\right)^{\frac{(k-1)}{k}}\right]} \tag{4.53}$$

It is considered that the gases' approach velocity upstream of the nozzle is low and may be disregarded in this situation. This is true if the nozzle throat area A_t and port area A_p, are sufficiently different from one another, or if the ratio of the two is more than around 4. We can also express R as $\frac{R'}{M}$. Hence the equation becomes:

$$v_2 = \sqrt{\frac{2k}{k-1} \frac{R'T_0}{M} \left[1 - \left(\frac{P_1}{P_2}\right)^{\frac{(k-1)}{k}}\right]} \tag{4.54}$$

4.7. Thrust and Thrust Coefficient

Rocket thrust using 2^{nd} and 3^{rd} law of Newton:

$F = m\,\ddot{x}$ and $F = Fr$

$$F = F_{momentum} + (P_e - P)A_e$$

$$= m(V_e - V_i)^{\cdot} + (P_e - P_c)A_e$$

Generally, **Thrust** for solid propellant rocket motors is given by:

$$F = \dot{m}v_2 + (P_2 - P_3)A_2 \tag{4.55}$$

The first element in the equation is the thrust due to momentum, which is calculated as the multiplication of the mass flow rate of the propellant with the velocity of its exhaust as it exits the vehicle. The second term represents the pressure thrust, which is made up of the product of the at the nozzle exit cros-sectional area (where the exhaust jet exits the vehicle) and the difference between the gas pressure at the exit and the surrounding fluid pressure.

After substituting the expressions of $\dot{m}$ *and* $v_2$and some manipulation, the thrust would be given by:

$$F = A_1 P_1 \sqrt{\frac{2k^2}{k\text{-}1} \left(\frac{2}{k+1}\right)^{\frac{(k+1)}{(K-1)}} \left[1\text{-} \left(\frac{P_1}{P_2}\right)^{\frac{(k-1)}{k}}\right]} + (P_2 - P_1)A_2 \tag{4.56}$$

Now, a thrust coefficient CF may be determined by dividing the thrust by the chamber pressure p1 and the throat area At. The thrust coefficient may be thought of as the amount of thrust that is increased as a result of the gas expanding in the supersonic nozzle as compared to the amount of thrust that would be created if the chamber pressure just had an impact on the throat area.

$$C_F = \frac{F}{P_1 A_t} = \sqrt{\frac{2k^2}{k-1}\left(\frac{2}{k+1}\right)^{\frac{(k+1)}{(K-1)}}\left[1-\left(\frac{P_1}{P_2}\right)^{\frac{(k-1)}{k}}\right]} + \frac{(P_2-P_1)}{P_1}\frac{A_2}{A_t} \quad (4.57)$$

$$F = C_F A_t P_1 \quad (4.58)$$

4.8. Motor Casing Structural Integrity Design

Solid propellant rocket motor casings, which are frequently a part of the flying vehicle construction, both encapsulate the propellant grain and act as highly loaded pressure vessels. When designing a case there are several things to be made under considerations. The frequently examined elements are: temperature changes that result in thermal stress and strain and adverse circumstances associated with space environments (vacuum or radiation).

The most common origins of force include: Internal Pressure, and aerodynamic surfaces of the case and items attached to the case. An approximate prediction of the stresses in solid propellant rocket chamber cases may be made using simplified membrane theory; this method assumes that the case walls won't flex and that all loads will be applied under tension. The longitudinal stress σ_l for a cylinder with radius *R* and thickness *t*, and chamber pressure P, is equal to half the tangential or hoop stress σ_θ. The total stresses must never be more than the material's operating stresses.

$$\sigma_\theta = 2\sigma_l = \frac{PR}{t} \quad (4.59)$$

The elongation in the longitudinal length and circumference of the casing created due to pressure inside is given by the following formula:

$$\Delta L = \frac{PLD}{4Ed}(1-2\nu) = \frac{\sigma_l L}{E}(1-2\nu) \quad (4.60)$$

$$\Delta D = \frac{PD^2}{4Ed}\left(1-\frac{\nu}{2}\right) = \frac{\sigma_\theta L}{2E}\left(1-\frac{\nu}{2}\right) \quad (4.61)$$

CHAPTER FIVE

5. RESULTS AND DISCUSSION

5.1. Thermo-physical and Performance Results from CEA NASA Software

The software called CEA NASA was used to evaluate the performance of the formulated fuel. To enhance the performance of the KNSU propellant fuel three different additives were used. The first additive was Mg. The amount of magnesium powder added ranged from 1% in mass to 5%. The following were the fuel samples tested:

Table 6: Chemical Composition of samples using Mg as additive

Sample	mol. of **KNO3**	Mg %	mol. of Mg	mol of **C**	SUC. %	mol. Of SUC.
1	6.44	0.50	0.21	1.67	32.50	0.95
2	6.44	1.00	0.42	1.67	32.00	0.94
3	6.44	1.50	0.63	1.67	31.50	0.92
4	6.44	e0	0.83	1.67	31.00	0.91
5	6.44	2.50	1.04	1.67	30.50	0.89
6	6.44	3.00	1.25	1.67	30.00	0.88
7	6.44	3.50	1.46	1.67	29.50	0.86
8	6.44	4.00	1.67	1.67	29.00	0.85
9	6.44	4.50	1.88	1.67	28.50	0.83
10	6.44	5.00	2.08	1.67	28.00	0.82

The addition of Mg (5%) resulted in increase in combustion temperature by around 250 K while only very slight change in molecular weight was observed from the data. However the specific impulse increased from 111 to around 117. The addition of magnesium have improved the specific impulse by 5.4 %. This is comparable to the performance increase result obtained (2.8%) by (Oyedeko K.F.K & Egwenu S. O., 2021).

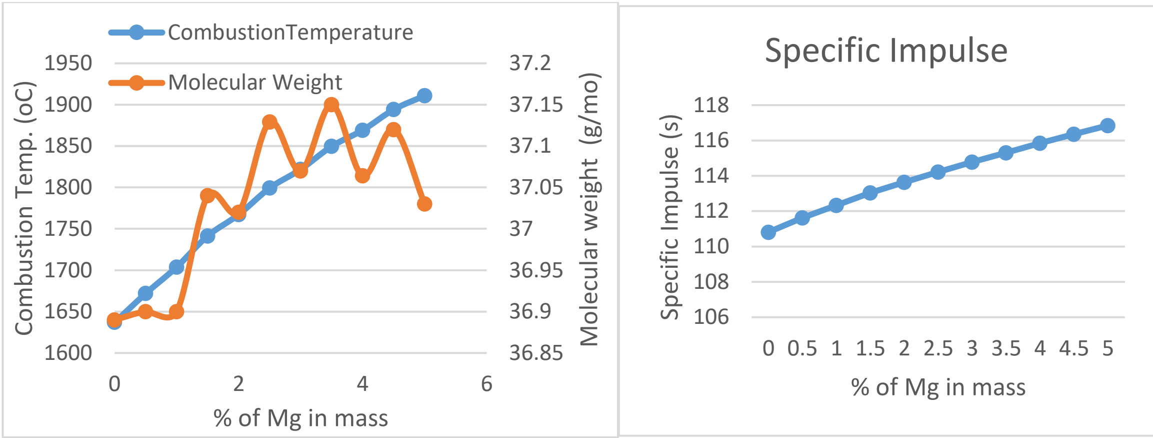

Figure 24: Thermochemical and Performance Result from CEA

The Second additive was aluminum powder. The aluminum added consisted of up to 10%. Ten samples were analyzed by increasing the concentration by 1%. The fuel's combustion temperature increased unsteadily with molecular weight.

Table 7: Chemical Composition of Samples using Al as additive

Sample	mol. of **KNO3**	**Al** %	mol. of **Al**	mol of **C**	SUC. %	mol. Of SUC.
1	6.44	1.00	0.37	1.67	32	0.94
2	6.44	2.00	0.74	1.67	31	0.91
3	6.44	3.00	1.11	1.67	30	0.88
4	6.44	4.00	1.48	1.67	29	0.85
5	6.44	5.00	1.85	1.67	28	0.82
6	6.44	6.00	2.22	1.67	27	0.79
7	6.44	7.00	2.59	1.67	26	0.76
8	6.44	8.00	2.96	1.67	25	0.73
9	6.44	9.00	3.33	1.67	24	0.70
10	6.44	10.00	3.70	1.67	23	0.67

However the specific impulse increased steadily as it is not dependent on temperature or molecular weight but on their ratio. The fuels performance is observed to increase with the addition of Al, until it reached nearly 10%. The finding is in agreement to the former work by (Kumar & Palekar, 2013).

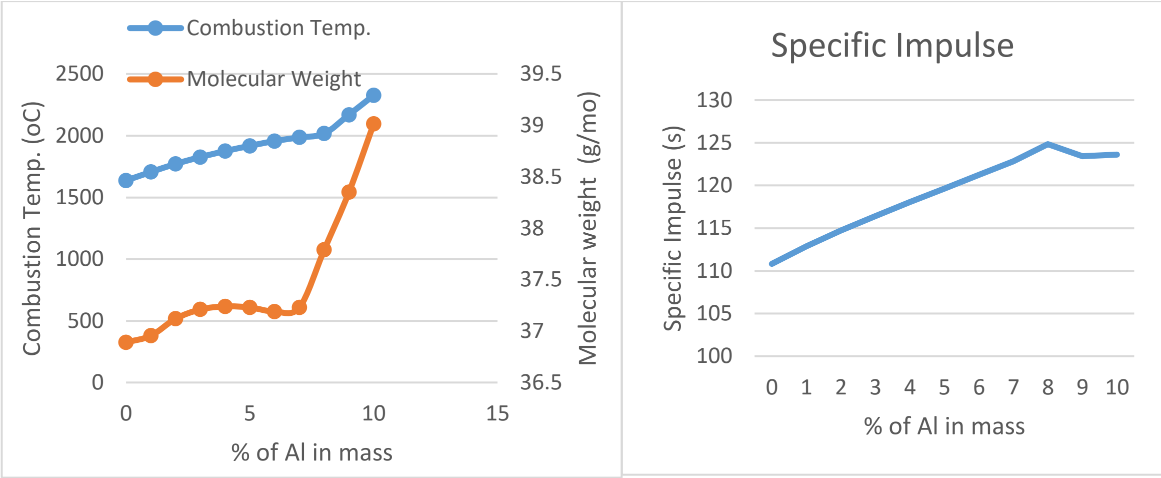

Figure 25: Thermochemical and Performance Result from CEA

The condensate produced when aluminum combustion products condense to liquid aluminum oxide is the main cause of the larger amount of heat released during combustion and hence increase in specific impulse.

The third additives were ammonium nitrate and epoxy. Ammonium nitrate is a strong oxidizing agent which have many atoms of oxygen ready to leave the oxidizer to oxidize the fuel. The epoxy (10% of the fuel by mass) was also added to enhance the mechanical property of the fuel. Ammonium nitrate composition varied from 0% of the composition by mass to 65%.

Table 8: Chemical Composition of Samples using ammonium nitrate and potassium nitrate as a multi-oxidizer

Samples	mass% of KNO3	Mol. of KNO3	mass % of NH4NO3	mol. of NH4NO3	mol. of Al	mol. Of C	mol. of SUC	mass% of Epoxy
1	63	6.24	2	0.25	3.70	1.67	0.29	13
2	61	6.04	4	0.5	3.70	1.67	0.29	13
3	59	5.84	6	0.75	3.70	1.67	0.29	13
4	57	5.64	8	1	3.70	1.67	0.29	13
5	55	5.45	10	1.25	3.70	1.67	0.29	13
6	53	5.25	12	1.5	3.70	1.67	0.29	13
7	51	5.05	14	1.75	3.70	1.67	0.29	13
8	49	4.85	16	2	3.70	1.67	0.29	13
9	47	4.65	18	2.25	3.70	1.67	0.29	13
10	45	4.46	20	2.5	3.70	1.67	0.29	13

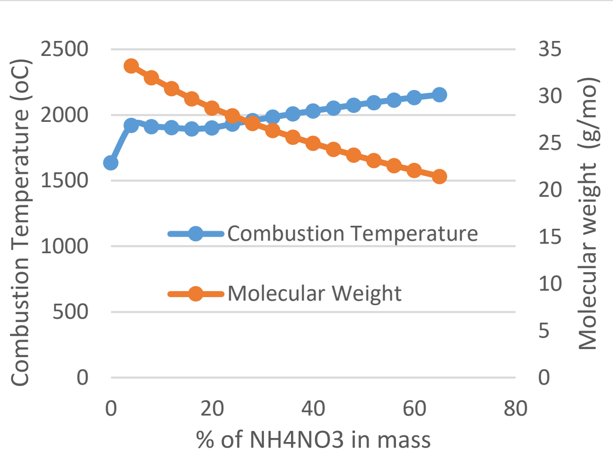

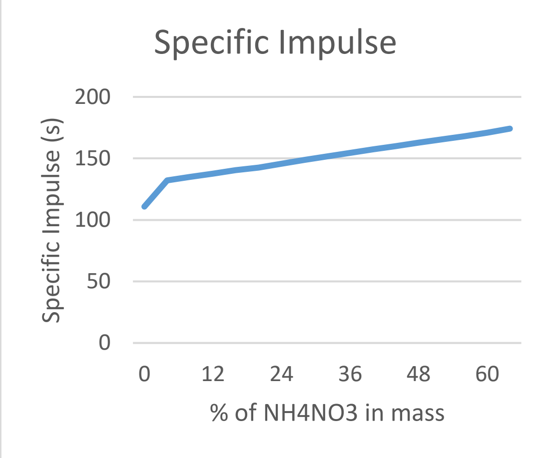

Figure 26: Thermo-physical and performance data results from NASA CEA

The substitution of the KNO3 by NH4NO3 resulted in the decrease in molar weight and increase in combustion temperature. The main reason for the observed decrease in molar weight is because of the low molar weight of ammonium nitrate. The addition of ammonium nitrate increased the specific impulse steadily from 110 s to 174 s. However when ammonium nitrate constitutes of all of the oxidizer amount, 65%, some demerits come with it. This is because of the low burn rate, hygroscopic nature of the compound (Oommen, 1999).

The final selected fuel has NH_4NO_3 the following combustion equation:

$$\mathbf{1.68KNO_3 + 6NH_4N0_3 + 0.38C_{12}H_{22}0_{11} + 3.7Al + 1.67C + 0.357C_{16}H_{24}O_4 \longrightarrow 11.46H_2 + 1.85\,Al_2O_3 + 10.36CO + 1.571CO_2 + 8.38H_2O + 1.19KOH + 6.84\,N_2 + 0.477K}$$

5.2. Design for the Rocket for an Apogee of 20km and payload of 1kg

5.2.1. Initial Design Consideration

The targeted apogee of the rocket is 20 km with a payload of 1kg. This height was selected to break the record held by African student space initiative. Solid rocket propulsion was selected because of its ease in manufacturing the fuel and motor hardware. Propellant to be used for the design is the mixture of potassium nitrate and Ammonium nitrate as oxidizer, sucrose and aluminum as a fuel and epoxy as a binder. Carbon black powder is added as an opacifier. The percentage composition by mass of KNO_3 is 17 %, NH_4NO_3 is 48 %, Al is 10 % and C is 2 %, sucrose is 13 % and epoxy is 10 %. The density of the solid fuel were computed to be 2067.7 kg/m^3 and combustion pressure targeted was 3447.4 kpa.

From PROPEP software, the following thermo-physical and performance parameters are presented in the table below.

Table 9: Chemical equilibrium and performance data obtained from CEA NASA

Molecular Weight	23.72 g/mol
Combustion Temperature	2074.82 K
Specific Heat Ratio, k	1.21
Specific Impulse	198.36 s
Characteristic velocity	4296.76 m/s
Effective Exhaust Velocity	1944.77 m/s

5.2.2. Fuel Grain Design

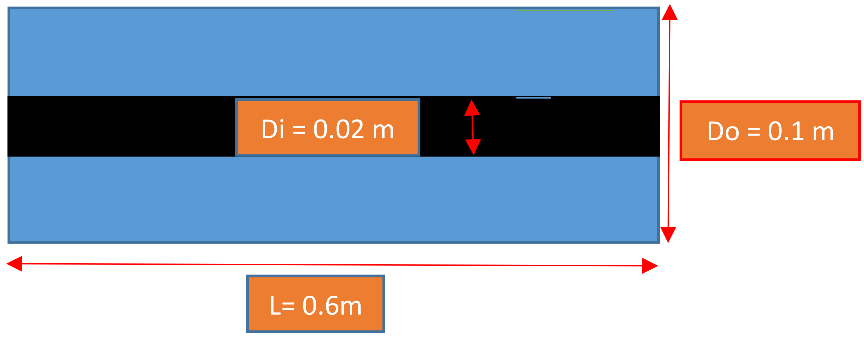

Figure 27: Fuel grain

Based on design consideration, the following fuel mass is used:

$$m = \rho V = \rho \frac{\pi(Do^2 - Di^2)L}{4} = 2067.7 * \frac{\pi * (0.1^2 - 0.02^2) * 0.6}{4} = 9.354\ Kg.$$

Table 10: Burn rate and burn time data (obtained by approximation)

Burn Rate, r	2.86mm/s	Guessed from previous experiment
Burn time, t_1	14 s	Calculated

5.2.3. Nozzle Design

To increase thrust and efficiency by effectively expanding and accelerating the high-pressure exhaust gases released by the rocket motor, converging-diverging nozzle, usually referred to as de Laval nozzles, is employed in this solid rocket motor. Due to the special nature of solid propellants, there are several additional considerations while designing a nozzle for a solid rocket engine. It is assumed that the flow through the nozzle is ideal and isentropic. The following are basic governing equations:

$$\frac{A}{A^*} = \frac{1}{M}\left[\left(\frac{2}{k+1}\right)\left(1+\frac{k-1}{2}\right)M^2\right]^{\frac{k+1}{2(k-1)}} \tag{5.1}$$

$$\frac{T_0}{T} = 1 + \left(\frac{k-1}{2}\right)M^2 \tag{5.2}$$

$$\frac{P_0}{P} = \left[1 + \left(\frac{k-1}{2}\right)M^2\right]^{\frac{k-1}{k}} \tag{5.3}$$

$$\frac{\rho_0}{\rho} = \left[1 + \left(\frac{k-1}{2}\right)M^2\right]^{\frac{1}{k-1}} \tag{5.4}$$

For this fuel's case we can observe the behavior of the above parameters by inserting k = 1.21.

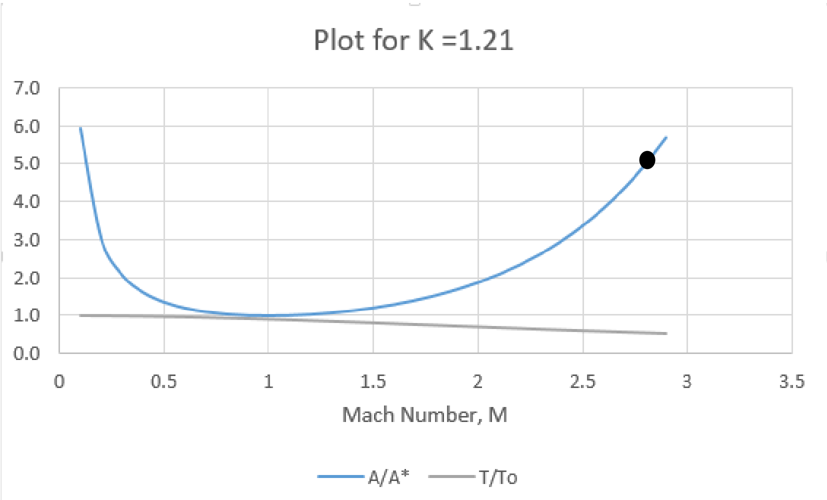

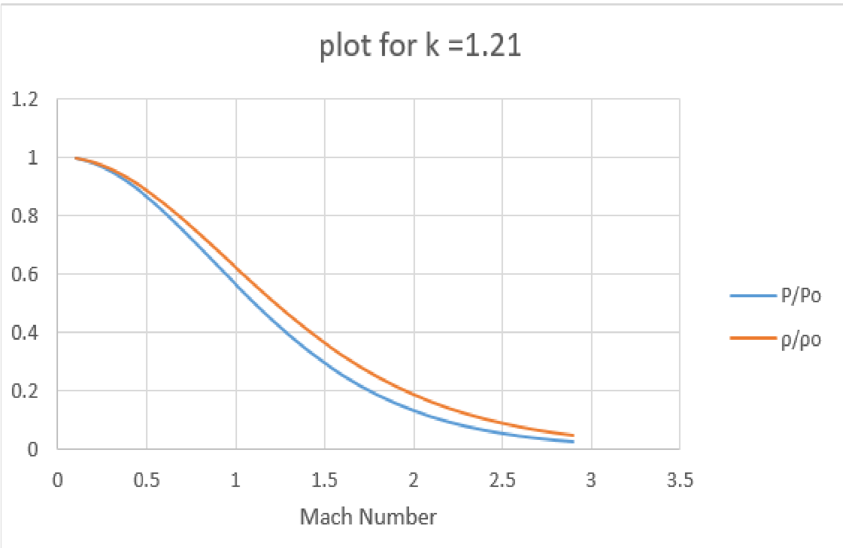

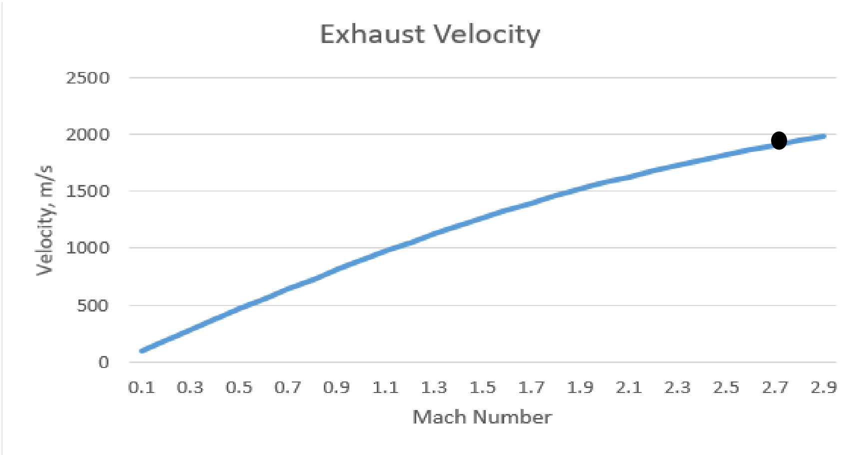

Figure 28: Area ratio, temperature ration, pressure ratio and exhaust velocity vs Mach number

The exhaust gas's velocity and hence the efficiency increases as the ration of exit area to throat area is increased but from manufacturing difficulty exit area ratio of 7.01 was selected. The throat area can be calculated by:

$$\dot{m} = \frac{Total\ Mass\ of\ Fuel}{Burn\ Time} = \frac{m_{f\ total}}{t} = \frac{9.354\ kg}{14\ s} = 0.668\ \frac{kg}{s}$$

From the definition of characteristic velocity:

$$A^{*}P = \dot{m}c^{*}$$

$$A^{*} = \frac{\dot{m}c^{*}}{P} = \frac{0.668\frac{kg}{s} * 4296.38\ m/s}{3447380\ Pa} = 5.8288 * 10^{-4}\ m^{2}$$

$$d^{*} = 0.03237m = 32.37\ mm$$

5.3. Flight Trajectory Simulation

We lay down the fundamental mathematical formulas, scientific rules, and presumptions in this portion of a model that enables us to calculate the theoretical trajectory of our rocket based on the values of its design parameters.

The simplified flight trajectory equation is given by Tsilkowiskey equation:

$$v_f = v_{eff} ln\left(\frac{m_i}{m_f}\right) - g_o t$$

Where, V_f is the final velocity of the rocket, m_i is initial mass of the rocket, mf is the final mass of the rocket, go is the gravity and t is the flight time. However this equation does not incorporate the aerodynamic drag on the rocket and

The flight trajectory is divided in to two: flight while the fuel is being burnt and flight after burnout. For the first case mass of the rocket continuously changes and also there is a thrust force from propulsion. But for the after burnout the rocket has already reached a velocity of V and height of h_o. The rocket is still travelling at very high speed and will continue to travel by inertia until maximum apogee is reached. The height as the function of time for each case is given as:

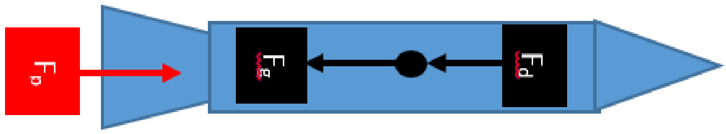

Figure 29: Force balance on the rocket while the fuel is burning

From force balance on the rocket:

$$a = \frac{Propulsion\ force\ (F_p) - Gravitational\ pull\ (F_g) - Aerodynamic\ force\ (F_a)}{m} \tag{5.5}$$

$$h(t) = h_o + Vt + \frac{F_T - (F_D + F_g)}{2m_t} t^2 \tag{5.6}$$

On the other hand we can obtain velocity to be:

$$V(t) = V + \frac{F_T - (F_D + F_g)}{m_t} t \tag{5.7}$$

Force due to thrust generated by rocket propulsion is given by:

$$F_T = \dot{m} * c_{eff} \tag{5.8}$$

Force due to gravity at any height is given by:

$$F_g = m_t g_o \frac{R^2}{[R+h]^2} \tag{5.9}$$

Force due to drag is given by:

$$F_D = \frac{1}{2} C_D A \rho V^2 \tag{5.10}$$

In simulating rocket flight, the atmosphere is important. It presents a number of variables that have an impact on a rocket's performance, trajectory, and general behavior during ascent. Even though atmosphere has influence on flight in numerous ways only the effect on aerodynamic force via the change in air density is taken into consideration. Density of air changes with height from sea level and can be approximated by:

$$\rho = \rho_o e^{\frac{h}{H}} \tag{5.11}$$

Mass of the fuel changes with time and is given by:

$$m_t = m_{initial} - \dot{m}t \tag{5.12}$$

Where H is the so-called "scale height" of the atmosphere, 8000 meters, and ρ_o is the air density at sea level.

However, there is no analytical solution to this problem. This is because the trajectory will continually change depending on a number of factors, such as v. As a result, we will need to use a numerical approach to determine the trajectory. The following algorithm was employed to solve the equation:

Step 1: Define the design constraints. V, m_o and h_o. C_D is seen as being equivalent to 0.4. Set simulation settings as well, such as the t-step time step size. The initial time, t_o, is specified to be 0.

Step 2: Using the atmospheric model, determine the air density the starting height.

Step 4: Update the object's velocity and object's height using the equation of height and velocity above.

Step 5: Use the atmospheric and mass model to update the air density and mass at the increased time and height.

Step 6: Keep performing steps 4 and 5 back-to-back until the rocket’s fuel mass becomes empty. The atmospheric characteristics from the preceding phase are taken into account at each stage.

Step 7: Go back to the step one with taking the updated velocity and height to go through up to step six to calculate the trajectory for the after burnout flight.

The preceding approach is now simple to include into a computer application. The python program was used to solve it.

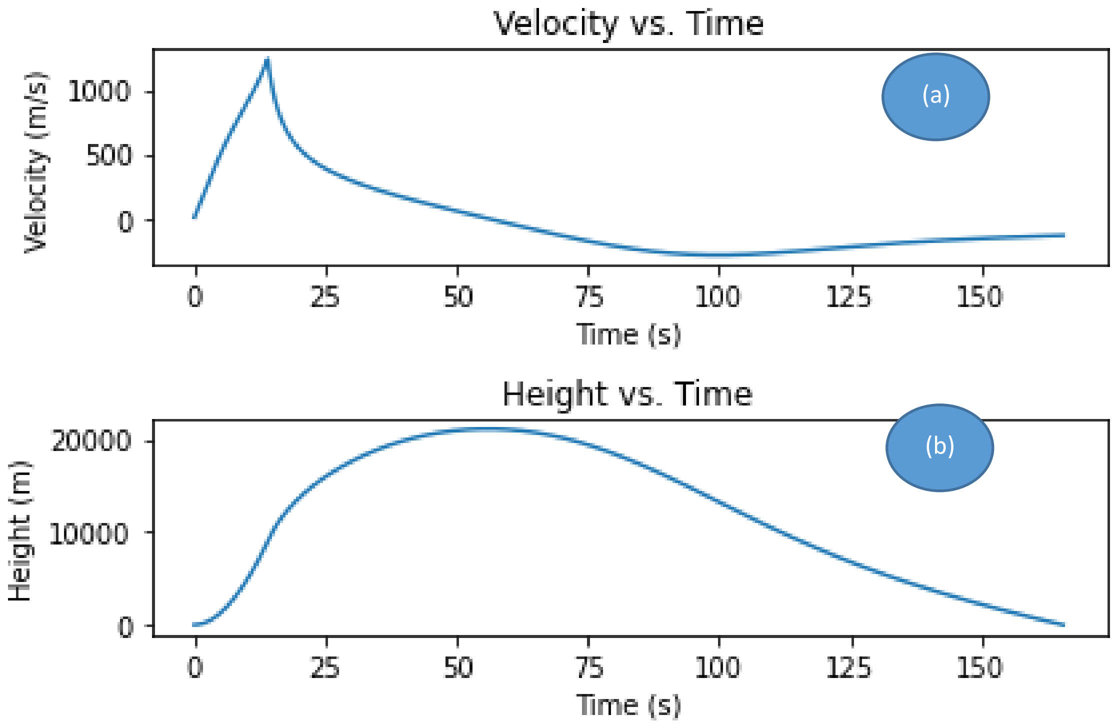

Figure 30: Flight trajectory (a) velocity vs time and (b) height vs time

Based on the simulation using Python, the solid rocket motor's flight trajectory resulted in several key parameters which has similar flight trajectory shape with (Milne et al., 2023). Let's expand on each of these aspects:

- Apogee: The rocket reached an apogee, which is the highest point in its trajectory, of close to 20 km. This indicates that the rocket achieved a significant altitude during its ascent phase before starting its descent back to the ground.
- Time to Apogee: The rocket took approximately 55 seconds to reach its apogee. This duration represents the time it took for the rocket to ascend to its highest point in the trajectory, where it reached the altitude of close to 20 km.
- Total Flight Time: The entire flight of the rocket, from the moment of launch until it touched the ground, lasted 165 seconds. This duration includes both the ascent and descent phases of the rocket's trajectory.
- Total Mass of the Rocket: The total mass of the rocket was selected to be 12.345 units. This value represents the combined mass of the rocket, including both the propellant (fuel) and the structural components.
- Fuel Mass Fraction: The fuel mass fraction indicates the proportion of the total mass of the rocket that is attributed to the propellant or fuel. In this case, the fuel mass fraction is 0.757, meaning that approximately 75.7% of the total mass is fuel.

CHAPTER SIX

6. CONCLUSION AND RECOMMENDATION

6.1. Conclusion

In conclusion, this thesis has successfully addressed the objective of designing a rocket capable of reaching an apogee of 20 km with a payload of 1 kg. The research focused on analyzing sucrose-based fuels with the incorporation of additives to enhance propulsion efficiency. To assess the performance of these fuels, a meticulously developed small-scale rocket motor test setup was employed, equipped with various sensors and a microprocessor for data logging.

The initial tests conducted on the setup served the purpose of verifying its functionality. Although the data logging system was not connected during the first two tests, it was confirmed that the setup performed as intended. The conventional KNSU fuel with a 65/35 oxidizer to fuel ratio was used for these tests. Subsequently, the second round of testing aimed to evaluate the electrical circuit, which exhibited flawless performance. However, it was noted that the thermocouples used for measuring exhaust gas temperature did not provide accurate readings due to their high thermal inertia and slow response time. This finding highlighted the challenge of accurately measuring temperature during the short-lived burn time of small-scale rockets.

For the fourth test, the focus shifted towards obtaining data necessary for calculating performance parameters. Once again, the conventional KNSU fuel with a 65/35 oxidizer to fuel ratio was utilized. The test results revealed a maximum pressure of 311.64 kpa and an average pressure of 63.4 kpa. In terms of thrust, the maximum and average values were recorded as 1.25 N and 0.73 N, respectively. The burn rate was measured to be 1 cm/s. The total impulse was calculated to be 9.54 Ns, while the specific impulse was determined to be 34.12 seconds. Although the thermocouples failed to accurately indicate the combustion and exhaust gas temperatures, they were able to mark the beginning and end of combustion, thus enabling the determination of the combustion duration.

Regrettably, the final test encountered a significant setback when the pressure chamber suddenly and violently exploded, resulting in extensive damage to the test setup. The pressure gradually increased during the first second but unexpectedly surged to 7680.76kpa, leading to the catastrophic failure. Despite this setback, the thesis employed the CEA NASA software to evaluate the performance of the formulated fuel.

To enhance the performance of the KNSU propellant fuel, three different additives were introduced and analyzed. The first additive, magnesium powder, was incorporated in varying amounts ranging from 1% to 5% of the fuel's mass. The inclusion of magnesium resulted in a notable improvement of 5.4% in specific impulse. The second additive, aluminum powder, was introduced in concentrations of up to 10%. Through the analysis of ten samples with increasing aluminum concentrations, a steady increase in specific impulse was observed until reaching nearly 10% concentration. Finally, ammonium nitrate and epoxy were used as the third additives. The gradual replacement of potassium nitrate with ammonium nitrate led to a consistent increase in specific impulse from 110 seconds to 174 seconds. However, it was noted that using ammonium nitrate as the sole oxidizer, constituting 65% of the mixture, presented some drawbacks.

The rocket design incorporated a converging-diverging nozzle, commonly known as a de Laval nozzle, with an exit area to throat area ratio of 5.0 and a throat area of $A^* = 8.225 * 10^{-4}\ m^2$. This design choice aimed to maximize the exhaust velocity and optimize the rocket's performance while considering manufacturing difficulty.

Finally, the flight trajectory and duration were simulated using Python. The results demonstrated that the rocket successfully reached an apogee close to the desired 20 km mark within approximately 55 seconds. The total flight time, from launch to touchdown, was estimated to be 165 seconds. The rocket's total mass was determined to be 12.345 kg, with a fuel mass fraction of 0.757.

In summary, this thesis has made a contributions to the field of rocket design and propulsion. By analyzing different fuel compositions and additives, as well as optimizing the nozzle design, the research has provided valuable insights into enhancing rocket performance. The flight trajectory simulations further validate the effectiveness of the design and provide a foundation for future rocket development and optimization endeavors.

6.2. Recommendation

This thesis dealt with thermochemical and performance analysis of sucrose based fuels with ways to improve them. Additionally design of the rocket, motor and nozzle were carried out. On top of that, flight trajectory of the rocket was simulated using computer analysis giving the maximum height and duration of the flight. Although large effort was applied and several attempts were undertaken to carry out this project, as the project is done with so much little resources and time, the project unveiled many areas open to further study and research. The following were recommended for further attempts on this area:

- Small scale rocket with larger size can be constructed which can hold larger amount of fuel. The smallness of the test setup with small throat area is believed to be the major cause for the restriction of the burned fuel in the nozzle ending up with explosion.
- To measure the exact temperature of the combustion and exhaust gas, other temperature measuring techniques, such as pyrometer, can be utilized.
- The use of software such as BurnSim to analyze internal ballistic performance of the designed rocket and the use of CHEMKIN software for the chemical kinetics of the propellant for validation of the analytical work and for better result.
- Complete design and manufacturing of the rocket can be done for the required apogee and payload with potential application in meteorology.
- The last but not the least is the incorporation due safety. Since the science of rocket is tied with very explosive chemicals, remote test site and proper safety precautions should be incorporated.

REFERENCES

Adeniyi, G. O., Nkere, I., Adetoro, L. M., & Sholiyi, O. S. (2021). Performance Analysis of a Dual-Fuel Sugar Based Solid Rocket Propellant. *European Journal of Engineering and Technology Research*, *6*(2), 34–41. https://doi.org/10.24018/ejeng.2021.6.2.2347

Armold, D., Boyer, J. E., Kuo, K., Fuller, J. K., Desain, J., & Curtiss, T. J. (2013, July 14). Test of Hybrid Rocket Fuel Grains with Swirl Patterns Fabricated Using Rapid Prototyping Technology. *49th AIAA/ASME/SAE/ASEE Joint Propulsion Conference*. 49th AIAA/ASME/SAE/ASEE Joint Propulsion Conference, San Jose, CA. https://doi.org/10.2514/6.2013-4141

Bachrach, W. (1987, June 29). Material development and the solid rocket motor. *23rd Joint Propulsion Conference*. 23rd Joint Propulsion Conference, San Diego,CA,U.S.A. https://doi.org/10.2514/6.1987-1819

Clare, S. (2021, February 12). *Nuclear Propulsion Could Help Get Humans to Mars Faster*. NASA Space Travel. https://www.nasa.gov/directorates/spacetech/nuclear-propulsion-could-help-get-humans-to-mars-faster

Elaine, M. M. (2004, April 12). What is a Sounding Rocket? *Research Aircraft*. https://www.nasa.gov/missions/research/f_sounding.html

Felix, W. G., Sammy, K. O., Jeff, M., Ian, K., Bernard, O., & Shohei, A. (2021, October 7). Development of Solid Propellant Motor for Low Altitude Model Rockets. *Sustainable Research and Innovation Conference*.

Fossumstuen, K., Tokerud, D., Biserod, H., Orbekk, E., Tenden, S., Kaiserman, M., Rodack, M., Spate, W., Winetrobe, S., Royce, B., & Wallace, S. (2005, July 10). The Hypervelocity Anti-Tank Missile Development Program; Rocket Motor Design and Development. *41st AIAA/ASME/SAE/ASEE Joint Propulsion*

Conference & Exhibit. 41st AIAA/ASME/SAE/ASEE Joint Propulsion Conference & Exhibit, Tucson, Arizona. https://doi.org/10.2514/6.2005-4172

Frederick, R. A., Whitehead, J. J., Knox, L. R., & Moser, M. D. (2007). Regression Rates Study of Mixed Hybrid Propellants. *Journal of Propulsion and Power, 23*(1), 175–180. https://doi.org/10.2514/1.14327

George, K., Panda, B. P., Mohanty, S., & Nayak, S. K. (2018). Recent developments in elastomeric heat shielding materials for solid rocket motor casing application for future perspective. *Polymers for Advanced Technologies*, *29*(1), 8–21. https://doi.org/10.1002/pat.4101

George, P. S., & Oscar, B. (2017). *Rocket Propulsion Elements* (9th ed.). John Wiley & Sons, Inc., Hoboken, New Jersey.

Goel, R. K., Yadav, C. S., Vishnoi, S., & Rastogi, R. (2021). Smart agriculture – Urgent need of the day in developing countries. *Sustainable Computing: Informatics and Systems*, *30*, 100512. https://doi.org/10.1016/j.suscom.2021.100512

Indian Space Research Organization,. (2022, November 11). Sounding Rockets. *Indian Space Research Organization, Department of Space*. https://www.isro.gov.in/soundingRockets.html#:~:text=Sounding%20rockets%20are%20one%20or,in%20launch%20vehicles%20and%20satellites.

Ji, Y., Han, S., Chen, Z., Wu, H., Guo, S., Yan, N., Li, H., & Luan, T. (2022). Understanding the Role of Carbon Fiber Skeletons in Silicone Rubber-Based Ablative Composites. *Polymers*, *14*(2), 268. https://doi.org/10.3390/polym14020268

Jonathan, R. S. (2018). *Development, Modeling and Testing of Thermal Protection Systems in Small, Slow-Burning Solid Rocket Motors*. Massachusetts Institute of Technology.

Kattus, J. R. (1957). Structural Materials for Missile Applications at Very High Temperatures. *Journal of Jet Propulsion*, *27*(6), 644–649. https://doi.org/10.2514/8.12898

M. Pavan Kumar & , Sanjeev. G. Palekar. (2013). *Design and Performance Analysis of Aluminized Sugar Aided Rocket Propulsion Using MATLAB*.

Mateduc Composites. (n.d.). FILAMENT WINDING. *Filament Winding*. Retrieved January 17, 2023, from https://www.mateduc-composites.com/en/process-products/our-3-technologies/filament-winding

Matthew, T. V. (2017). *Development, Modeling and Testing of a Slow -Burning Solid Rocket Propulsion System*. Massachusetts Institute of Technology.

McClain, M. S., Gunduz, I. E., & Son, S. F. (2019, January 7). Additive Manufacturing of Carbon Fiber Reinforced Silicon Carbide Solid Rocket Nozzles. *AIAA Scitech 2019 Forum*. AIAA Scitech 2019 Forum, San Diego, California. https://doi.org/10.2514/6.2019-0408

Michael, M., Aaron, E. L., & Josh, M. (Directors). (2021, April 12). *Animation: The James Webb Space Telescope's Orbit: NASA's Goddard Space Flight Center*. https://www.youtube.com/watch?v=6cUe4oMk69E&list=TLGG8tIphgpDAHkxNzAxMjAyMw&t=1s

Milne, B., Samson, S., Carrese, R., Gardi, A., & Sabatini, R. (2023). High-Fidelity Dynamics Modelling for the Design of a High-Altitude Supersonic Sounding Rocket. *Designs*, *7*(1), 32. https://doi.org/10.3390/designs7010032

Mohan, K., Usha, K. M., Anandapadmanabhan, E. N., & Chakravarthy, P. (2017). Effect of Fibre Orientation on the Properties and Functional Performance of Ablative Materials for Solid Rocket Motors. *Transactions of the Indian Institute of Metals*, *70*(9), 2407–2413. https://doi.org/10.1007/s12666-017-1102-1

Moody, K. J., Walsh, A. M., Ngo, A. D., Whyte, S., Stottlemyre, A., & Rouser, K. P. (2020, January 6). Development of Sorbitol-Based Solid Rocket Motors for Propulsion Education. *AIAA Scitech 2020 Forum*. AIAA Scitech 2020 Forum, Orlando, FL. https://doi.org/10.2514/6.2020-0067

Mosa, M., Mokhtar Kotb, M., Fouda, H., & Gobara, M. (2022). Study of Elastomeric Heat Shielding Materials for Solid Rocket Motor Insulation. *Journal of Physics: Conference Series*, *2305*(1), 012037. https://doi.org/10.1088/1742-6596/2305/1/012037

NASA, Goddard Space Flight Center. (n.d.). A Solar Orbit. *James Webb Space Telescope*. Retrieved January 13, 2023, from https://webb.nasa.gov/content/about/orbit.html

Nowakowski, P., Okninski, A., Pakosz, M., Cieslinski, D., Bartkowiak, B., & Wolanski, P. (2017). Development of small solid rocket boosters for the ILR-33 sounding rocket. *Acta Astronautica*, *138*, 374–383. https://doi.org/10.1016/j.actaastro.2017.06.007

Oommen, C. (1999). Ammonium nitrate: A promising rocket propellant oxidizer. *Journal of Hazardous Materials*, *67*(3), 253–281. https://doi.org/10.1016/S0304-3894(99)00039-4

Ouzemou, J.-E., El Harti, A., Lhissou, R., El Moujahid, A., Bouch, N., El Ouazzani, R., Bachaoui, E. M., & El Ghmari, A. (2018). Crop type mapping from pansharpened Landsat 8 NDVI data: A case of a highly fragmented and intensive agricultural system. *Remote Sensing Applications: Society and Environment*, *11*, 94–103. https://doi.org/10.1016/j.rsase.2018.05.002

Oyedeko K.F.K & Egwenu S. O. (2021). Modelling of the formulated solid rocket propellant characteristics. *Global Journal of Engineering and Technology Advances*, *6*(2), 061–073. https://doi.org/10.30574/gjeta.2021.6.2.0017

Rao, G. V. R. (1961). Recent Developments in Rocket Nozzle Configurations. *ARS Journal*, *31*(11), 1488–1494. https://doi.org/10.2514/8.5837

Rossi, C., Orieux, S., Larangot, B., Do Conto, T., & Estève, D. (2002). Design, fabrication and modeling of solid propellant microrocket-application to micropropulsion. *Sensors and Actuators A: Physical*, *99*(1–2), 125–133. https://doi.org/10.1016/S0924-4247(01)00900-1

Sandra, M. (2017, August 7). What Is Rocket. *NASA Educational Technology Services*. https://www.nasa.gov/audience/forstudents/k-4/stories/nasa-knows/what-is-a-rocket-k4.html

Sapozhnikov, I., Leitner, A., Natan, B., & Mograbi, E. (2022). Investigation of the Ablative Properties of an EPDM\Kevlar Insulator in a Solid Rocket Motor. *Propellants, Explosives, Pyrotechnics*, *47*(1). https://doi.org/10.1002/prep.202100051

Simonetta, D. P. (2022, December). *Space Technology and the Implementation of the 2030 Agenda*. UN Chronicle. https://www.un.org/en/chronicle/article/space-technology-and-implementation-2030-agenda

Singh, D. A. (2015). *Sugar Based Rocket Propulsion System-Making, Analysis & Limitations*. *2*(5).

Vernacchia, M. T., Mathesius, K. J., & Hansman, R. J. (2022). Low-Thrust Solid Rocket Motors for Small, Fast Aircraft Propulsion: Design and Development. *Journal of Propulsion and Power*, *38*(1), 122–134. https://doi.org/10.2514/1.B38104

Weinzierl, M. (2018). Space, the Final Economic Frontier. *Journal of Economic Perspectives*, *32*(2), 173–192. https://doi.org/10.1257/jep.32.2.173

Wondwosen, T. (2022, March 24). *Space science capabilities depend on quality education*. University World News, Africa Edition.

https://www.universityworldnews.com/post.php?story=20220320165742925#:~:text=For%20too%20long%2C%20space%20science,plays%20in%20their%20national%20aspirations

Zolla, P. M., Migliorino, M. T., Bianchi, D., Nasuti, F., Pellegrini, R. C., & Cavallini, E. (2021). A Computational Tool for the Design of Hybrid Rockets. *Aerotecnica Missili & Spazio*, *100*(3), 253–262. https://doi.org/10.1007/s42496-021-00085-3

APPENDIXES

A. Small Scale Rocket Motor Test Results

Five tests have been conducted. The first two tests were conducted to check whether the test setup developed performed as it was designed for. The data logging system has not been connected for these two tests. The fuel was the conventional KNSU with 65/35 oxidizer to fuel ratio. The tests were carried out successfully. The measured average burn rate for both the tests were 1 cm/s. It was measured by dividing the length of the combustion chamber in which the fuel is filled to the measured burn time. The length of the fuel was 10cm while also the burn duration was around 10 seconds. The ratio of the combustion chamber diameter, which is the diameter of the fuel strand, to the diameter of the nozzle were 7. The fuel burning mode were end burning where the fuel burned from one end to the opposite end longitudinally.

Figure 31: The captions of first round tests

The fuel burned smoothly from the start to the end. However the hot flame from the nozzle, the mass flow rate, noise and hence thrust increased very much on the last final second of the burn. The major reason for this was because of the crack formed in the thermal protection system which increased the fuel accumulated around at the bottom. The second possible reason is because of the difference in the compactness of the fuel longitudinally. The compaction difference came in the process of adding the fuel to the chamber little by little followed by compression. The fuel added first was around one third of the chamber length after it was compressed. Hence the fuel is added and compressed three times until the chamber was full. This increases the fuel added first to be compressed about three times which might have increased the burn rate, pressure and hence mass flow rate and thrust. But on the final test the problem was partially resolved by refilling the cracks in the thermal protection system.

After the first test was conducted and the setup was checked for its proper functionality, the data logging setup was installed and one additional test was carried out to verify that the circuit and all the components performed right. The test was conducted successfully with confirmation that all the components worked as intended. The data was properly recorded on computer. However, the thermocouple used to measure the exit temperature recorded maximum of 50 ^{0}C which is very small compared to the values obtained by NASA CEA software and also values from other literature which are above 1000^{0}c. This implied exhaust gas temperature measurement of small scale rockets cannot be measured properly for such short lived burn time. This is because of the high thermal inertia and response time of the thermocouples.

Figure 32: Caption of second round test

The fourth test was undertaken to obtain the data used to calculate performance parameters. Again the fuel used were conventional KNSU with 65/35 oxidizer to fuel ration. A slightly erratic burning pattern and pressure buildup in the chamber were observed. This is obviously the problem that this propellant composition always has. The formulation has a quick burn rate and weak mechanical properties, which causes the propellant burning region to abruptly expand up and produce a lot of combustion gas flux.

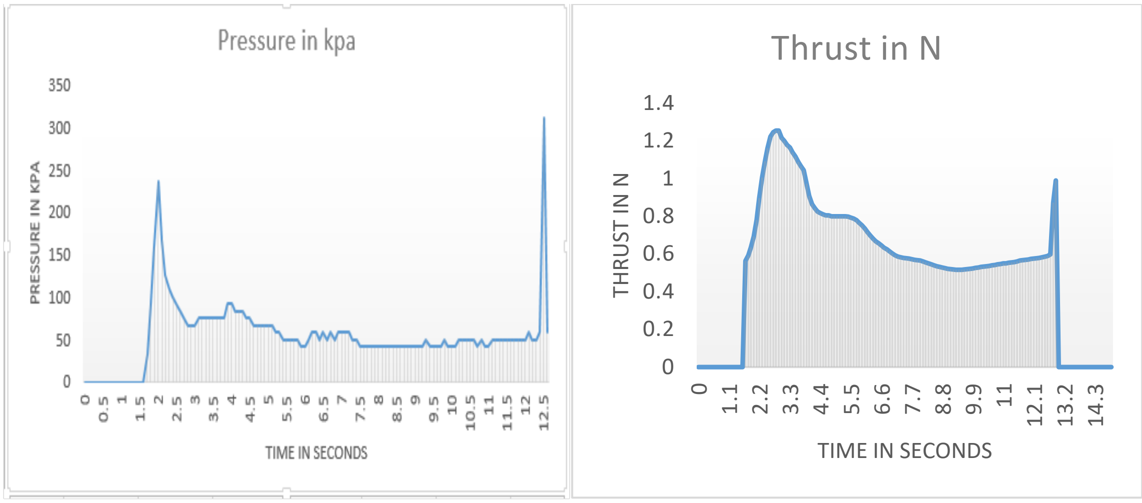

Figure 33: Pressure and thrust vs time

The maximum and average pressure was 311.6 and 63.4 kpa respectively. Whereas maximum and average thrust generated was 1.25N and 0.73N respectively. The sharp pressure rise at start and end were because of the cavities formed while manufacturing the combustion chamber and also during compression of the fuel by hammering. The length of the fuel strand were 11 cm and the burn time was 11 seconds. Hence the burn rate was 1cm/s. The measured total impulse was 9.54 whereas specific impulse was 34.12 sec.

B. CEA NASA chemical equilibrium analysis and performance parameter result for 5% of Mg powder by mass.

```
FileEditor:ppp.out


 *******************************************************************************

         NASA-GLENN CHEMICAL EQUILIBRIUM PROGRAM CEA2, MAY 21, 2004
                   BY  BONNIE MCBRIDE AND SANFORD GORDON
      REFS: NASA RP-1311, PART I, 1994 AND NASA RP-1311, PART II, 1996

 *******************************************************************************



 problem
     rocket  equilibrium  tcest,k=2000
   p,psia=500,
   sup,ae/at=2,
 react
   fuel=KNO3(a) moles=6.44  t,k=298.15
   name=Mg(cr) moles=2.08  t,k=298.15
   name=C(gr) moles=1.67  t,k=298.15
   fuel=Sucrose  moles=0.82  t,k=298.15
     h,kj/mol=-2226.4  C 12 H 22 O 11
 output
      siunits short
 end




              THEORETICAL ROCKET PERFORMANCE ASSUMING EQUILIBRIUM

           COMPOSITION DURING EXPANSION FROM INFINITE AREA COMBUSTOR

 Pin =   500.0 PSIA
 CASE =

             REACTANT                    MOLES         ENERGY      TEMP
                                                      KJ/KG-MOL      K
 FUEL        KNO3(a)                   6.4400000   -493999.998    298.150
 NAME        Mg(cr)                    2.0800000         0.000    298.150
 NAME        C(gr)                     1.6700000         0.000    298.150
 FUEL        Sucrose                   0.8200000  -2226400.000    298.150

 O/F=    0.00000  %FUEL=100.000000  R,EQ.RATIO= 1.317572  PHI,EQ.RATIO= 0.000000

                 CHAMBER   THROAT     EXIT
 Pinf/P            1.0000   1.7213   7.3767
 P, BAR            34.474   20.028   4.6733
 T, K             1910.86  1820.96  1615.69
 RHO, KG/CU M    9.4570 0 5.8247 0 1.5755 0
 H, KJ/KG        -4995.02 -5187.29 -5651.99
 U, KJ/KG        -5359.55 -5531.13 -5948.61
 G, KJ/KG        -18279.6 -17846.9 -16884.5
 S, KJ/(KG)(K)     6.9522   6.9522   6.9522

 M, (1/n)          43.585   44.033   45.289
 MW, MOL WT        37.030   37.177   37.594
```

FileEditor:ppp.out

```
 (dLV/dLP)t      -1.10963 -1.10190 -1.07818
 (dLV/dLT)p        2.4104   2.3958   2.2437
 Cp, KJ/(KG)(K)    5.0614   5.2176   5.2604
 GAMMAs            1.1228   1.1183   1.1081
 SON VEL,M/SEC      639.8    620.1    573.3
 MACH NUMBER        0.000    1.000    1.999

 PERFORMANCE PARAMETERS

 Ae/At                      1.0000   2.0000
 CSTAR, M/SEC                954.4    954.4
 CF                         0.6497   1.2010
 Ivac, M/SEC                1174.6   1405.0
 Isp, M/SEC                  620.1   1146.3


 MOLE FRACTIONS

 *CO              0.23422  0.22994  0.21799
 *CO2             0.11730  0.11825  0.12171
 *H               0.00004  0.00003  0.00001
 *H2              0.09352  0.09922  0.11550
 H2O              0.19899  0.19907  0.19799
 *K               0.00921  0.00906  0.00803
 KCN              0.00001  0.00001  0.00000
 KH               0.00006  0.00004  0.00001
 KOH              0.07308  0.06588  0.04648
 K2               0.00001  0.00001  0.00000
 K2CO3            0.00012  0.00011  0.00007
 K2O2H2           0.00410  0.00324  0.00153
 NH3              0.00001  0.00001  0.00000
 *N2              0.11894  0.11941  0.12076
 *OH              0.00001  0.00000  0.00000
 K2CO3(L)         0.07354  0.07857  0.09190
 MgO(cr)          0.07683  0.07714  0.07801

  * THERMODYNAMIC PROPERTIES FITTED TO 20000.K
```

C. CEA NASA chemical equilibrium analysis and performance parameter result for 10% of Al powder by mass.

```
*******************************************************************************

        NASA-GLENN CHEMICAL EQUILIBRIUM PROGRAM CEA2, MAY 21, 2004
                  BY  BONNIE MCBRIDE AND SANFORD GORDON
     REFS: NASA RP-1311, PART I, 1994 AND NASA RP-1311, PART II, 1996

*******************************************************************************



problem
    rocket  equilibrium  tcest,k=2000
  p,psia=500,
  sup,ae/at=2,
react
  fuel=KNO3(a) moles=6.44  t,k=298.15
  name=AL(cr) moles=3.70  t,k=298.15
  name=C(gr) moles=1.67  t,k=298.15
  fuel=Sucrose  moles=0.67  t,k=298.15
    h,kj/mol=-2226.4  C 12 H 22 O 11
output
     siunits short
end




             THEORETICAL ROCKET PERFORMANCE ASSUMING EQUILIBRIUM

          COMPOSITION DURING EXPANSION FROM INFINITE AREA COMBUSTOR

Pin =   500.0 PSIA
CASE =

            REACTANT                         MOLES         ENERGY      TEMP
                                                          KJ/KG-MOL      K
FUEL        KNO3(a)                        6.4400000   -493999.998    298.150
NAME        AL(cr)                         3.7000000         0.000    298.150
NAME        C(gr)                          1.6700000         0.000    298.150
FUEL        Sucrose                        0.6700000  -2226400.000    298.150

O/F=    0.00000  %FUEL=100.000000  R,EQ.RATIO= 1.332334  PHI,EQ.RATIO= 0.00000

                 CHAMBER   THROAT     EXIT
Pinf/P            1.0000   1.7347   6.8181
P, BAR            34.474   19.873   5.0562
T, K             2326.86  2174.56  1986.00
RHO, KG/CU M    8.1244 0 5.0090 0 1.3889 0
H, KJ/KG        -4671.49 -4897.56 -5406.60
U, KJ/KG        -5095.81 -5294.30 -5770.65
G, KJ/KG        -20817.2 -19986.5 -19187.1
S, KJ/(KG)(K)     6.9388   6.9388   6.9388

M, (1/n)          45.595   45.572   45.358
MW, MOL WT        39.015   38.999   38.841
```

```
FileEditor:ppp.out

 (dLV/dLP)t      -1.00642 -1.00651 -1.00673
 (dLV/dLT)p        1.0447   1.0463   0.0000
 Cp, KJ/(KG)(K)    1.5564   1.5480   0.0000
 GAMMAs            1.1383   1.1396   0.9933
 SON VEL,M/SEC      695.0    672.4    601.3
 MACH NUMBER        0.000    1.000    2.016

 PERFORMANCE PARAMETERS

 Ae/At                      1.0000   2.0000
 CSTAR, M/SEC               1023.5   1023.5
 CF                         0.6569   1.1846
 Ivac, M/SEC                1262.4   1512.8
 Isp, M/SEC                  672.4   1212.5


 MOLE FRACTIONS

 *CO              0.26402  0.26065  0.25235
 *CO2             0.11466  0.11787  0.12466
 *H               0.00047  0.00027  0.00017
 *H2              0.07056  0.07329  0.07665
 H2O              0.17420  0.17211  0.17150
 *K               0.02206  0.02323  0.03051
 KCN              0.00001  0.00000  0.00000
 KH               0.00019  0.00013  0.00007
 KO               0.00003  0.00002  0.00001
 KOH              0.08279  0.08165  0.07489
 K2               0.00003  0.00002  0.00002
 K2CO3            0.00002  0.00002  0.00001
 K2O2H2           0.00084  0.00084  0.00042
 *NO              0.00001  0.00000  0.00000
 *N2              0.12557  0.12553  0.12503
 *OH              0.00021  0.00010  0.00004
 KALO2(I)         0.00000  0.00000  0.11483
 KALO2(L)         0.14430  0.14425  0.02883

  * THERMODYNAMIC PROPERTIES FITTED TO 20000.K
```

D. Measuring Instrument Description and Specifications

MAX6675 Thermocouple: The following are some of the most notable characteristics of the MAX6675 Thermocouple Temperature Module with Probe.

- The module incorporates the MAX6675 IC, capable of handling temperature readings ranging from 0°C to 1024°C.
- It includes a thermocouple probe featuring a threaded tip with a 1/4″-20 size.
- The module offers a resolution of 0.25°C with an accuracy of ±3°C.
- The module operates within a voltage range of 3 to 5.5V.

HX711-20 Load Cell: This load cell and amplifier board may be used to build a specific scale that works with a microcontroller. The HX711 24-bit analog-to-digital converter (ADC) on the amplifier board properly transforms the analog input from the load cell into weight measurements.

Specifications:

- Model: HX711-20
- Measuring range: Up to 20 kg
- Load cell resolution (0.01g)
- Accuracy: ±0.02% of Full Scale (F.S.)
- Supply voltage: 2.6 to 5.25 V
- Current consumption: Less than 1.5 mA

1000 psi Industrial Pressure Transducer: This pressure transducer is designed to measure pressure in various mediums such as oil, fuel, air, and water. It features a G1/4" input connection for easy installation. The transducer operates on a 5V power supply and provides an output voltage range of 0.5-4.5V or 0-5V, depending on the configuration.

Specifications:

- Input connection: G1/4"
- Power supply: 5V
- Output voltage range: 0.5-4.5V or 0-5V
- Suitable for measuring pressure up to 1000 PSI (pounds per square inch)
- Constructed with stainless steel for durability and resistance to corrosion

E. Arduino Code for the Test Stand

The following Arduino code was developed to interface the sensors with microprocessor and to log data on Arduino serial port which is then saved to notepad for analysis.

```
/////LOAD CELL/////
#include <HX711_ADC.h>
#include <EEPROM.h>
const int HX711_dout = 11;
const int HX711_sck = 12;
HX711_ADC LoadCell(HX711_dout, HX711_sck);
const int calVal_eepromAdress = 0;
```

```
long t;
////TEMPERATURE////
#include "max6675.h"
int thermoDO1  = 2;
int thermoCS1  = 3;
int thermoCLK1  = 4;
MAX6675 thermocouple1 (thermoCLK1, thermoCS1, thermoDO1);
int thermoDO2  = 5;
int thermoCS2  = 6;
int thermoCLK2  = 7;
MAX6675 thermocouple2 (thermoCLK2, thermoCS2, thermoDO2);
int thermoDO3 = 8;
int thermoCS3 = 9;
int thermoCLK3 = 10;
MAX6675 thermocouple3 (thermoCLK3, thermoCS3, thermoDO3);
/////PRESSURE////
const int pressureInput = A0; //select the analog input pin for the pressure
transducer
const int pressureZero = 102.4; //analog reading of pressure transducer at
0psi
const int pressureMax = 921.6; //analog reading of pressure transducer at
100psi
const int pressuretransducermaxPSI = 1000; //psi value of transducer being
used
const int sensorreadDelay = 100; //constant integer to set the sensor read
delay in milliseconds
float pressureValue = 0; //variable to store the value coming from the
pressure transducer
void setup() {
  Serial.begin(19200); delay(10);
  Serial.println();
  Serial.println("Measuring in a second");
  delay(1000);
  LoadCell.begin();
  float calibrationValue;
  calibrationValue = 117.24;
  #if defined(ESP8266)|| defined(ESP32)
  #endif
```

```
  long stabilizingtime = 2000; // preciscion right after power-up can be
improved by adding a few seconds of stabilizing time
  boolean _tare = true; //set this to false if you don't want tare to be
performed in the next step
  LoadCell.start(stabilizingtime, _tare);
  if (LoadCell.getTareTimeoutFlag()) {
    Serial.println("Timeout, check MCU>HX711 wiring and pin designations");
    while (1);
  }
  else {
    LoadCell.setCalFactor(calibrationValue);
    Serial.println("Startup is complete");
  }
}
void loop() {
  for (int i = 1; i <= 3; i++) {
    if(i==1){
      static boolean newDataReady = 0;
      const int serialPrintInterval = 0;
      // check for new data/start next conversion:
      if (LoadCell.update()) newDataReady = true;
      // get smoothed value from the dataset:
      if (newDataReady) {
        if (millis() > t + serialPrintInterval) {
          float i = LoadCell.getData();
          Serial.print(i);
          newDataReady = 0;
          t = millis();
        }
      }
     pressureValue = analogRead(pressureInput);
     pressureValue = ((pressureValue-
pressureZero)*pressuretransducermaxPSI)/(pressureMax-pressureZero);
//conversion equation to convert analog reading to psi
     Serial.print("\t");
     Serial.println(pressureValue, 1); //prints value from previous line to
serial
     delay(100);
```

```
    }
    else{
      /////LOAD CELL////
      static boolean newDataReady = 0;
      const int serialPrintInterval = 0;
      // check for new data/start next conversion:
      if (LoadCell.update()) newDataReady = true;
      // get smoothed value from the dataset:
      if (newDataReady) {
       if (millis() > t + serialPrintInterval) {
         float i = LoadCell.getData();
         Serial.print("\t\t\t");
         Serial.print(i);
         newDataReady = 0;
         t = millis();
        }
      }
      ////PRESSURE////
      pressureValue = analogRead(pressureInput);
      pressureValue = ((pressureValue-
pressureZero)*pressuretransducermaxPSI)/(pressureMax-pressureZero);
//conversion equation to convert analog reading to psi
      Serial.print("\t");
      Serial.println(pressureValue, 1); //prints value from previous line to
serial
      delay(100);
    }
  }
  Serial.print(thermocouple1.readCelsius());
  Serial.print("\t");
  Serial.print(thermocouple2.readCelsius());
  Serial.print("\t");
  Serial.print(thermocouple3.readCelsius());
  Serial.print("\t");
}
```

F. Python Code for the Flight Trajectory Simulation

The following python code was developed to solve the flight trajectory simulation by iteratively updating velocity, mass, height and air density with time.

```
import math

import matplotlib.pyplot as plt

# Step 1: Define design constraints and simulation settings

C_D = 0.4  # Drag coefficient

t_step = 0.1  # Time step size

t_o = 0  # Initial time

m_flow =0.668

# Step 2: Determine initial air density

def get_air_density(h):

    density = 1.225*2.72**(-h/8000)

     return density

def update_mass(m_t):

        m_new = m_t - m_flow*t_step

        return m_new

# Step 4: Update velocity and height

def update_velocity_height(v, h, density, m_new):

    if v >= 0:

        # Calculate the thrust force

        m_flow =0.668

        c_eff = 1944.77

        F_T =m_flow*c_eff

        # Calculate the drag force

        A = 0.00785  # Reference cross-sectional area (m^2)

        F_d = 0.5 * C_D * density * A * v**2  # Drag force
```

```
        # Calculate the gravity force
        F_g = m_new*9.81*((6378400/(6378400 + h))**2)
        # Update velocity and height
        v_new = v + ( (F_T-(F_g + F_d) )/ m_new ) * t_step  # New velocity
        h_new = h + v * t_step + ( (F_T - (F_g + F_d)) / (2*m_new) ) *
t_step**2  # New height
        return v_new, h_new
def update_velocity_height2(v, h, density):
        if v >= 0:
        # Calculate the drag force
        A = 0.00785  # Reference cross-sectional area (m^2)
        F_d = 0.5 * C_D * density * A * v**2  # Drag force
        # Calculate the gravity force
        F_g = m_f*9.81*((6378400/(6378400 + h))**2)
        # Update velocity and height
        v_new = v - ( (F_g + F_d) / m_f ) * t_step  # New velocity
        h_new = h + v * t_step - ( (F_g + F_d) / (2*m_f) ) * t_step**2  # New
height
    else:
        # Calculate the drag force
        A = 0.00785  # Reference cross-sectional area (m^2)
        F_d = 0.5 * C_D * density * A * v**2  # Drag force
        # Calculate the gravity force
        F_g = m_f*9.81*((6378400/(6378400 + h))**2)
        # Update velocity and height
        v_new = v - ( (F_g - F_d) / m_f ) * t_step  # New velocity
        h_new = h + v * t_step - ( (F_g - F_d) / (2*m_f) ) * t_step**2
```

```
    return v_new, h_new

# Lists to store time, velocity, and height values

time_list = []

velocity_list = []

height_list = []

# Step 6: Perform simulation until the object reaches the ground

v = 0  # Initial velocity

h = 0  # Initial height

m =9.354+3

while m >= 3:

    density = get_air_density(h)  # Step 5: Update air density

    m = update_mass(m)

    v, h = update_velocity_height(v, h, density, m)  # Step 4: Update velocity
and height

        # Print the current state

    # Store the current state

    time_list.append(t_o)

    velocity_list.append(v)

    height_list.append(h)

    print(f"Time: {t_o:.2f}s, Height: {h:.2f}m, Velocity: {v:.2f}m/s")

    t_o += t_step  # Update time

m_f = 3

while h >= 0:

    density = get_air_density(h)  # Step 5: Update air density

    v, h = update_velocity_height2(v, h, density)  # Step 4: Update velocity
and height

    # Print the current state
```

```python
    # Store the current state
    time_list.append(t_o)
    velocity_list.append(v)
    height_list.append(h)
    print(f"Time: {t_o:.2f}s, Height: {h:.2f}m, Velocity: {v:.2f}m/s")
    t_o += t_step  # Update time
print("The object has touched the ground.")
# Plotting velocity vs. time
plt.subplot(2, 1, 1)
plt.plot(time_list, velocity_list)
plt.xlabel('Time (s)')
plt.ylabel('Velocity (m/s)')
plt.title('Velocity vs. Time')
# Plotting height vs. time
plt.subplot(2, 1, 2)
plt.plot(time_list, height_list)
plt.xlabel('Time (s)')
plt.ylabel('Height (m)')
plt.title('Height vs. Time')
# Display the graphs
plt.tight_layout()
plt.show()
```

G. Drawings of Test Stand and Solid Rocket

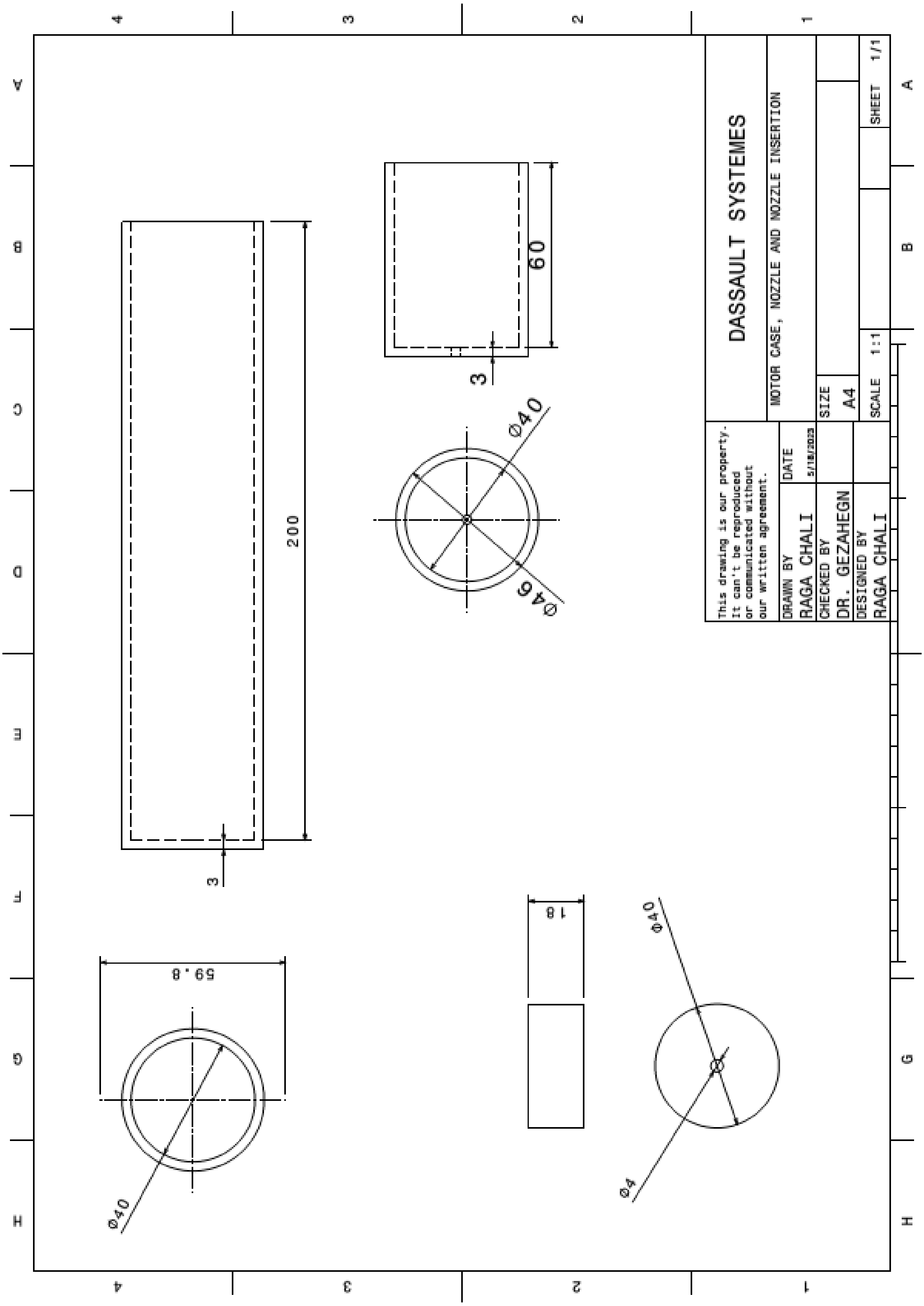

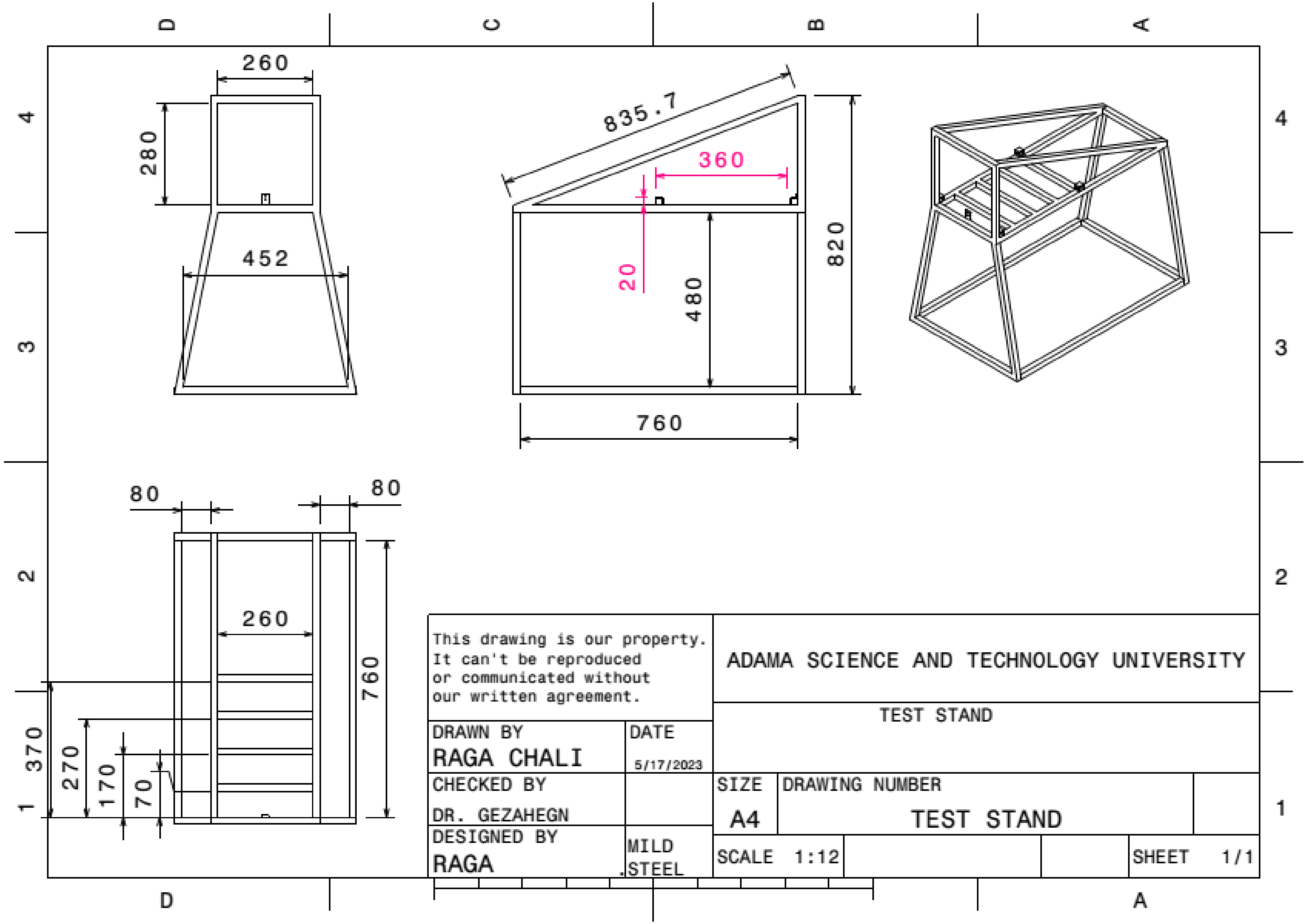
260
280
452
835.7
360
20
480
820
760
80
80
260
760
370
270
170
70
This drawing is our property.
It can't be reproduced
or communicated without
our written agreement.
ADAMA SCIENCE AND TECHNOLOGY UNIVERSITY
TEST STAND
DRAWN BY
RAGA CHALI
DATE
5/17/2023
CHECKED BY
DR. GEZAHEGN
DESIGNED BY
RAGA
MILD
.STEEL
SIZE
A4
DRAWING NUMBER
TEST STAND
SCALE 1:12
SHEET 1/1

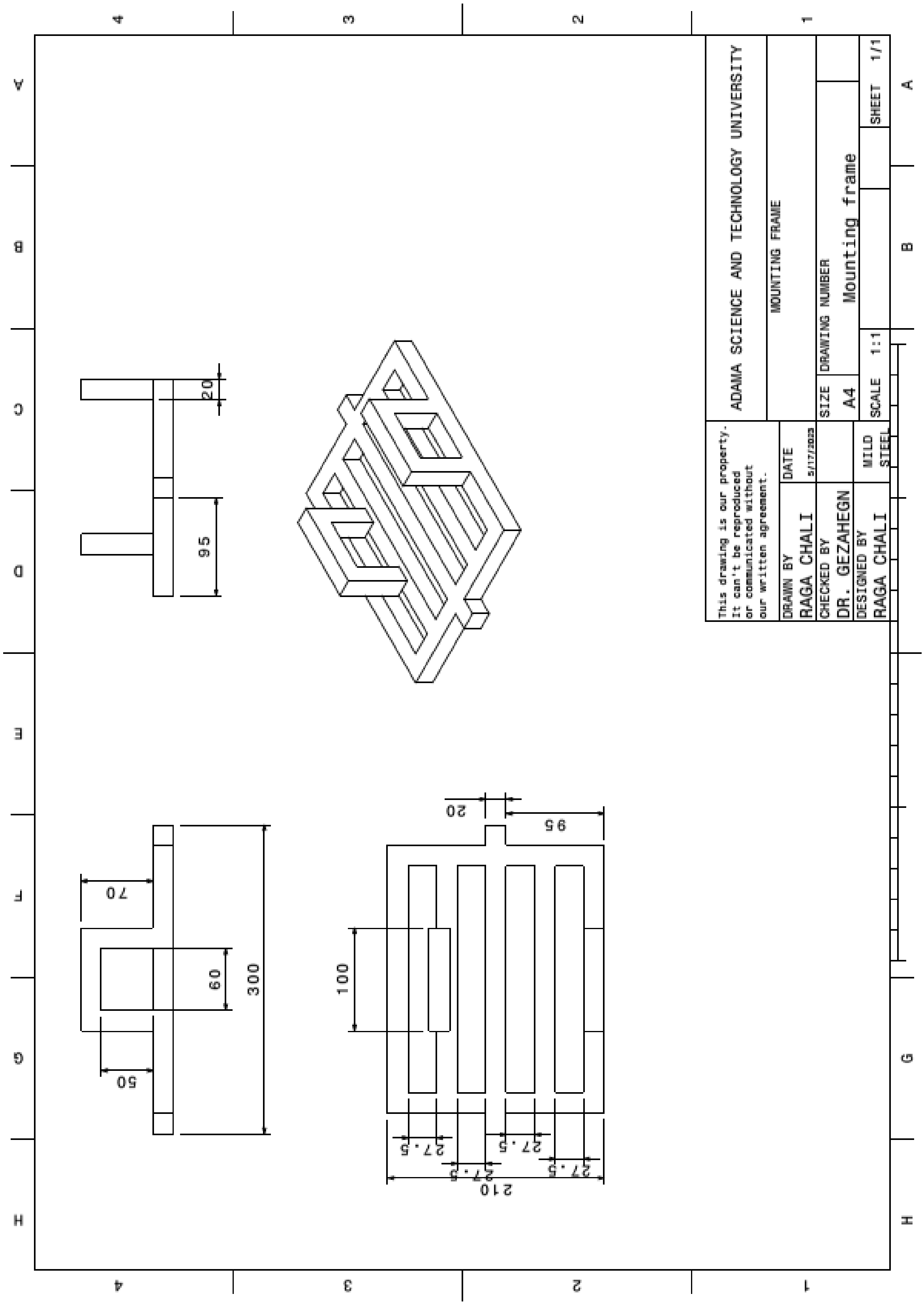
ADAMA SCIENCE AND TECHNOLOGY UNIVERSITY
MOUNTING FRAME
SIZE A4
DRAWING NUMBER
Mounting frame
SCALE 1:1
SHEET 1/1
This drawing is our property. It can't be reproduced or communicated without our written agreement.
DRAWN BY RAGA CHALI
DATE 5/17/2023
CHECKED BY DR. GEZAHEGN
DESIGNED BY RAGA CHALI
MILD STEEL
20
95
70
60
300
50
100
210
27.5

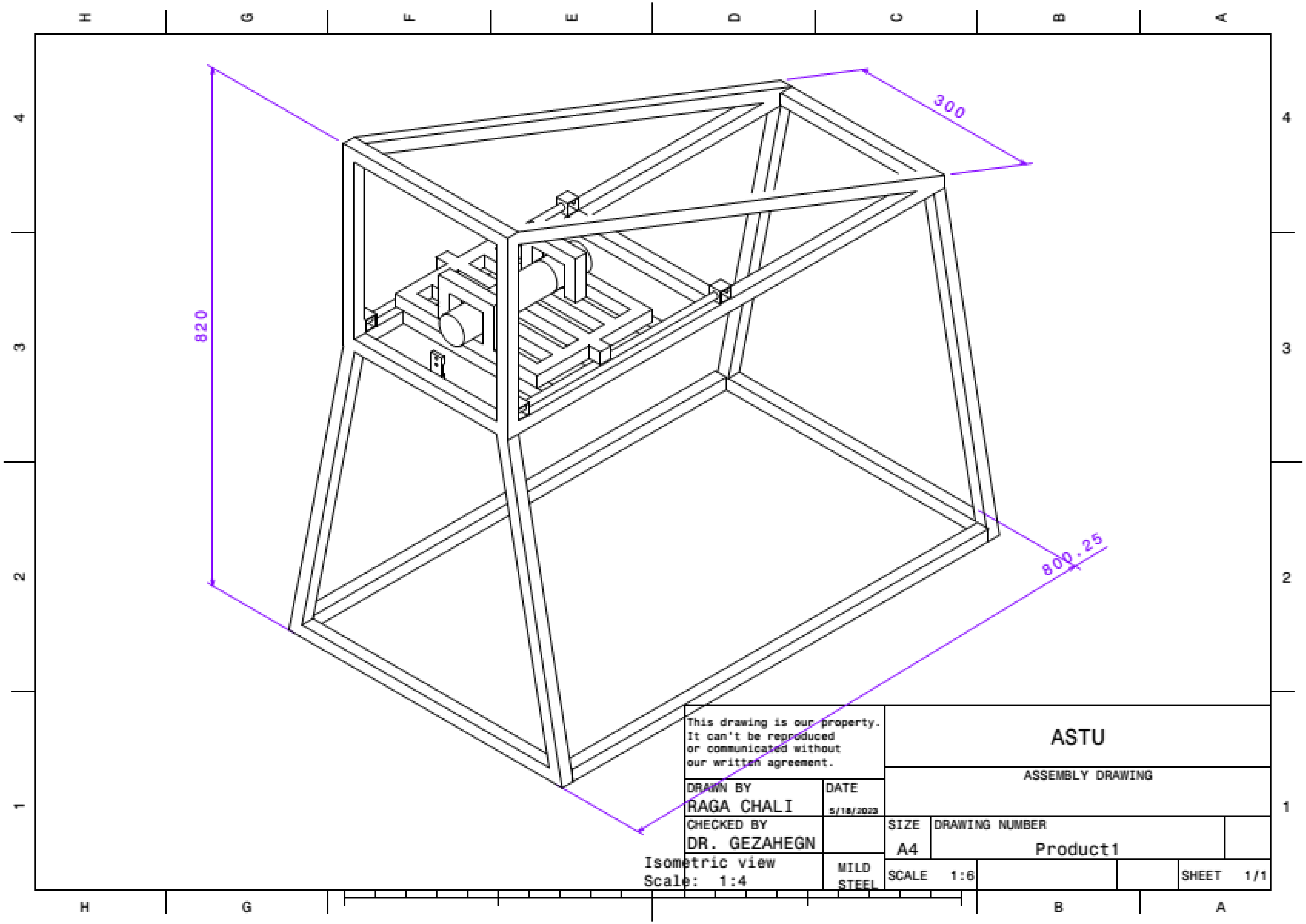
300
820
800.25
This drawing is our property.
It can't be reproduced
or communicated without
our written agreement.
DRAWN BY
RAGA CHALI
DATE
5/18/2023
CHECKED BY
DR. GEZAHEGN
Isometric view
Scale: 1:4
MILD STEEL
ASTU
ASSEMBLY DRAWING
SIZE
A4
DRAWING NUMBER
Product1
SCALE 1:6
SHEET 1/1

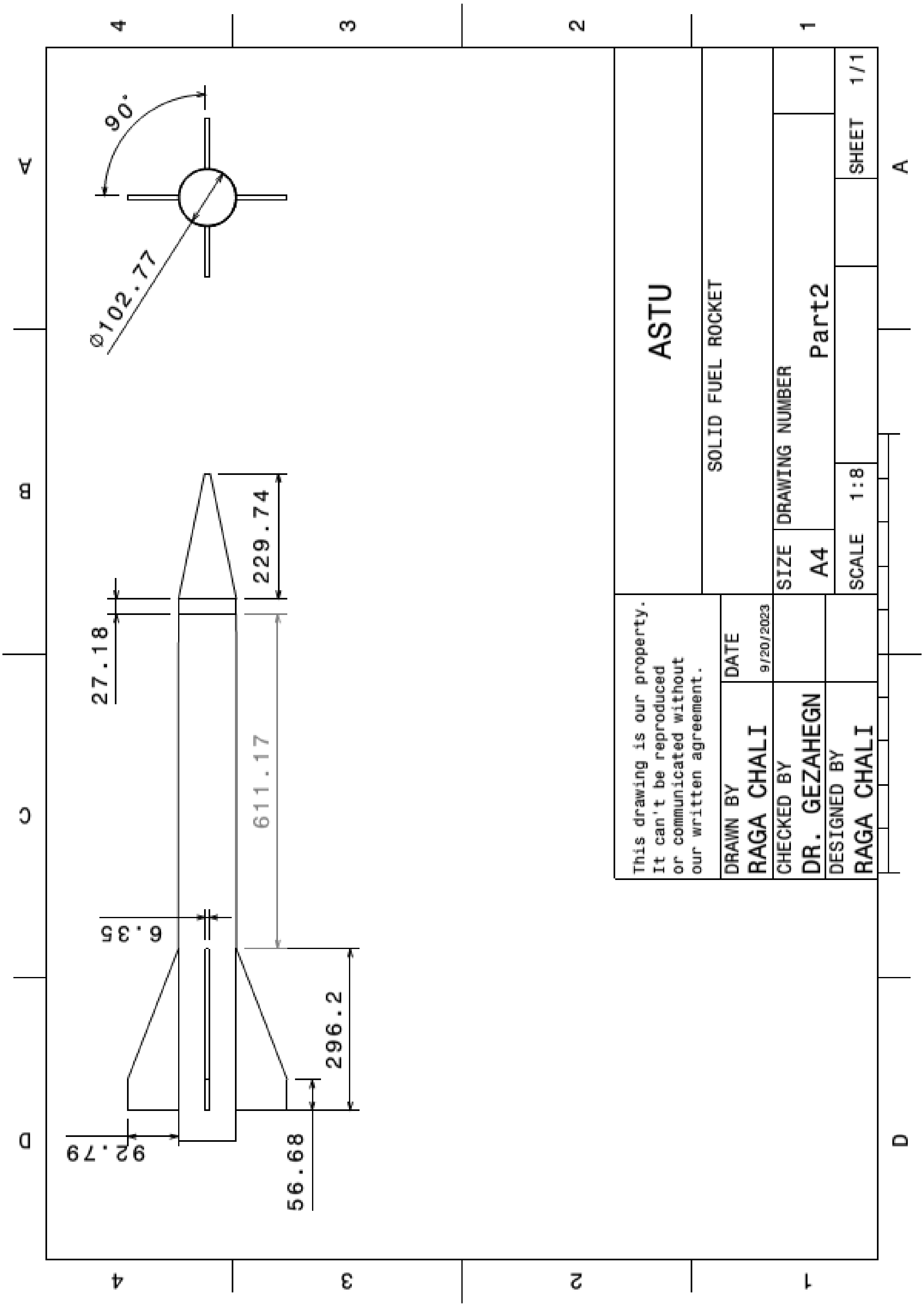

ASTU
SOLID FUEL ROCKET
This drawing is our property.
It can't be reproduced
or communicated without
our written agreement.
DRAWN BY
RAGA CHALI
DATE
9/20/2023
CHECKED BY
DR. GEZAHEGN
DESIGNED BY
RAGA CHALI
SIZE
A4
DRAWING NUMBER
Part2
SCALE 1:8
SHEET 1/1
Ø102.77
90°
229.74
27.18
611.17
6.35
296.2
92.79
56.68

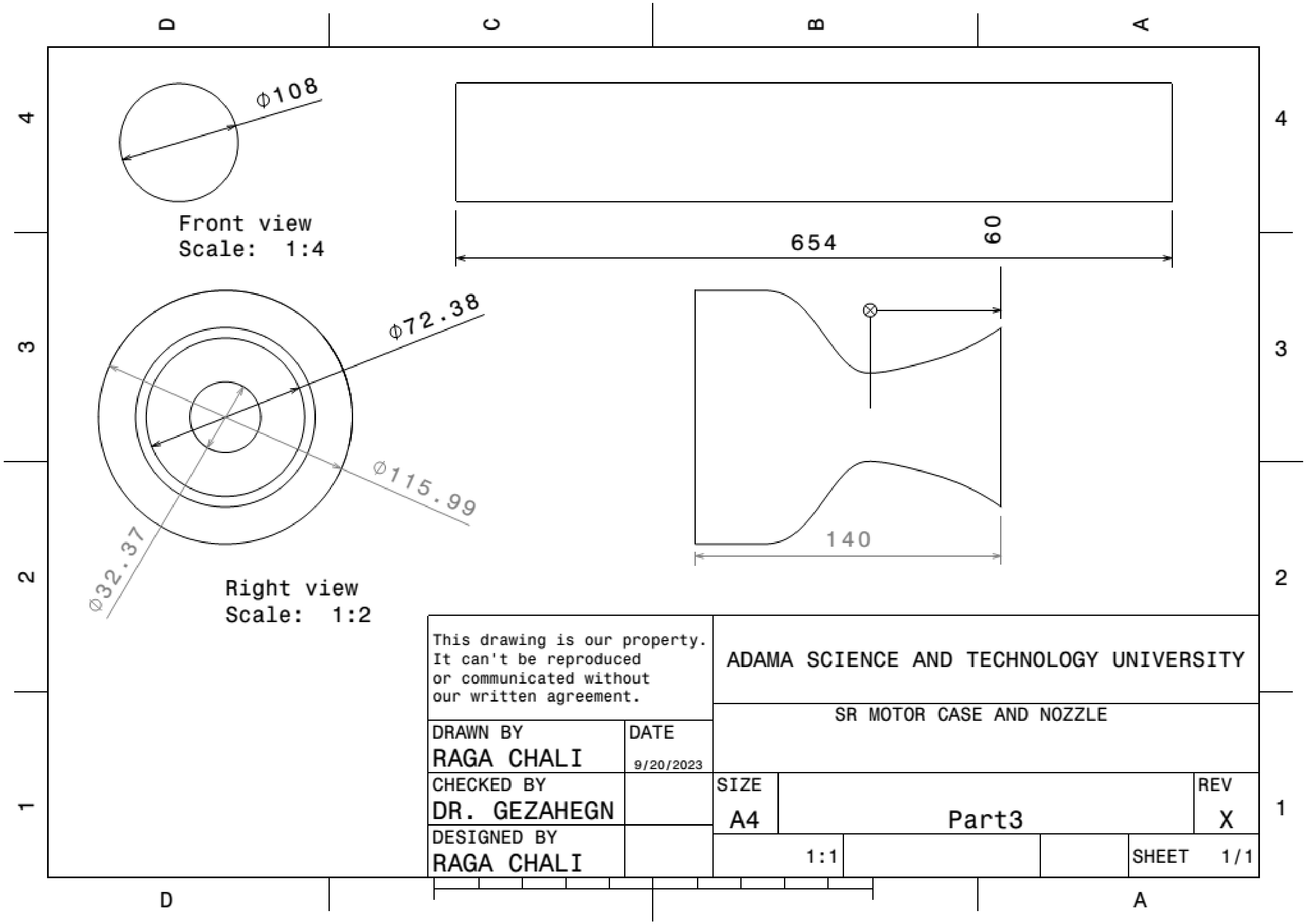
D
C
B
A
4
3
2
1
ϕ108
Front view
Scale: 1:4
654
60
ϕ72.38
ϕ115.99
ϕ32.37
140
Right view
Scale: 1:2
This drawing is our property.
It can't be reproduced
or communicated without
our written agreement.
ADAMA SCIENCE AND TECHNOLOGY UNIVERSITY
SR MOTOR CASE AND NOZZLE
DRAWN BY
RAGA CHALI
DATE
9/20/2023
CHECKED BY
DR. GEZAHEGN
DESIGNED BY
RAGA CHALI
SIZE
A4
Part3
REV
X
1:1
SHEET 1/1

SPECIAL ACKNOWLEDGEMENT

This research project is funded by Adama Science and Technology University under the grant number ASTU/SM-R/654/22, Adama, Ethiopia.